Rapporter och meddelanden 141

Geology of the Northern Norrbotten ore province, northern Sweden

Paper 5 (13)

Editor: Stefan Bergman




SGU
Sveriges geologiska undersökning
Geological Survey of Sweden

Rapporter och meddelanden 141

Geology of the Northern Norrbotten ore province, northern Sweden

Editor: Stefan Bergman

Sveriges geologiska undersökning
2018

ISSN 0349-2176
ISBN 978-91-7403-393-9

Cover photos:
Upper left: View of Torneälven, looking north from Sakkaravaara, northeast of Kiruna. ***Photographer:*** Stefan Bergman.
Upper right: View (looking north-northwest) of the open pit at the Aitik Cu-Au-Ag mine, close to Gällivare. The Nautanen area is seen in the background. ***Photographer:*** Edward Lynch.
Lower left: Iron oxide-apatite mineralisation occurring close to the Malmberget Fe-mine. ***Photographer:*** Edward Lynch.
Lower right: View towards the town of Kiruna and Mt. Luossavaara, standing on the footwall of the Kiruna apatite iron ore on Mt. Kiirunavaara, looking north. ***Photographer:*** Stefan Bergman.

Head of department, Mineral Resources: Kaj Lax
Editor: Stefan Bergman

Layout: Tone Gellerstedt och Johan Sporrong, SGU
Print: Elanders Sverige AB

Geological Survey of Sweden
Box 670, 751 28 Uppsala
phone: 018-17 90 00
fax: 018-17 92 10
e-mail: sgu@sgu.se
www.sgu.se

Table of Contents

Introduktion

Stefan Bergman & Ildikó Antal Lundin

Den här rapporten presenterar de samlade resultaten från ett delprojekt inom det omfattande tvärvetenskapliga Barentsprojektet i norra Sverige. Projektet initierades av Sveriges geologiska undersökning (SGU) som ett första led i den svenska mineralstrategin. SGU fick ytterligare medel av Näringsdepartementet för att under en fyraårsperiod (2012–2015) samla in nya geologiska, geofysiska och geokemiska data samt för att förbättra de geologiska kunskaperna om Sveriges nordligaste län. Det statligt ägda gruvbolaget LKAB bidrog också till finansieringen. Projektets strategiska mål var att, genom att tillhandahålla uppdaterad och utförlig geovetenskaplig information, stödja prospekterings- och gruvindustrin för att förbättra Sveriges konkurrenskraft inom mineralnäringen. Ny och allmänt tillgänglig geovetenskaplig information från den aktuella regionen kan hjälpa prospekterings- och gruvföretag att minska sina risker och prospekteringskostnader och främjar därigenom ekonomisk utveckling. Dessutom bidrar utökad geologisk kunskap till en effektiv, miljövänlig och långsiktigt hållbar resursanvändning. All data som har samlats in i projektet lagras i SGUs databaser och är tillgängliga via SGU.

Syftet med det här delprojektet var att få en djupare förståelse för den stratigrafiska uppbyggnaden och utvecklingen av de mineraliserade ytbergarterna i nordligaste Sverige. Resultaten, som är en kombination av ny geologisk kunskap och stora mängder nya data, kommer att gynna prospekterings- och gruvindustrin i regionen i många år framöver.

Norra Norrbottens malmprovins står för en stor del av Sveriges järn- och kopparmalmsproduktion. Här finns fyra aktiva metallgruvor (mars 2018) och mer än 500 dokumenterade mineraliseringar. Fyndigheterna är av många olika slag, där de viktigaste typerna är stratiforma kopparmineraliseringar, järnformationer, apatitjärnmalm av Kirunatyp och epigenetiska koppar-guldmineraliseringar. En vanlig egenskap hos de flesta malmer och mineraliseringar i Norr- och Västerbotten är att de har paleoproterozoiska vulkaniska och sedimentära bergarter som värdbergart. För undersökningarna valdes ett antal nyckelområden med bästa tillgängliga blottningsgrad. De utvalda områdena representerar tillsammans en nästan komplett stratigrafi i ytbergarter inom åldersintervallet 2,5–1,8 miljarder år.

Rapporten består av tretton kapitel och inleds med en översikt över de geologiska förhållandena, som beskriver huvuddragen i de senaste resultaten. Översikten följs av fyra kapitel (2–5) som huvudsakligen handlar om litostratigrafi och åldersbestämningar av ytbergarterna. Huvudämnet för de därpå följande fem kapitlen (6–10) är 3D-geometri och strukturell utveckling. Därefter kommer två kapitel (11–12) som fokuserar på U-Pb-datering av en metamorf respektive intrusiv händelse. Rapporten avslutas med en studie av geokemin hos morän i Norra Norrbottens malmprovins (kapitel 13).

Introduction

Stefan Bergman & Ildikó Antal Lundin

This volume reports the results from a subproject within the Barents Project, a major programme in northern Sweden. The multidisciplinary Barents Project was initiated by SGU as the first step in implementing the Swedish National Mineral Strategy. SGU obtained additional funding from the Ministry of Enterprise and Innovation to gather new geological, geophysical and till geochemistry data, and generally enhance geological knowledge of northern Sweden over a four-year period (2012–2015). The state-owned iron mining company LKAB also helped to fund the project. The strategic goal of the project was to support the exploration and mining industry, so as to improve Sweden's competitiveness in the mineral industry by providing modern geoscientific information. Geological knowledge facilitates sustainable, efficient and environmentally friendly use of resources. New publicly available geoscientific information from this region will help exploration and mining companies to reduce their risks and exploration costs, thus promoting economic development. All data collected within the project are stored in databases and are available at SGU.

This subproject within the Barents Project aims to provide a deeper understanding of the stratigraphy and depositional evolution of mineralised supracrustal sequences in northernmost Sweden. The combined results in the form of new geological knowledge and plentiful new data will benefit the exploration and mining industry in the region for many years to come.

The Northern Norrbotten ore province is a major supplier of iron and copper ore in Sweden. There are four active metal mines (March 2018) and more than 500 documented mineralisations. A wide range of deposits occur, the most important types being stratiform copper deposits, iron formations, Kiruna-type apatite iron ores and epigenetic copper-gold deposits. A common feature of most deposits is that they are hosted by Palaeoproterozoic metavolcanic or metasedimentary rocks. A number of key areas were selected across parts of the supracrustal sequences with the best available exposure. The areas selected combine to represent an almost complete stratigraphic sequence.

This volume starts with a brief overview of the geological setting, outlining some of the main recent achievements. This is followed by four papers (2–5) dealing mainly with lithostratigraphy and age constraints on the supracrustal sequences. 3D geometry and structural evolution are the main topics of the next set of five papers (6–10). The following two contributions (11–12) focus on U-Pb dating of a metamorphic event and an intrusive event, respectively. The volume concludes with a study of the geochemical signature of till in the Northern Norrbotten ore province (13).

Authors, paper 5:
Fredrik A. Hellström
Geological Survey of Sweden
Department of Mineral Resources
Uppsala, Sweden

Risto Kumpulainen
Stockholm University,
Department of Geological Sciences,
Stockholm, Sweden

Cecilia Jönsson
Geological Survey of Sweden
Department of Mineral Resources
Uppsala, Sweden

Tonny B. Thomsen
Geological Survey of Denmark & Greenland,
Department of Petrology & Economic Geology,
Copenhagen, Denmark

Hannu Huhma
Geological Survey of Finland,
Espoo, Finland

Olof Martinsson
Luleå University of Technology,
Division of Geosciences and Environmental Engineering,
Luleå, Sweden

5. Age and lithostratigraphy of Svecofennian volcanosedimentary rocks at Masugnsbyn, northernmost Sweden – host rocks to Zn-Pb-Cu- and Cu ±Au sulphide mineralisations

Fredrik A. Hellström, Risto Kumpulainen, Cecilia Jönsson, Tonny B. Thomsen, Hannu Huhma, Olof Martinsson

ABSTRACT

This study focuses on the Svecofennian volcanosedimentary rock units of the Pahakurkio and Kalixälv groups in the Masugnsbyn area, approximately 90 km to the S-SE of Kiruna in northeasternmost Sweden, with the aim of constraining their depositional timing and environment. The Pahakurkio group comprises pelitic to arenitic metasedimentary rocks lying on top of the Karelian Veikkavaara greenstone group. It is divided into four subunits, two sandstones and two shale units. The sandstones are immature arkoses to subarkoses, originating predominantly from rocks in the upper continental crust. The overlying Kalixälv group consists of similar metasedimentary rocks, i.e. originally shales and sandstone, now sillimanite-bearing mica schist, migmatitic paragneisses and quartzites. Both successions were deposited in a marine coastal environment with the presence of wave activity and change in vertical facies from shallow to deeper water where, in part, graphite-bearing shales represent deposition in stagnant waters beneath the storm wave base. The Kalixälv group differs from the Pahakurkio group in that it contains a much greater abundance of volcanic and volcanogenic sedimentary rocks. Extensive volcanism is a potentially important heat source driving hydrothermal alteration and generation of the minor Zn-Pb-Cu and Cu ±Au sulphide mineralisations that occur along the border zone between the Pahakurkio and Kalixälv groups, but the partly vein-hosted nature of the ore deposits suggests a later, epigenetic, hydrothermal origin, with mineralisations formed from boron-rich fluids. Sandstones from the Pahakurkio and Kalixälv group record similar negative $\varepsilon_{Nd(1.89Ga)}$ values at -3.0 and -3.9, respectively, consistent with mixing of debris from predominantly 2.2–1.9 Ga and 3.0–2.6 Ga-old rocks, a theory supported by U-Pb provenance zircon dating. The lower sandstone in the Pahakurkio group shows a zircon age distribution pattern dominated by 2.15–1.90 Ga (66%) and 2.95–2.62 Ga ages (30%), with a maximum depositional age of approximately 1.91 Ga, similar to age data from the upper sandstone unit with a maximum depositional age of approximately 1.90 Ga. A sandstone of intermediate composition in the Kalixälv group is dominated by 2.15–1.86 Ga (81%) and 2.96–2.55 Ga zircon ages (11%), and deposition is suggested to have occurred at approximately 1.89–1.88 Ga, contemporaneous with emplacement of andesitic rock within the same group. Overall, the zircon age distribution patterns are consistent with the Kalixälv group being younger than the

Pahakurkio group, according with way-up determinations. The lower quantity of Archaean zircons in the Kalixälv group sample suggests that the Archaean basement was covered by Svecofennian rocks as the Svecokarelian orogeny progressed, and thus erosion and deposition of debris from the latter was the main source. The Sakarinpalo intermediate to felsic metavolcanic rocks occur north of, and spatially associated with, rocks of the Veikkavaara greenstone group. However, U-Pb SIMS zircon data of a meta-andesite give a Svecofennian age of 1 890 ±5 Ma, and possibly indicate inverted younging of the stratigraphy in this area due to poly-phase folding. Strongly scapolite-biotite-altered intermediate rocks of the Pahakurkio group show a similar trace element pattern to volcanic rocks in the Sakarinpalo suite, suggesting that these units can be correlated. One sample from the Kalixälv group intermediate metavolcanic rocks is dated at 1 887 ±5 Ma and is thus similar in age to the Sakarinpalo suite. In a regional context, the metavolcanic rocks in the Masugnsbyn area are of a similar age to, or are possibly slightly older than, similar intermediate metavolcanic rocks in northernmost Sweden, i.e. possibly correlated with the Porphyrite group in the Kiruna–Tjårrojokka area, the Sammakkovaara group in the Pajala area and the Muorjevaara group in the Gällivare area. It is suggested that overall negative initial ε_{Nd} signatures of metavolcanic rocks from the Sakarinpalo and Kalixälv groups ($\varepsilon_{Nd(1.89Ga)}$ at -3.9 and -2.2) are a result of juvenile arc-generated melts mixed with variable amounts of anatexis and assimilated older Archaean continental crust, and related to partial melting above a subduction zone dipping underneath the Archaean Norrbotten craton.

INTRODUCTION

Northern Sweden is one of the most important mining regions in Europe, with world-class mineral deposits such as the Kiruna and Malmberget iron ores and the Aitik copper ore. Apart from the major deposits, a large number of sub-economic to economic deposits containing Fe and Cu ±Au are known (e.g. Weihed et al. 2005, Martinsson & Wanhainen 2013, Martinsson et al. 2016). Nearly all mineralisations are hosted by supracrustal rocks and, in SGU's Barents Project, key areas were selected to cover the complete supracrustal stratigraphy with the aim of characterising and improving the understanding of the stratigraphy, geochemical signature and age of these rocks.

This chapter focuses on Svecofennian supracrustal successions at Masugnsbyn in the northeast of the Norrbotten ore province (Figs. 1–3), an area with abundant mineralisations, including stratiform quartz-banded iron ores, skarn iron ores, graphite, dolomite, Cu-Zn-Pb ±Au sulphide mineralisations (see summary review in Hellström & Jönsson 2014, Bergman et al. 2015). The lower part of the stratigraphy in Masugnsbyn, including the Veikkavaara greenstone group, is presented in Lynch et al. (2018b, Fig. 2). The upper, Svecofennian, part presented here includes pelitic to arenitic metasedimentary rocks and subordinate intermediate metavolcanic rocks. Age and geochemical data for the volcanosedimentary units in the Pahakurkio and Kalixälv groups, as well as for metavolcanic rocks of the Sakarinpalo suite (Padget 1970, Witschard 1970, Niiniskorpi 1986) put constraints on depositional timing, environment and provenance of sedimentary units and petrogenesis of the volcanic rocks, and enable comparison and correlation with similar rocks across the Norrbotten ore province. These data also increase knowledge of the stratigraphy and the geological evolution of the region, which is also of importance for further mineral exploration.

GEOLOGICAL OVERVIEW

Precambrian bedrock in northern Sweden includes a 3.2–2.6 Ga Archaean granitoid-gneiss basement, which is non-conformably overlain by Palaeoproterozoic volcanic and sedimentary successions (e.g. Ödman 1957, Witschard 1984, Bergman et al. 2001, Martinsson 2004, Kathol & Weihed 2005, Weihed et al. 2005, Martinsson & Wanhainen 2013, Lauri et al. 2016). Sm-Nd isotopic analyses of Proterozoic granitoids and metavolcanic rocks approximately delineate the Archaean palaeoboundary zone between the reworked Archaean craton in the north and more juvenile Palaeoproterozoic domains to the south, along the Luleå–Jokkmokk zone in Sweden and along the Raahe–Ladoga zone in Finland (Fig. 1, e.g. Huhma 1986, Vaasjoki & Sakko 1988, Öhlander et al. 1993, Mellqvist et al. 1999, Nironen 1997). This approximate boundary zone defines the border between the Norrbotten and the Bothnia–Skellefteå lithotectonic provinces (Stephens, pers. comm). In Norrbotten County rift-related 2.5–2.0 Ga Karelian basic metavolcanic rocks and associated metasedimentary rocks of the Kovo and Greenstone groups rest on the Archaean basement. These are overlain by terrestrial to shallow water, approximately 1.90–1.87 Ga arc-related Svecofennian successions, represented by the calc-alkaline, andesite-dominated Porphyrite group, the mildly alkaline volcanic rocks of the Kiirunavaara group (Martinsson 2004) and, in the uppermost stratigraphic level, younger clastic sedimentary rocks. The Greenstone group contains stratiform–stratabound base metal and iron deposits in the middle and upper parts (Martinsson & Wanhainen 2013), whereas the Kiirunavaara group hosts economically important apatite iron ores, e.g. the Kiirunavaara and Malmberget deposits. Sub-aerial volcanic rocks extend south of the Archaean palaeoboundary in the predominantly volcanic 1.88–1.87 Ga Arvidsjaur group (Skiöld et al. 1993, Kathol & Triumf 2004, Kathol & Weihed 2005, Kathol & Persson 2007). The volcanic rocks of the Arvidsjaur group are commonly grouped together with similar volcanic rocks north of the Archaean palaeoboundary, such as the Kiruna–Arvidsjaur porphyry group (Perdahl & Frietsch 1993). Palaeoproterozoic supracrustal rocks are intruded by the calc-alkaline 1.89–1.88 Ga Haparanda suite and the alkali-calcic 1.88–1.86 Ga Perthite monzonite suite, considered to be comagmatic with the Svecofennian volcanic rocks of the Porphyrite and Kiirunavaara–Arvidsjaur groups, respectively (Witschard 1984, Bergman et al. 2001). It has been suggested that the Aitik Cu-Au-Ag deposit is a porphyry copper system related to a 1.89 Ga quartz monzodiorite that was later modified by hydrothermal and metamorphic events (Wanhainen et al. 2012). Minimum-melt granites and pegmatites, referred to as Lina granite, intruded at 1.80–1.79 Ga and occupy large areas of Norrbotten (Öhlander et al. 1987a). Coeval with the S-type rocks of the Lina suite are approximately 1.80 Ga I- to A-type GSDG-type (Granite-syenite-diorite-gabbro) magmatic rocks in Norrbotten belonging to the Edefors suite. These rocks are related to the Transscandinavian igneous belt that forms a 1 500 km long, north–south-trending belt along the western part of the Svecokarelian orogen (Högdahl et al. 2004).

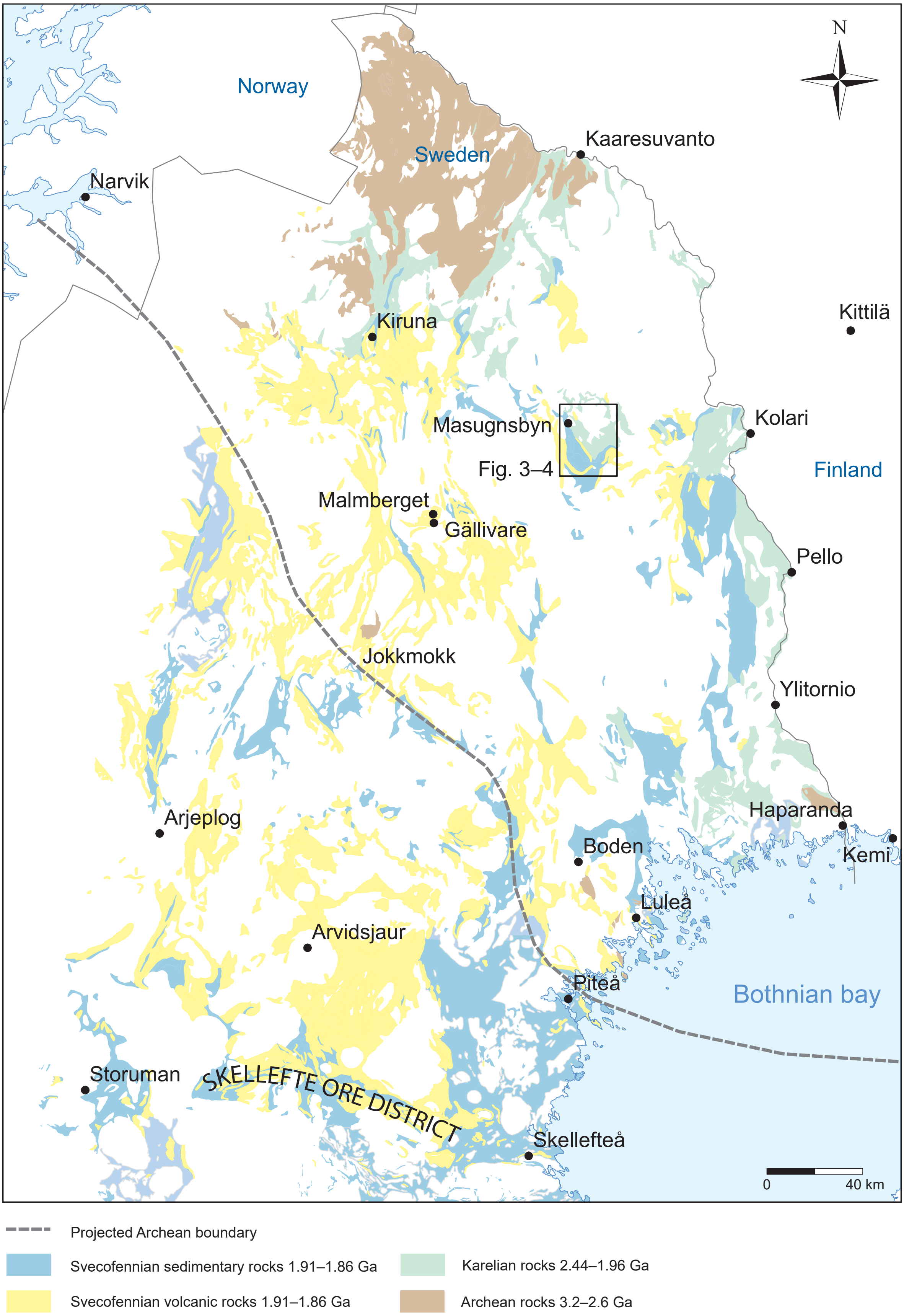

Figure 1. Geological outline of northern Sweden, showing selected lithological units (from SGU bedrock 1:M bedrock database).

Super-unit	Unit	Sub-unit	Rock units	(m)
Svecofennian supracrustal rocks	Rissavaara quartzite	4	Quartz sandstone (quartzite)	
	Kalixälv grp	3b	Semipelitic,-pelitic-, basic schists, migmatitic paragneiss	
		3a	Conglomerate, meta-sandstone, intermediate metavolcanic rocks	
	Sakarinpalo suite		Intermediate-felsic metavolcanic rocks	
	Pahakurkio grp	upper sandstone (2d)	Subarkosic metasandstone	1800
		upper shale (2c)	Pelitic micaschist, graphite schist, marble	1000
		lower sandstone (2b)	Subarkosic-arkosic metasandstone, greenshist	430
		lower shale (2a)	Pelitic micaschist	600
Karelian supracrustal rocks	Veikkavaara greenstone grp	Masugnsbyn fm (1c)	Graphite schist, skarnbanded chert (BIF), marble	370
		Tuorevaara greenstone fm (1c)	Metabasaltic tuff, graphite schist, metadolerite sills	1000
		Suinavaara fm (1b)	Pelitic schist and quartzite (Suinavaara quartzite)	100
		Nokkokorvanrova greenstone fm (1a)	Basaltic greenstone	2000

Figure 2. Schematic stratigraphy of the Masugnsbyn area, modified from Padget (1970) & Witschard (1970). The names used in Padget (1970) have been partly modified, and new informal names have been added. The alphanumerical names for the sub-units used by Padget (1970) are within brackets. Names of units within the Veikkavaara group follow Lynch et al. (2018b); grp = group, fm = formation.

Geology of the Masugnsbyn area

In the Masugnsbyn area, approximately 90 km east-southeast of Kiruna, Karelian greenstones of the Veikkavaara greenstone group are overlain by Svecofennian supracrustal rocks of the Pahakurkio and Kalixälv groups (Figs. 1–4; Padget 1970). The Veikkavaara greenstones constitute the upper part of the Greenstone group, whereas the Pahakurkio and Kalixälv groups have been included in the Middle sediment group of Witschard (1984). Intermediate volcanic rocks north of, and spatially associated with, the Veikkavaara greenstone are referred to as the Sakarinpalo suite (Witschard 1970).

The Veikkavaara greenstones form a V-shaped area in the eastern part of the Masugnsbyn area and predominantly consist of mafic volcaniclastic rocks (Fig. 3, Padget 1970, Lynch et al. 2018b). Metadoleritic sills appear to be concordant with the basaltic tuffs and are considered to have intruded shortly after the deposition of the basaltic sandstones, possibly representing near-surface intrusions related to the contemporary volcanism. A 40 m wide dolerite sill was dated by U-Pb in zircon at 2 139 ±4 Ma (2σ), and is also suggested to constrain the age of the Veikkavaara greenstone group (Lynch et al. 2018b). The uppermost part of the Veikkavaara greenstone group is referred to as the Masugnsbyn formation and consists of chemically deposited metasediments, including skarn-banded chert (silicate facies banded iron formation), graphite schist and calcitic to dolomitic marble (see Lynch et al. 2018b). Martinsson et al. (2013) used the name Vinsa formation for the uppermost part of the Veikkavaara greenstone group, defined in the Käymäjärvi area to the east (see Martinsson et al. 2018b).

The Sakarinpalo suite consists of altered acid to intermediate metavolcanic rocks and occurs immediately north of the Veikkavaara greenstones (Fig. 3, Witschard 1970). The magnetic anomaly pattern suggests that the Sakarinpalo metavolcanic rocks are spatially related to rocks of the Greenstone group (Fig. 4), and can possibly be correlated with units within the Viscaria formation in the Kiruna Greenstone group (cf. Martinsson 1997). But the area is poorly exposed and no contacts have been observed between the Veikkavaara greenstones and the Sakarinpalo suite.

The Pahakurkio group comprises arenitic to pelitic metasedimentary rocks, west of, and concordantly on top of, the Veikkavaara greenstone group (Fig. 3). Cross-bedding is common in the metasandstones, and numerous way-up determinations consistently show younging to the west (Padget 1970).

Layers of strongly scapolite-altered rocks of basic to intermediate composition occur within the meta-sandstones and may represent volcanic material. Graphite-bearing schists and carbonate rocks occur within the metapelites of the Pahakurkio group (Niiniskorpi 1986).

The *Kalixälv group* has a basal conglomerate, suggesting an unconformable contact with the Pahakurkio group. Distinct cross-bedding shows that the steeply dipping beds in meta-sandstones young to the west, and the Kalixälv group therefore overlies the Pahakurkio group (Padget 1970). In part, the contact between the groups is tectonic, i.e. along the Kalixälv fault. Niiniskorpi (1986) noted that both the Pahakurkio and the Kalixälv groups consist of similar types of metasedimentary rocks, metapelites and quartzites. However, metavolcanic rocks are much more frequent in the Kalixälv group than the Pahakurkio group (Niiniskorpi 1986). To the west and south, migmatisation increases and no natural, upper stratigraphic limit for the group is known.

Structures

The supracrustal sequence in the Masugnsbyn area is deformed into large-scale fold structures and cut by faults. Structures have northeast or northwest trends, thereby intersecting at high angles. Main tectonic features include the Kalixälv dome, the Masugnsbyn syncline, the Saittajärvi anticline and the Oriasvaara syncline with the associated Kalixälv fault (Fig. 3, Padget 1970). Fold axial planes strike northwest–southeast, except for the Oriasvaara syncline, which has a northeast–southwest trend, parallel to the Kalixälv fault. The Oriasvaara syncline is bounded to the northwest by the northeasterly-oriented Kalixälv fault. Movements along that fault have down-thrown the southeastern block, creating the tectonic contact between the Pahakurkio and Kalixälv groups. The dip of the beds in the Kalixälv dome is low to moderate but increases away from the centre of the dome, and must have resulted from combining at least two fold phases. The magnetic anomaly map reveals the complexly folded internal structure of the Veikkavaara greenstones and the presence of a possible earlier phase of isoclinal folding with a north-northwest-oriented axial plane in addition to the north-oriented axial plane of the Saitajärvi anticlinal. The fold structures in the Masugnsbyn area are evaluated by Grigull et al. (2018). Geophysical modelling supports the interpretation of the Saittajärvi fold as a synform structure.

Metamorphic constraints

Metamorphic mineral associations in the metapelitic rocks, with andalusite, sillimanite and cordierite, and the absence of kyanite, indicate amphibolite facies conditions of relatively high temperature and low to moderate pressures (Padget 1970). The composition of the plagioclase (An_{10-50}) and the presence of hornblende together with almandine suggest the rocks of the Veikkavaara greenstones are in the garnet amphibolite facies of regional metamorphism (Padget 1970). Partial melting in the migmatitic paragneisses in the south of the area suggests even upper amphibolites facies grade of metamorphism have been reached. Migmatisation in the paragneiss is dated at 1878 ±3 Ma and is suggested to be caused by heat from large volumes of contemporaneous early orogenic Svecokarelian intrusions (Hellström 2018).

Contact metamorphic alterations of the upper part of the Veikkavaara greenstones containing banded iron formations and carbonate rocks also resulted in skarn formation and remobilisation of iron to higher grades to form the Masugnsbyn skarn iron ores. Later metamorphic/hydrothermal events are possible, as recorded by a U-Pb monazite age of approximately 1.86 Ga of an andalusite bearing mica schist (Bergman et al. 2006), as well as U-Pb analyses of a single fractions of titanite plotting weakly discordant at approximately 1.80 Ga (Veikkavaara Cu-sulphide mineralisation), at approximately 1.78 Ga (Sakarinpalo, metadacite) and at 1.76 Ga (Tiankijoki, pyroxene skarn in metasedimentary rock, Martinsson et al. 2016). This is supported by the presence of deformation and high-grade metamorphism within the Pajala deformation belt to the west, which occurred in the 1.83–1.78 Ga interval (Bergman et al. 2006, Luth et al. 2016, Hellström & Bergman 2016, Luth et al. 2018), possibly overprinting earlier structures.

Mineralisations

Mineralisations of economic interest in the Masugnsbyn area include layers of iron and dolomite between the greenstones and metasedimentary rocks, and graphite layers and base-metal sulphide mineralisations within the volcaniclastic greenstones as well as in the Svecofennian supracrustal rocks (Fig. 3, Geijer 1929, Padget 1970, Witschard et al. 1972, Grip & Frietsch 1973, Niiniskorpi 1986, Frietsch 1997, Martinsson et al. 2013, 2016, Hellström & Jönsson 2014, Bergman et al. 2015). Greenstone-hosted mineralisations are described in Lynch et al. (2018b); a short summary of the mineralisations hosted by rocks in the Pahakurkio and Kalixälv groups is given below.

The Kurkkionvaara Zn-Pb-Cu mineralisation is located approximately 15 km south of Masugnsbyn at the contact between metasedimentary rocks of the Pahakurkio group and metasedimentary and intermediate metavolcanic rocks of the Kalixälv group (Fig. 3; Niiniskorpi, 1986, summarised below). The mineralisations occur as scattered sulphide veins or fracture fillings with sphalerite and galena, mainly in the metasedimentary rocks of the Pahakurkio groups but also in the overlying conglomerate. Locally, richer mineralisations occur in some fracture zones, with total Zn-Pb content up to a few per cent over 0.4–2.0 m. Impregnations of pyrrhotite and pyrite occur in metre-wide zones, where the highest concentrations of Fe-sulphides occur in the 10–20 m wide conglomerate horizon above the Pahakurkio group as an impregnation within the matrix. Veins of pyrrhotite generally occur parallel to bedding in the metasedimentary rocks, whereas the Pb-Zn-filled fractures usually dip steeply and crosscut bedding. There is a positive correlation between B and Zn + Pb content in lithochemical analyses, suggesting a hydrothermal system with boron-rich fluids containing base metals (Niiniskorpi 1986). At Kurkkionvaara, tourmaline-rich layers (tourmalinites) occur in the pelitic metasedimentary rocks, but tourmaline-rich pegmatites are also seen. Boron-rich fluids probably have a source in the metapelites, originally deposited as marine sediments. The sulphide mineralisations may have resulted from boron-rich fluids formed during migmatisation of the pelitic sediments, but the fracture style of Zn-Pb mineralisation suggests that this type of mineralisation post-dates migmatisation and ductile deformation. The age of migmatisation at 1.88 Ga thus provides a maximum age of the fracture-type Pb-Zb mineralisation at Kurkkionvaara (Hellström 2018).

The Maunuvaara Cu-Au quartz-veined-hosted mineralisations (also named Magnovaara, Geijer 1918, Hermelin 1804, Tegengren 1924) occur in a more than 5 km long north–south-trending zone located in the western part of the Masugnsbyn area (Fig. 3). The small scattered mineralisations consist of chalcocite, with small amounts of bornite and chalcopyrite in veins, together with quartz and amphibole in a fine-grained, gneissic andesite. Malachite and azurite are present, as well as zeolites, including aggregates of stilbite (desmin) and chabazite. Copper concentrations in mineralised rocks are generally low, but may reach a few per cent. Gold content is generally below 2 ppm, but one sample contained 6.5 ppm. Anomalously high molybdenum (200 ppm) and tungsten (2 900 ppm) are seen in a few rock samples (Niiniskorpi 1982).

The Rappukoski copper mineralisation occurs approximately 18 km south-southeast of Masugnsbyn in metasedimentary rocks of the Pahakurkio group, mainly quartzitic mica schist, that are cut by granite and pegmatite (Fig. 3, Ödman 1939, Grip & Frietsch 1973, Padget 1970). The mineralisation is located in a layer of calcareous skarn in outcrops on both sides of the river Kalixälven. A system of tension fractures created during folding is filled with quartz, calcite, hornblende, chalcopyrite, bornite and molybdenite. To some extent, chalcopyrite is also disseminated within the wall rock. The width of the mineralised zones is usually 0.1–0.3 m, but may reach 2 m in conjunction with folding. The mineralisation contains 1–2% copper and traces of molybdenum.

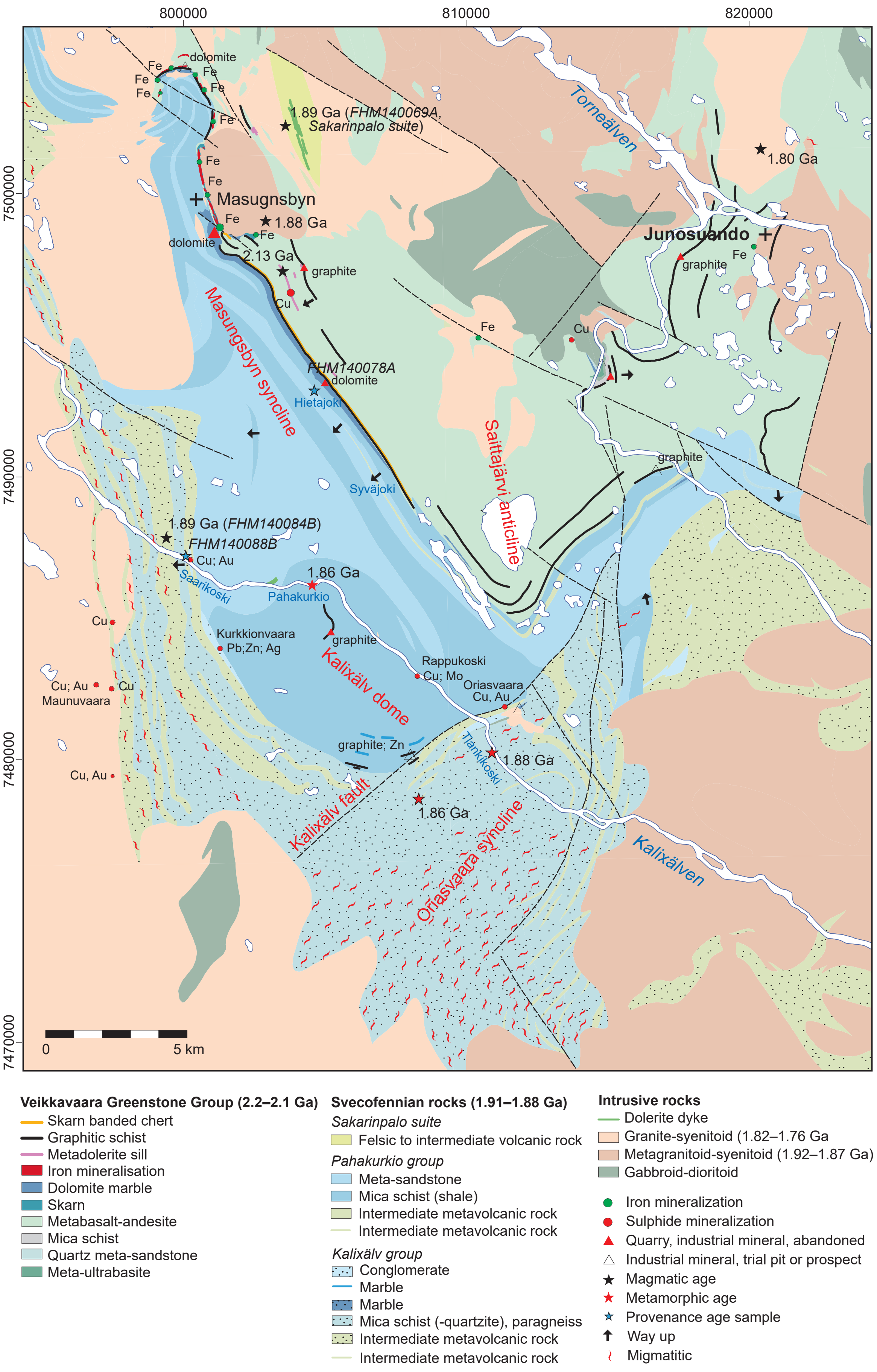
800000
810000
820000
7500000
7490000
7480000
7470000
dolomite
Fe
Fe, Fe
1.89 Ga (FHM140069A, Sakarinpalo suite)
Torneälven
1.80 Ga
Masungsbyn
1.88 Ga
dolomite
2.13 Ga
graphite
Cu
Junosuando
graphite
Fe
Masungsbyn syncline
Cu
FHM140078A
dolomite
Hietajoki
Saittajärvi anticline
Syväjoki
graphite
1.89 Ga (FHM140084B)
FHM140088B
Cu; Au
1.86 Ga
Saarikoski
Pahakurkio
Kurkkionvaara
Pb;Zn; Ag
graphite
Kalixälv dome
Rappukoski
Cu; Mo
Oriasvaara
Cu, Au
Cu; Au
Maunuvaara
graphite; Zn
1.88 Ga
Tiänkikoski
Cu, Au
1.86 Ga
Kalixälv fault
Oriasvaara syncline
Kalixälven
0
5 km
Veikkavaara Greenstone Group (2.2–2.1 Ga)
Skarn banded chert
Graphitic schist
Metadolerite sill
Iron mineralisation
Dolomite marble
Skarn
Metabasalt-andesite
Mica schist
Quartz meta-sandstone
Meta-ultrabasite
Svecofennian rocks (1.91–1.88 Ga)
Sakarinpalo suite
Felsic to intermediate volcanic rock
Pahakurkio group
Meta-sandstone
Mica schist (shale)
Intermediate metavolcanic rock
Intermediate metavolcanic rock
Kalixälv group
Conglomerate
Marble
Marble
Mica schist (-quartzite), paragneiss
Intermediate metavolcanic rock
Intermediate metavolcanic rock
Intrusive rocks
Dolerite dyke
Granite-syenitoid (1.82–1.76 Ga
Metagranitoid-syenitoid (1.92–1.87 Ga)
Gabbroid-dioritoid
Iron mineralization
Sulphide mineralization
Quarry, industrial mineral, abandoned
Industrial mineral, trial pit or prospect
Magmatic age
Metamorphic age
Provenance age sample
Way up
Migmatitic

◄ Figure 3. Bedrock geological map of the Masugnsbyn area (modified from Padget 1970, Niiniskorpi 1986). Age determinations are from Bergman et al. (2006), Hellström (2018), Lynch et al. (2018b), Martinsson et al. (2018a) and this study (FHM140069A, FHM140078A, FHM140084B, FHM140088B).

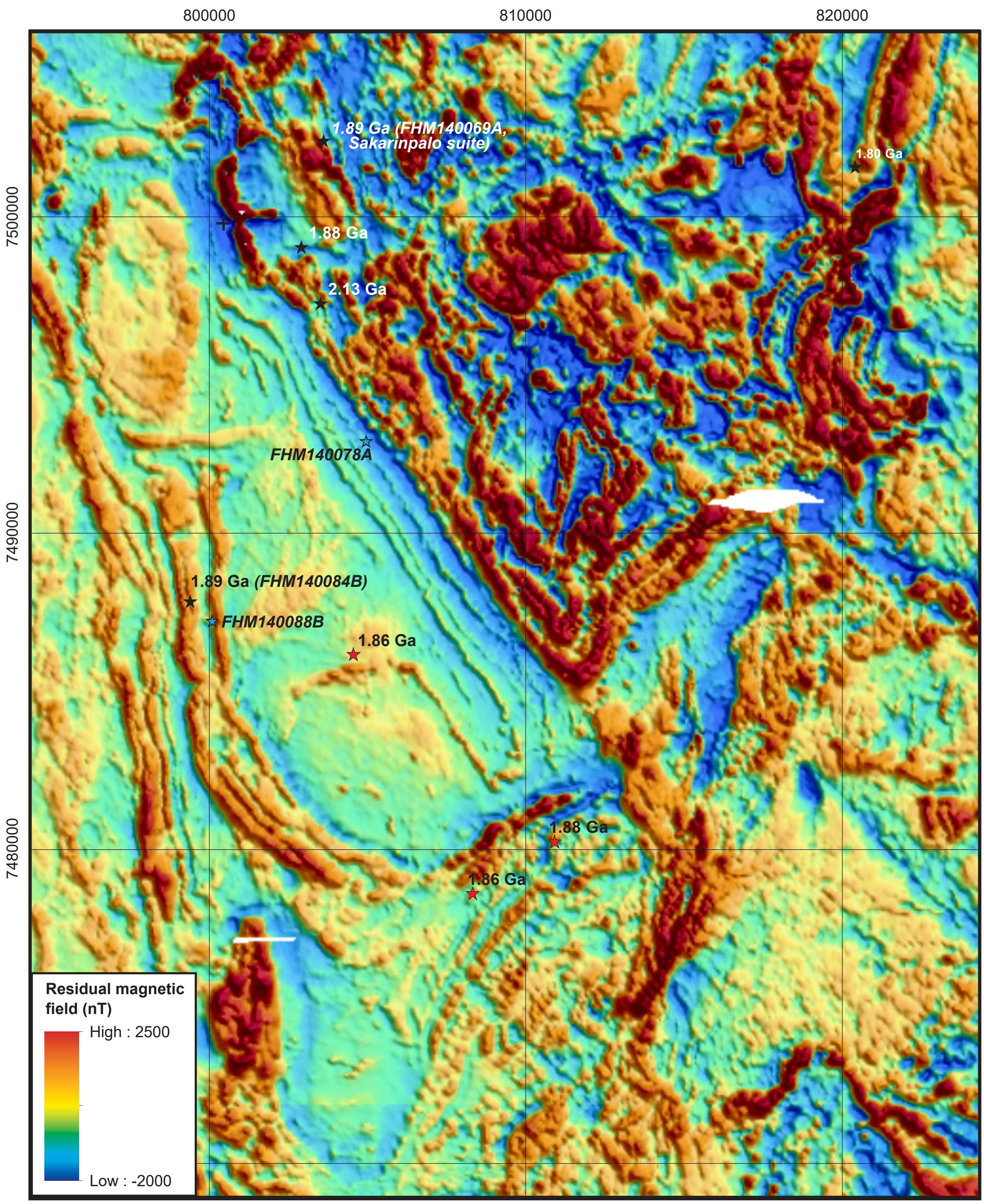

Figure 4. Magnetic anomaly map of the Masugnsbyn area with same extent as in Figure 3. Map is gridded from SGU data.

The Oriasvaara copper-gold mineralisation is located approximately 20 km south-southeast of Masugnsbyn, just east of the road to Tärendö and approximately 1 km north of the mountain Oriasvaara (Fig. 3). The Cu-Au mineralisation is spatially associated with a deformation zone: the Kalixälv fault. Two zones of mineralisation have been recognised in supracrustal rocks that have been assigned to the lower part of the Kalixälv group (Quezada 1976, Carlson 1982a, Carlson 1982b). The eastern mineralisation contains an irregular and fine-grained impregnation of pyrrhotite, chalcopyrite and pyrite in limestone. The mineralisation is locally richer in skarn-altered parts, occurring as impregnations or in bands. The western mineralisation occurs in a greenstone with zones of strong silicification and has an impregnation of sulphides, including pyrrhotite, pyrite, chalcopyrite and traces of bornite. The scapolite-altered rocks form an approximately 180 m thick unit, which generally strikes southwest–northeast and is bounded by mica schist to the north and east, and by pegmatite to the south. The richest section contains 0.5 wt. % Cu and 0.64 ppm Au over 4 m, as obtained from geochemical assays in an exploration trench in the western part (Petersson 1986).

The Sakarinpalo suite

Northeast of Masugnsbyn, at Pahtajänkkä, intermediate-felsic metavolcanic rocks referred to as the Sakarinpalo suite occur, which on a regional scale lie within the Veikkavaara greenstones (Figs. 3–5, Witschard 1970). The area is, however, poorly exposed and no contacts have been observed between the Veikkavaara greenstones and the Sakarinpalo suite. Felsic to intermediate metavolcanic rocks form a north–south-striking, steeply west-dipping unit and appear to be surrounded by granites of the Lina suite. In the west, metavolcanic rocks are bordered by a few outcrops of granite and pegmatite, but a high magnetic anomaly pattern further west cannot be explained by the low-magnetic granite (Fig. 4). The high magnetic anomaly pattern instead resembles that of the Veikkavaara greenstones, which outcrop along strike to the south, suggesting that the Sakarinpalo suite occurs within the greenstone package. Newly discovered outcrops confirm the presence of mafic rocks to the west, including dolerite and layered basaltic tuff. The metavolcanic rocks are sodium and potassium-altered and, in part, also scapolite-altered with net veining of amphibole and epidote (Fig. 5). The volcanic rocks are commonly feldspar porphyric, but volcaniclastic tuffs with alternating beds of different composition are also observed (Fig. 5).

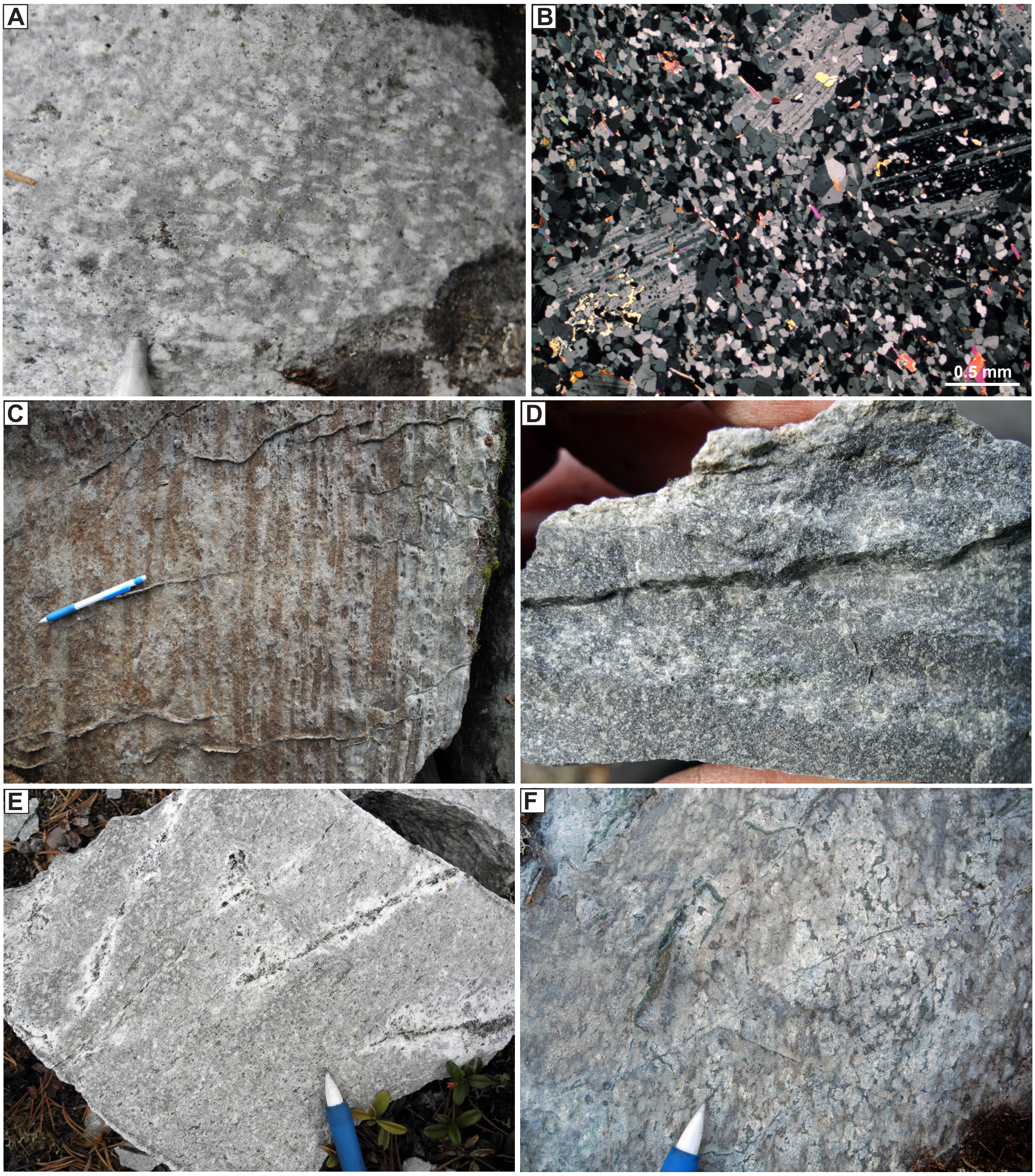

Figure 5. Metavolcanic rocks of the Sakarinpalo suite. **A.** Plagioclase porphyric meta-trachyte. (7502355 / 803715) **B.** Thin-section cross-polarised light views of plagioclase porphyric meta-trachyte. The plagioclase is sericite- and epidote-altered (7502300 / 803745). **C.** Layered volcaniclastic tuff with alternating beds of different composition (weathered outcrop surface; 7502060 / 804478). **D.** Sample of layered volcanoclastic tuff (same as in C but fresh surface; 7502060 / 804478). **E.** Albite alteration seen as bleaching next to amphibole veins in metadacite. **F.** Strongly scapolite-epidote-amphibole-altered meta-andesite (7502154 / 804535). Coordinates are given in SWEREF 99TM. All photographs by Fredrik Hellström.

The Pahakurkio group

The Pahakurkio group comprises pelitic to arenitic metasedimentary rocks to the west and on top of the Veikkavaara greenstone group (Figs. 2, 3, 7, Geijer 1930, Eriksson 1954, Padget 1970, Niiniskorpi 1986, Kumpulainen 2000). Shales have been metamorphosed to biotite-andalusite (±sillimanite) mica schists and sandstones have been recrystallised into quartzites and carry metamorphic biotite (Fig. 7E–F). The lowermost beds of the Pahakurkio group are poorly exposed, but no indications of conglomerates or any marked discordance to the uppermost unit of marble in the Veikkavaara greenstones have been observed. The magnetic anomaly pattern suggests that the Pahakurkio and Veikkavaara groups are concordant (Fig. 4). Padget (1970) studied the succession in the area between Masungsbyn and Pahakurkio along the Kalixälven river. He divided that succession into a lower shale, a lower sandstone, an upper shale and an upper sandstone. Kumpulainen (2000) later studied the sedimentological aspects of the succession; some of them are included in the text below. The Pahakurkio group is best exposed along Kalixälven between Pahakurkio and Saarikoski and at Syväjoki and Hietajoki, south-southeast of Masugnsbyn (Fig. 3).

In the *Hietajoki area*, the poorly exposed, grey, *lower shale* is succeeded by the grey, *lower sandstone*, which is further sub-divided into a horizontally-bedded, grey lower arkose (~ 150m) and a grey, low-angle to hummocky cross-bedded upper arkose (approximately 300 m, Fig. 6). Dark bands in cross-bedded quartzites contain heavy minerals such as rutile, tourmaline, zircon, ilmenite and apatite, but are not significantly magnetic. This upper arkose unit contains a poorly stratified (<2.5 m thick) conglomerate unit approximately 75 m above its base. The conglomerate clasts are predominantly quartzite; a few jasper clasts are also found. In the upper part of the upper arkose, cross-bedding is

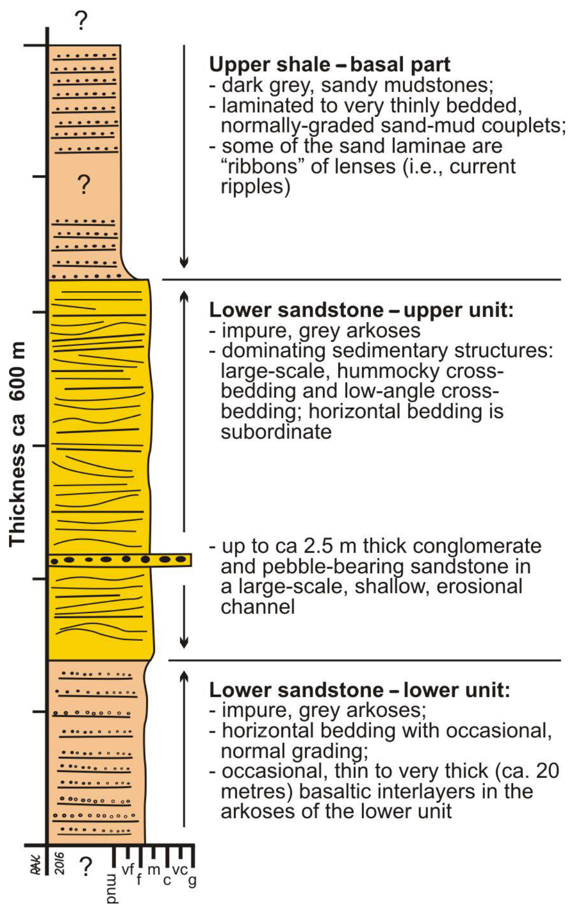

Figure 6. Stratigraphic section of the Pahakurkio group at Hietajoki, south of Masugnsbyn.

► Figure 7. Rocks of the Pahakurkio group. **A.** Trough cross-bedding in meta-sandstone at Syväjoki (7489841/806895). **B.** Cross bedding in arkosic meta-sandstone at Hietajoki (7492866/804620). **C.** Alternating beds of meta-sandstone and mica schist, originally sandy and pelitic beds at Hietajoki (7492325/804671) **D.** Wave ripples in flat dipping beds of meta-sandstone at Pahakurkio (7486133 / 803332). **E.** Deformed and folded andalusite porphyryblasts in mica schist at Hietajoki (7492168/804653). **F.** Photomicrograph in cross-polarised light of mica schist with fibrolitic sillimanite aggregate at Pahakurkio (7486176/804583). **G.** Strongly scapolite-altered intermediate rock at Syväjoki (7489838 / 806809). **H.** Photomicrograph in plane polarised light of scapolite-altered intermediate rock (7489838/806809). Coordinates are given in SWEREF 99TM. All photographs by Fredrik Hellström.

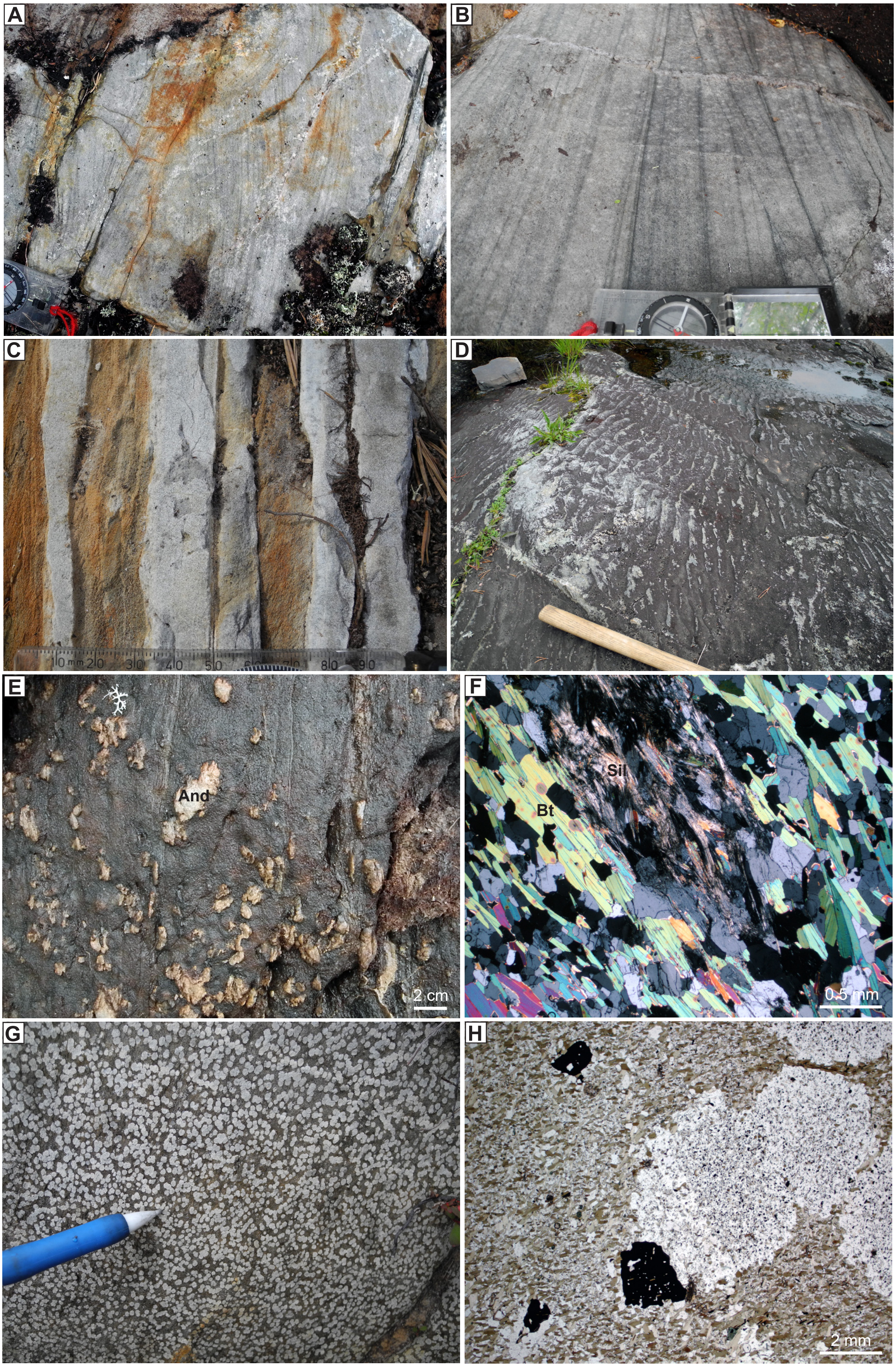
A
B
C
D
E
And
2 cm
F
Si
Bt
0.5 mm
G
H
2 mm

gradually replaced by horizontal bedding and laminations give way-up to the grey, *upper shale* unit (Figs. 2, 7E–F). The upper shale unit is predominantly horizontally laminated and contains very thin beds and lenses of sandstone (Fig. 7C). Some of these sand lenses are normally graded.

Strongly scapolite-altered, probably basic-intermediate volcanic rocks (Fig. 7G–H, "greenschist" of Padget 1970), occur within the lower sandstone unit, and seem to have a considerable lateral extent, as is evident from the aeromagnetic map (Figs. 3–4). Similar magnetic bands occur in the upper shale unit. *The Syväjoki section* is located 3.5 km southeast of Hietajoki at the corresponding stratigraphic level and there exposes a similar stratigraphic succession (Padget 1970). Trough cross-bedding is observed locally in the arkose below the basaltic-andesitic unit (Fig. 7A).

Further south, the *Pahakurkio Canyon* of the river Kalixälven (Pahakurkio, *bad rapids* – i.e. not easy to negotiate by boat) exposes a gradual transition from the uppermost part of the grey, *upper shale* (andalusite-sillimanite-bearing mica schist) into the pale grey, *upper sandstone* (quartzite). Some very thin beds and laminas display normal grading in the transition zone. Further up the section, horizontal bedding and rare low-angle cross-bedding is encountered, and further up still, wave ripples and lunate current ripple structures are observed (Fig. 7D). The upper shale is locally graphite bearing, and layers of carbonate rocks also occur (Ödman 1939, Niiniskorpi 1986).

The Kalixälv group

Structurally and stratigraphically above the Pahakurkio group is the Kalixälv group, which is poorly exposed west and south of the former group (Fig. 3; Ödman 1939, Eriksson 1954. Padget 1970, Niiniskorpi 1986). The aeromagnetic map reveals alternating high-magnetic and low-magnetic bands, in contrast to the overall low-magnetic intensity of the Pahakurkio group (Fig. 4). These high-magnetic bands consist of intermediate volcanic or volcanogenic sedimentary rocks, and seem to alternate with low-magnetic arenitic to pelitic rocks (Fig. 8). An increasing degree of migmatisation is observed to the west and south, and no natural, upper stratigraphic limit for the group is known.

The base of the Kalixälv group is marked by an 20–30 m thick conglomerate that crops out along the river Kalixälven at Saarikoski and 13 km downstream at Tiankikoski. The conglomerate is also seen in drill core at the Kurkkionvaara Zn-Pb-Cu sulphide mineralisation (Niiniskorpi 1986). The rounded pebbles in the conglomerate consist of chert (quartz) or quartzite, and intermediate to basic volcanic rocks in a dark matrix (Fig. 8A). Ödman (1939) also noted pebbles of gabbro, syenite, granite, felsic volcanic rocks in the Tiankijoki conglomerate; thus it is indeed polymict. In the western part at Saarikoski (Fig. 3) the conglomerate grades into a dark hornblende-bearing sandstone of intermediate composition, probably consisting in part of volcanogenic material (Fig. 8B). Locally, a planar lamination with alternating laminas enriched in magnetite and light-coloured laminas is seen (Fig. 8C). The dark sandstone displays cross-bedding (Fig. 8B) similar to the structures in the underlying Pahakurkio group, which shows that both groups young westwards in this area (Padget 1970).

About 1 km above the basal conglomerate at Saarikoski, an outcrop area coincides with a positive north–south-trending magnetic anomaly band, which can be correlated with a plagioclase porphyric meta-andesite with high-magnetic susceptibility (Fig. 4). Volcanoclastic or volcanogenic sandstones,

► Figure 8. Rocks of the Kalixälv group. **A.** Polymict conglomerate at Tiankikoski, with clasts mainly of chert and mafic-intermediate rocks (7481257 / 810646) **B.** Steeply dipping, cross-bedded and amphibole-bearing meta-sandstone at Saarikoski showing way-up to the west. **C.** Photomicrograph in plane polarised light of amphibole-bearing meta-sandstone with alternating laminas enriched in magnetite. **D.** Migmatitic meta-sandstone at Tiankikoski. **E.** Photomicrograph in cross-polarised light of sillimanite-cordierite-bearing paragneiss at Tiankijoki (7480253 / 810919) **F.** Photomicrograph in plane polarised light of sillimanite-cordierite-bearing paragneiss at Tiankijoki (7480253 / 810919). **G.** Volcanoclastic, meta-andesitic tuff constitutes the host rock to the Maunuvaara Cu-Au quartz vein-hosted mineralisations (7482513 / 797469) **H.** Plagioclase porphyric meta-andesite north of Saarikoski (7487854 / 799400). Coordinates are given in SWEREF 99 TM. All photographs by Fredrik Hellström except B by Veikko Niiniskorpi.

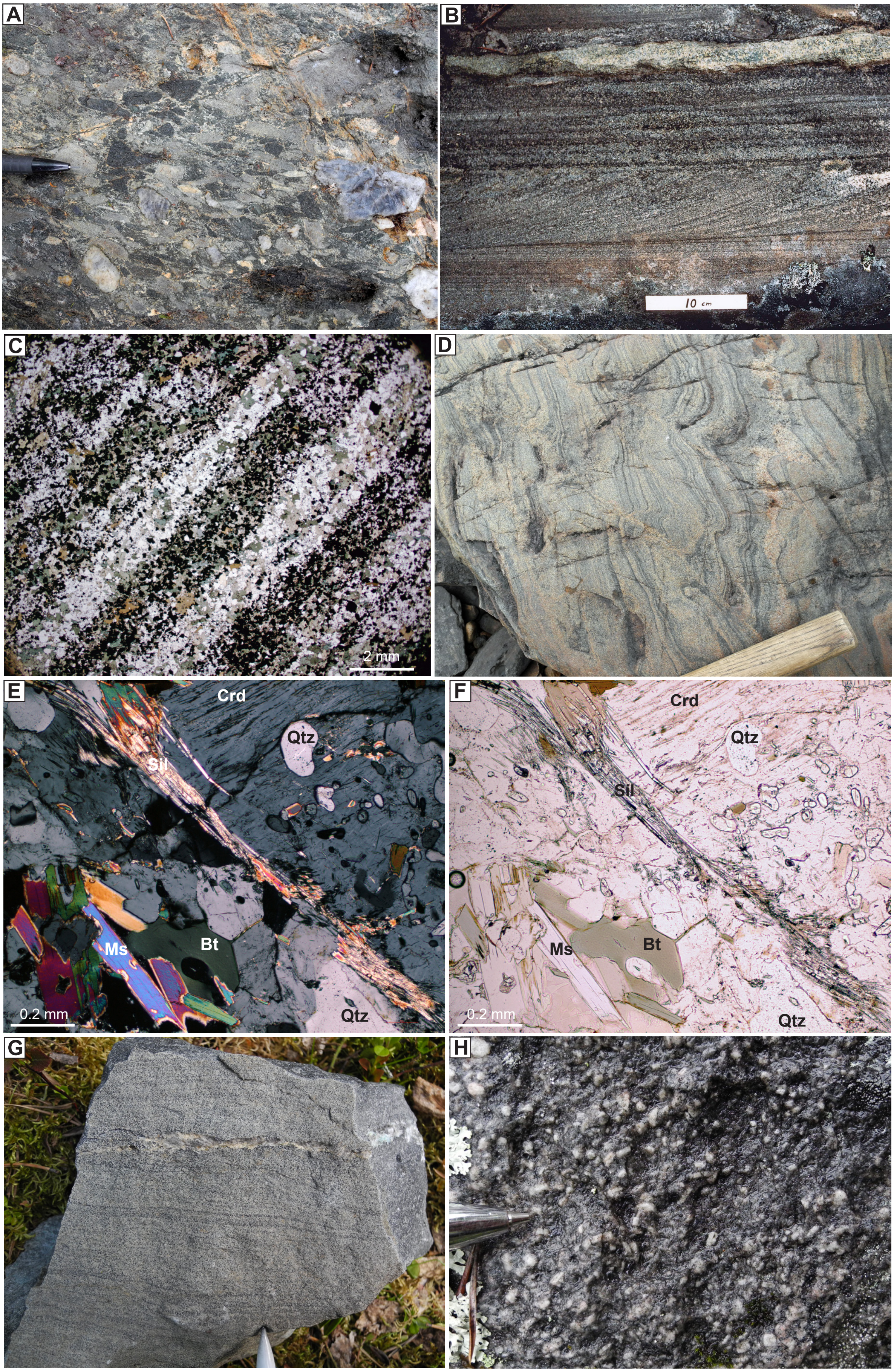
A
B
10 cm
C
2 mm
D
E
Crd
Qtz
Sil
Ms
Bt
0.2 mm
Qtz
F
Crd
Qtz
Sil
Ms
Bt
0.2 mm
Qtz
G
H

with common skarn alteration bands, and conglomeratic layers with pebbles of chert and intermediate volcanic rock occur (Niiniskorpi 1986). Modelling of magnetic data suggests that units have a steep, near vertical dip corroborating field observations of bedding (Jönberger et al. 2018).

In the south of the area (Fig. 3), sillimanite- and andalusite-bearing mica schists or migmatitic paragneisses with interlayers of quartzic sandstones are found (Fig. 8D). Niiniskorpi (1986) noted that both the Pahakurkio and the Kalixälv groups consist of similar types of metasedimentary rocks, metapelites and quartzites, which makes it difficult to distinguish between these units. Occurrences of graphite-bearing schists and carbonate rocks within the Pahakurkio group also complicate the distinction between the Pahakurkio and Veikkavaara groups.

Lithogeochemistry

Methods

Sample preparation was carried out by ALS Minerals in Piteå (Sweden) and subsequent analytical work performed at ALS Minerals lab in Vancouver (Canada). Preparation involved crushing samples and pulverising to a powder using low-chrome steel grinding mills. The lithogeochemical analysis at ALS was conducted using the whole-rock major and trace element package CCP-PKG01, a combination of different methods. Lithium metaborate fusion ICP-AES (ME-ICP06) was used for major elements. Total carbon and sulphur was analysed using a LECO analyser (ME-IR08), where the sample (0.01 to 0.1 g) is heated to approximately 1350°C in an induction furnace while passing a stream of oxygen through the sample. Total sulphur and carbon is measured by an IR detection system. Trace elements, including the full rare earth element suite, are reported from three types of sample digestion with either ICP-AES or ICP-MS analysis: lithium borate fusion for the resistive elements (ME-MS81), four-acid digestion for the base metals (ME-4ACD81), and aqua regia digestion for the volatile gold-related trace elements (ME-MS42). In addition to the new data, some old chemical analyses (SGU data & Niiniskorpi 1986) were used, in which major and trace elements were analysed by XRF, ICP-AES and ICP-MS. Geochemical diagrams were made using GCD kit software (Janoušek et al. 2006).

Metavolcanic rocks

Many metavolcanic rock samples are sodium- or potassium-altered according to the diagram by Hughes (1973, Fig. 9A), but immobile trace element, mantle-normalised spider plots show nearly identical patterns between averaged values of altered and unaltered samples within the groups (Fig. 9F). Strongly scapolite- and biotite-altered rocks within the Pahakurkio group are strongly potassium enriched, but show a trace element signature similar to volcanic rocks in the Kalixälv group. Most samples contain 52–66% SiO_2, and are thus intermediate to weakly acid in composition (Table 1, Fig. 9C). Rocks of the Sakarinpalo suite are generally more silica rich (54.0–72.6% SiO_2), than volcanic rocks in the Pahakurkio and Kalixälv groups (48.6–63.5% SiO_2,); the latter even includes a few samples of basic composition (Fig. 9C). Using the Nb/Y – Zr/TiO_2 classification plot of Pearce (1996), most samples classify as andesite, with a few samples as basalt, trachy-andesite, trachyte and rhyolite-dacite (Fig. 9B). Based on the Al – Fe_t + Ti – Mg ternary classification diagram of Jensen (1976), most samples plot in the basalt-andesite fields and a few samples in the dacite-rhyolite fields, along a low Fe-Ti, calc-alkaline trend. The TiO_2 content of the volcanic rocks in the Masugnsbyn area is relatively low, averaging 0.74% (±0.16, 1σ, n = 26, Fig. 9E) and similar to the volcanic rocks in Norrbotten classified as belonging to the "Porphyrite group" (Offerberg 1967, Martinsson & Perdahl 1995, Bergman et al. 2001). The stratigraphically higher Kiirunavaara group rocks are generally more evolved, with higher values for Ti and Zr (e.g. Bergman et al. 2001).

Volcanic rocks in the Masugnsbyn area record similar chondrite-normalised (Boynton 1984) rare earth element (REE) patterns, enriched in light REEs over heavy REEs, $(La/Yb)_N = 10.5$ ±3.3

(Fig. 9H, 1σ, n = 26). The La-Sm section has a steeper slope ($(La/Sm)_N = 3.8 \pm 0.67$ (1σ)) than the Gd-Lu section, which shows an almost flat profile $(Gd/Lu)_N = 1.6 \pm 0.38$ (1σ). Volcanic rocks from the Sakarinpalo and Pahakurkio groups generally have a weak negative Eu anomaly ($Eu/Eu^* = 0.78 \pm 0.17$ (1σ, n = 13)), in contrast to the volcanic rocks of the Kalixälv group, which have no significant Eu anomaly.

The primitive mantle-normalised (McDonough & Sun 1995) spider diagram shows enrichment in the large ion lithophile elements, with a pronounced negative Nb-Ta anomaly, but also negative anomalies in Ti and P (Fig. 9G). The patterns for the averaged values of the different groups are similar, but rocks in the Sakarinpalo suite and Pahakurkio groups show a strong negative anomaly in Sr compared with rocks in the Kalixälv group. Although very similar element patterns are seen for all rocks, the volcanic rocks from the southeastern part of the Masugnsbyn area can be grouped with the Kalixälv group, and the highly altered rocks in the Pahakurkio group with Sakarinpalo suite. The spider diagram pattern shows a typical upper continental crustal signature, except for the low amounts of Sr, which may be due to post-depositional alteration.

Metasedimentary rocks

Sediment maturity can be expressed by SiO_2 content and the SiO_2/Al_2O_3 ratio, reflecting the abundance of quartz, clay (mica) and feldspar. Herron (1988) proposed a geochemical classification diagram of terrigenous sands and shales using log (Fe_2O_3/K_2O) versus log (SiO_2/Al_2O_3). The SiO_2/Al_2O_3 ratio separates Si-rich quartz-arenites from Al-rich shales, with other sand types showing intermediate values. The Fe_2O_3t/K_2O ratio separates lithic sands (litharenites and sublitharenites) from feldspathic sands (arkoses and subarkoses). Shale is identified on the basis of a very low SiO_2/Al_2O_3 ratio. Sandstones from the Pahakurkio group are classified as arkoses to mainly subarkoses, whereas mica schists from the same group are classified as shales to wackes, except one sample that falls in the arkose field (Fig. 10A). The amphibole-bearing dark sandstone and conglomerate from the Kalixälv group also classify as wackes, except for one more quartz-rich leucocratic sandstone that classifies as arkose (Fig. 10A).

Another useful index of chemical maturity is the alkali content (Na_2O+K_2O), which corresponds to the feldspar and clay (mica) content. The K_2O/Na_2O ratio reflects the relative abundance of potassic feldspar and mica versus plagioclase, but is also affected by the compositions of the feldspars present. In a K_2O/Na_2O versus SiO_2 plot (Fig. 10B), the dark, amphibole-bearing sandstone and conglomerate samples in the Kalixälv group have lower K_2O/Na_2O ratios (0.31–0.59) and SiO_2 (58.9–61.5%, Table 2) content than the more mature, quartz-rich sandstones within the Kalixälv and Pahakurkio groups (SiO_2: 75.6–85.4 % and K_2O/Na_2O ratios: 0.90–29.1). The difference in sodium and potassium content is also seen in a triangular Na_2O–$MgO+Fe_2O_3t$–K_2O diagram (Fig. 10E). This shows that the dark Kalixälv sandstone has a more plagioclase-rich, intermediate composition, similar to that of the meta-andesitic volcanic rocks, suggesting these contain a significant proportion of volcanoclastic or volcanogenic sedimentary material. The more mafic character of the dark sandstone is also reflected in the elevated magnesium and iron content illustrated in Figure 10E or in a bivariate plot of Al_2O_3/SiO_2 versus ($MgO+Fe_2O_3t$; Fig. 10C); the latter has also been used to discriminate sandstone from different tectonic settings (Bathia 1983). The "arc-setting" of the dark Kalixälv sandstones possibly reflects their volcanogenic nature, also seen in Figure 10B. Mica schist samples also have elevated K_2O/Na_2O ratios, as well as fairly high magnesium and iron content, reflecting their biotite (muscovite)- rich nature. A discriminate function diagram for provenance signatures of sandstone-mudstone suites using major element ratios has been proposed by Roser & Korsch (1988, Fig. 10D). The dark Kalixälv group sandstone and conglomerate samples have intermediate or mafic igneous signatures, whereas the remaining samples have a felsic igneous or quartzose signature. A trace element plot using, e.g., Sc, Th and Zr (Fig. 10F) also highlights the difference between the sandstones from the Kalixälv and Pahakurkio groups, with the more mafic sandstones showing higher Sc and lower Zr content.

Table. 1. Lithochemistry of selected metavolcanic rock samples.

Sample	Unit	Method	FHM140069A	FHM140070A	FHM140071A	FHM140074A	FHM140075A	FHM150021A	FHM140065A	FHM140065B	FHM140079A	FHM140028A	FHM140084B	FHM150018A
N		ALS-code	7502412	7502355	7502300	7502253	7502154	7502060	7489838	7489838	7493028	7482513	7487854	7485723
E			803618	803715	803745	804278	804535	804478	806809	806809	804661	797469	799400	816571
Rock			Trachy-andesite	Trachyte	Trachyte	Dacite (Ab)	Andesite (Scp)	Andesite	Andesite (Scp)	Andesite (Scp)	Andesite (Scp)	Andesite (Cu)	Andesite	Andesite
Stratigraphic unit			Sakarinpalo suite	Sakarinpalo suite	Sakarinpalo suite	Sakarinpalo suite	Sakarinpalo suite	Sakarinpalo suite	Pahakurkio group	Pahakurkio group	Pahakurkio group	Kalixälv group	Kalixälv group	Kalixälv group
SiO_2	%	ME-ICP06	61.60	63.30	62.50	72.60	56.20	61.00	57.70	53.30	55.70	63.10	60.40	59.70
Al_2O_3	%	ME-ICP06	17.00	19.20	19.70	13.70	15.40	14.90	15.20	17.10	15.95	17.45	15.45	16.10
Fe_2O_3t	%	ME-ICP06	7.85	3.25	3.12	0.69	7.37	5.19	8.38	8.71	11.05	4.82	7.30	7.20
CaO	%	ME-ICP06	1.72	2.93	4.71	2.54	6.19	5.53	1.61	3.84	0.72	6.05	2.89	4.21
MgO	%	ME-ICP06	1.62	0.55	0.48	2.80	5.34	3.81	5.22	6.87	5.44	2.40	2.53	3.69
Na_2O	%	ME-ICP06	1.53	2.57	3.39	7.48	2.37	4.73	1.42	1.05	1.40	4.07	6.05	4.47
K2O	%	ME-ICP06	5.85	7.60	3.96	0.17	4.80	2.56	7.00	6.03	7.82	0.96	2.41	3.00
Cr_2O_3	%	ME-ICP06	0.01	<0.01	<0.01	0.01	0.02	0.02	0.04	0.04	0.04	0.02	0.01	0.01
TiO_2	%	ME-ICP06	0.73	0.54	0.54	0.34	0.92	0.62	0.76	0.87	0.82	0.67	0.66	0.70
MnO	%	ME-ICP06	0.11	0.10	0.08	0.04	0.19	0.13	0.07	0.08	0.04	0.08	0.06	0.12
P_2O_5	%	ME-ICP06	0.22	0.17	0.16	0.09	0.11	0.08	0.15	0.13	0.15	0.19	0.24	0.22
SrO	%	ME-ICP06	<0.01	<0.01	<0.01	<0.01	<0.01	<0.01	<0.01	<0.01	<0.01	0.04	0.02	0.06
BaO	%	ME-ICP06	0.13	0.31	0.25	<0.01	0.03	0.03	0.15	0.20	0.10	0.05	0.05	0.09
LOI	%	OA-GRA05	1.40	0.77	0.53	0.78	1.88	1.57	0.79	0.99	0.88	0.52	0.65	1.29
Total	%	TOT-ICP06	99.77	101.29	99.42	101.24	100.82	100.17	98.49	99.21	100.11	100.42	98.72	100.86
C	%	C-IR07	0.01	<0.01	<0.01	0.10	0.37	0.21	<0.01	0.05	0.01	0.02	0.09	<0.01
S	%	S-IR08	<0.01	<0.01	<0.01	<0.01	<0.01	0.02	<0.01	0.02	<0.01	0.06	0.01	0.01
Ba	ppm	ME-MS81	1150	2640	2180	13.3	250	234	1390	1745	902	449	473	987
Ce	ppm	ME-MS81	77.4	69.2	79.2	48.0	42.0	48.9	32.1	83.0	50.6	34.0	52.7	63.7
Cr	ppm	ME-MS81	80	10	10	70	150	110	270	310	300	100	70	90
Cs	ppm	ME-MS81	7.08	7.71	4.49	0.03	2.09	0.81	10.6	10.55	10.35	1.18	1.34	1.67
Dy	ppm	ME-MS81	3.03	2.34	2.94	2.6	3.31	2.53	3.16	3.51	3.72	2.69	3.5	3.41
Er	ppm	ME-MS81	1.85	1.31	1.67	1.36	1.92	1.54	2.21	1.76	2.1	1.6	2.05	1.89
Eu	ppm	ME-MS81	1.14	0.94	1.14	0.96	0.92	0.95	0.73	1.39	0.93	1.35	1.15	1.28
Ga	ppm	ME-MS81	24.6	20.4	18.1	15.1	19.6	20.2	21.2	23.6	23.4	19.5	19.1	22.6
Gd	ppm	ME-MS81	3.93	2.92	3.7	1.96	3.33	3.17	2.9	4.89	3.52	3.21	4.09	3.72
Hf	ppm	ME-MS81	4.7	7.7	7.4	5.3	4.9	5.7	3.5	3.3	3.8	3.0	4.4	4.6
Ho	ppm	ME-MS81	0.65	0.48	0.58	0.52	0.70	0.49	0.69	0.60	0.70	0.59	0.61	0.70
La	ppm	ME-MS81	36.3	34.7	41.2	21.7	22.1	24.8	13.7	44.0	26.9	15.6	26.6	36.6
Lu	ppm	ME-MS81	0.25	0.19	0.24	0.18	0.23	0.24	0.27	0.19	0.27	0.19	0.24	0.29
Nb	ppm	ME-MS81	12.2	13.4	14.3	4.8	8.0	5.8	9.2	9.9	9.4	5.9	9.6	10.8
Nd	ppm	ME-MS81	31.7	26.1	30.9	20.4	18.5	22.0	13.1	35.4	21.6	19.3	24.6	30.1
Pr	ppm	ME-MS81	8.55	7.49	8.86	5.45	4.75	5.15	3.56	9.58	5.75	4.84	6.11	7.62

Table. 1 continues

Sample	Unit	Method	FHM140069A	FHM140070A	FHM140071A	FHM140074A	FHM140075A	FHM150021A	FHM140065A	FHM140065B	FHM140079A	FHM140028A	FHM140084B	FHM150018A
N		ALS-code	7502412	7502355	7502300	7502253	7502154	7502060	7489838	7489838	7493028	7482513	7487854	7485723
E			803618	803715	803745	804278	804535	804478	806809	806809	804661	797469	799400	816571
Rock			Trachy-andesite	Trachyte	Trachyte	Dacite (Ab)	Andesite (Scp)	Andesite	Andesite (Scp)	Andesite (Scp)	Andesite (Scp)	Andesite (Cu)	Andesite	Andesite
Stratigra-phic unit			Sakarinpalo suite	Sakarinpalo suite	Sakarinpalo suite	Sakarinpalo suite	Sakarinpalo suite	Sakarinpalo suite	Pahakurkio group	Pahakurkio group	Pahakurkio group	Kalixälv group	Kalixälv group	Kalixälv group
Rb	ppm	ME-MS81	231	305	198	1.3	152.5	69.5	201	233	200	25.5	79.8	109
Sm	ppm	ME-MS81	5.50	4.28	4.86	3.84	3.54	3.48	2.84	6.27	4.10	3.72	4.38	6.24
Sn	ppm	ME-MS81	2	<1	<1	<1	1	1	1	2	2	1	2	4
Sr	ppm	ME-MS81	35.4	154	180	16	45.1	56.8	90.6	115	33.3	580	140.5	485
Ta	ppm	ME-MS81	0.7	0.8	0.8	0.3	0.9	0.6	0.7	0.7	1	0.3	0.7	0.7
Tb	ppm	ME-MS81	0.61	0.42	0.46	0.46	0.54	0.38	0.47	0.60	0.56	0.50	0.53	0.56
Th	ppm	ME-MS81	12.50	12.75	13.40	7.34	10.50	9.00	8.28	9.14	9.11	4.94	9.93	10.75
Tm	ppm	ME-MS81	0.24	0.20	0.25	0.17	0.27	0.24	0.29	0.25	0.29	0.18	0.29	0.29
U	ppm	ME-MS81	1.50	2.50	3.89	0.92	2.34	2.25	2.31	2.30	2.06	4.23	2.98	3.60
V	ppm	ME-MS81	81	40	29	14	129	86	145	183	171	134	150	165
W	ppm	ME-MS81	4	1	3	<1	<1	1	<1	<1	1	2	2	1
Y	ppm	ME-MS81	18.2	13.6	15.5	13.9	17.5	14.9	17.9	18.2	19.4	14.8	17.1	21.5
Yb	ppm	ME-MS81	1.99	1.51	1.99	1.28	1.88	1.59	2.14	1.96	2.08	1.58	1.77	2.07
Zr	ppm	ME-MS81	175	299	307	206	169	210	125	116	124	129	158	195
As	ppm	ME-MS42	1	3.1	3.5	<0.1	1	1.1	0.4	0.7	0.2	1.1	1.2	2
Bi	ppm	ME-MS42	<0.01	0.01	0.01	<0.01	0.04	<0.01	0.02	0.06	0.05	4.04	0.01	0.06
Hg	ppm	ME-MS42	0.007	<0.005	<0.005	<0.005	<0.005	0.006	<0.005	<0.005	<0.005	<0.005	0.005	<0.005
Sb	ppm	ME-MS42	0.06	0.09	0.11	0.08	0.28	0.29	0.14	0.11	0.45	0.17	0.2	0.31
Se	ppm	ME-MS42	0.4	0.2	0.2	0.3	0.3	<0.2	0.5	0.6	0.3	1.5	0.3	0.3
Te	ppm	ME-MS42	<0.01	<0.01	<0.01	0.03	0.01	<0.01	0.01	0.01	0.01	0.11	<0.01	0.02
Ag	ppm	ME-4ACD81	<0.5	<0.5	<0.5	<0.5	<0.5	<0.5	<0.5	<0.5	<0.5	1.9	<0.5	<0.5
Cd	ppm	ME-4ACD81	<0.5	<0.5	<0.5	<0.5	<0.5	<0.5	<0.5	<0.5	<0.5	0.8	<0.5	<0.5
Co	ppm	ME-4ACD81	9	4	4	3	14	9	30	40	34	13	14	19
Cu	ppm	ME-4ACD81	1	<1	1	1	<1	2	2	1	82	3600	9	17
Li	ppm	ME-4ACD81	40	40	30	<10	10	<10	70	70	90	20	10	10
Mo	ppm	ME-4ACD81	1	<1	<1	<1	<1	<1	<1	<1	<1	<1	<1	<1
Ni	ppm	ME-4ACD81	16	2	2	11	45	31	148	167	152	16	20	19
Pb	ppm	ME-4ACD81	<2	<2	<2	<2	<2	<2	<2	<2	2	3	3	3
Sc	ppm	ME-4ACD81	16	4	5	4	15	10	21	27	23	14	16	17
Zn	ppm	ME-4ACD81	4	6	6	4	16	9	30	37	120	31	21	117
Au	ppm	PGM-ICP23	<0.001	<0.001	<0.001	<0.001	<0.001	<0.001	<0.001	<0.001	<0.001	0.023	<0.001	<0.001
Cl	ppm	Cl-IC881	<50	<50	<50	<50	6090	na	880	2050	530	140	340	na

Lithogeochemical analysis were conducted at ALS Minerals in 2014 & 2015 using analytical packages referred to as CCP-PKG01, PGM-ICP23, Cl-IC881.

ALS method code refers to analytical method used for each element and is described in ALS methodology factsheets at www.alsglobal.com; see also the main text.

All rocks are metamorphic, with prefix meta- to be added to the rock names. Ab = albite altered, Scp = Scapolite altered, Cu = Cu-sulphide mineralised. Am = Amphibole bearing

Table. 2. Lithochemistry of meta-sandstone samples.

Sample	Unit	Method code	FHM140080A	FHM140078A	FHM140090A	FHM140087A	FHM140088A	FHM140088B
N			7492866	7493033	7486133	7487718	7487141	7487141
E			804620	804679	803332	799248	800148	800148
Rock			Sandstone	Sandstone	Sandstone	Sandstone	Sandstone	Sandstone
Stratigraphic unit			Pahakurkio group	Pahakurkio group	Pahakurkio group	Kalixälv group	Kalixälv group	Kalixälv group
SiO_2	%	ME-ICP06	85.40	85.90	77.70	75.90	61.50	63.70
Al_2O_3	%	ME-ICP06	6.56	5.66	11.35	8.13	15.55	15.35
Fe_2O_3t	%	ME-ICP06	2.23	3.65	2.24	5.09	7.63	5.88
CaO	%	ME-ICP06	0.08	0.07	0.86	3.52	3.76	5.44
MgO	%	ME-ICP06	1.30	0.67	0.90	1.39	3.30	2.08
Na_2O	%	ME-ICP06	0.08	1.22	3.46	1.47	4.54	4.54
K_2O	%	ME-ICP06	2.33	2.65	3.12	2.10	2.68	1.52
Cr_2O_3	%	ME-ICP06	0.01	0.03	0.01	0.01	0.01	0.01
TiO_2	%	ME-ICP06	0.28	0.59	0.39	0.46	0.65	0.63
MnO	%	ME-ICP06	0.02	0.01	0.03	0.16	0.08	0.09
P_2O_5	%	ME-ICP06	0.05	0.04	0.13	0.13	0.20	0.18
SrO	%	ME-ICP06	<0.01	<0.01	0.02	0.01	0.05	0.06
BaO	%	ME-ICP06	0.04	0.10	0.09	0.03	0.08	0.09
LOI	%	OA-GRA05	1.10	0.41	0.36	1.50	0.62	1.14
Total	%	TOT-ICP06	99.48	101.00	100.66	99.90	100.65	100.71
C	%	C-IR07	<0.01	<0.01	0.04	0.31	0.01	0.12
S	%	S-IR08	0.01	0.01	<0.01	0.02	0.01	<0.01
Ba	ppm	ME-MS81	434	919	825	234	662	755
Ce	ppm	ME-MS81	11.8	30.4	70.4	29.0	45.9	46.4
Cr	ppm	ME-MS81	80	210	70	90	80	100
Cs	ppm	ME-MS81	2.43	0.77	1.96	1.86	6.18	0.37
Dy	ppm	ME-MS81	1.95	2.54	3.88	2.37	2.41	2.83
Er	ppm	ME-MS81	1.48	1.33	2.23	1.34	1.45	1.72
Eu	ppm	ME-MS81	0.36	0.74	1.18	0.64	0.95	1.15
Ga	ppm	ME-MS81	8.1	6.6	11.8	9.2	16.7	16.1
Gd	ppm	ME-MS81	1.44	2.65	4.87	2.55	3.25	3.57
Hf	ppm	ME-MS81	2.7	4.5	7.8	3.2	2.4	3.7
Ho	ppm	ME-MS81	0.47	0.46	0.74	0.52	0.49	0.55
La	ppm	ME-MS81	4.3	13.3	35.3	13.7	23.3	23.3
Lu	ppm	ME-MS81	0.19	0.20	0.30	0.19	0.20	0.23
Nb	ppm	ME-MS81	4.6	4.4	6.1	4.0	5.6	5.0
Nd	ppm	ME-MS81	4.7	15.8	32.3	14.0	21.8	23.5
Pr	ppm	ME-MS81	1.32	3.75	8.33	3.45	5.45	5.56
Rb	ppm	ME-MS81	80.7	47.6	85	75.1	125	26.1
Sm	ppm	ME-MS81	1.18	3.27	5.89	2.81	3.94	4.56
Sn	ppm	ME-MS81	2	1	1	1	1	4
Sr	ppm	ME-MS81	7.5	14.4	136.5	49.1	406	524
Ta	ppm	ME-MS81	0.4	0.4	0.6	0.3	0.4	0.4
Tb	ppm	ME-MS81	0.25	0.32	0.60	0.43	0.45	0.50
Th	ppm	ME-MS81	6.01	3.71	9.55	4.92	4.30	4.59
Tm	ppm	ME-MS81	0.19	0.18	0.29	0.19	0.19	0.26
U	ppm	ME-MS81	0.76	1.28	1.93	1.47	1.08	1.64
V	ppm	ME-MS81	65	100	45	109	125	117
W	ppm	ME-MS81	2	2	2	4	2	2
Y	ppm	ME-MS81	12.9	11.4	21.2	12.6	14	15.9
Yb	ppm	ME-MS81	1.48	1.19	2.17	1.35	1.4	1.62
Zr	ppm	ME-MS81	98	169	294	123	94	130
As	ppm	ME-MS42	0.4	0.2	0.1	0.9	0.6	0.9
Bi	ppm	ME-MS42	0.03	0.02	0.06	0.04	0.01	0.05
Hg	ppm	ME-MS42	<0.005	<0.005	0.005	<0.005	<0.005	<0.005
Sb	ppm	ME-MS42	0.05	0.07	<0.05	0.25	0.05	0.17
Se	ppm	ME-MS42	<0.2	<0.2	0.3	0.2	0.2	0.3
Te	ppm	ME-MS42	<0.01	<0.01	<0.01	0.01	<0.01	<0.01
Ag	ppm	ME-4ACD81	<0.5	<0.5	<0.5	<0.5	<0.5	<0.5

Table. 2 continues

Sample	Unit	Method code	FHM140080A	FHM140078A	FHM140090A	FHM140087A	FHM140088A	FHM140088B
N			**7492866**	**7493033**	**7486133**	**7487718**	**7487141**	**7487141**
E			**804620**	**804679**	**803332**	**799248**	**800148**	**800148**
Rock			**Sandstone**	**Sandstone**	**Sandstone**	**Sandstone**	**Sandstone**	**Sandstone**
Stratigraphic unit			**Pahakurkio group**	**Pahakurkio group**	**Pahakurkio group**	**Kalixälv group**	**Kalixälv group**	**Kalixälv group**
Cd	ppm	ME-4ACD81	<0.5	<0.5	<0.5	<0.5	<0.5	<0.5
Co	ppm	ME-4ACD81	8	14	6	10	19	21
Cu	ppm	ME-4ACD81	2	5	<1	12	4	21
Li	ppm	ME-4ACD81	20	10	20	20	30	10
Mo	ppm	ME-4ACD81	<1	1	<1	<1	<1	<1
Ni	ppm	ME-4ACD81	32	36	18	23	28	23
Pb	ppm	ME-4ACD81	<2	<2	4	<2	2	<2
Sc	ppm	ME-4ACD81	5	4	7	10	14	16
Zn	ppm	ME-4ACD81	15	9	31	16	36	35
Au	ppm	PGM-ICP23	<0.001	<0.001	<0.001	0.001	<0.001	<0.001
Cl	ppm	Cl-IC881	110	160	50	1310	690	940

Lithogeochemical analysis were conducted at ALS Minerals in 2014 & 2015 using analytical packages referred to as CCP-PKG01, PGM-ICP23, Cl-IC881.

ALS method code refers to analytical method used for each element and is described in ALS methodology factsheets at www.alsglobal.com, see also the main text.

All rocks are metamorphic, with prefix meta- to be added to the rock names.

The metasedimentary rocks record similar chondrite-normalised rare earth element (REE) patterns, enriched in light REEs over heavy REEs (Fig. 11A), with averaged values very similar to mean values for volcanic rocks in the Masugnsbyn area (Fig. 11C). A primitive mantle-normalised spider diagram shows a typical upper continental crustal signature, except for the low amounts of Sr, which are seen in both sedimentary and volcanic rocks of the Pahakurkio group (Fig. 11B, D). The normalised element pattern is characterised by enrichment in the large ion lithophile elements with a pronounced negative Nb-Ta anomaly, but also negative anomalies in Ti and P, in addition to the negative Sr anomaly in the Pahakurkio group rocks. In contrast, basalts of the Veikkavaara greenstone group show a flat REE profile, and an enriched MORB trace element signature (Fig. 11E, Lynch et al. 2018b). However, graphite schist and skarn-banded chert in the Veikkavaara group show an LREE-enriched pattern and a negative Nb-Ta anomaly, suggesting an upper continental crustal source for these sediments (Fig. 11E–F).

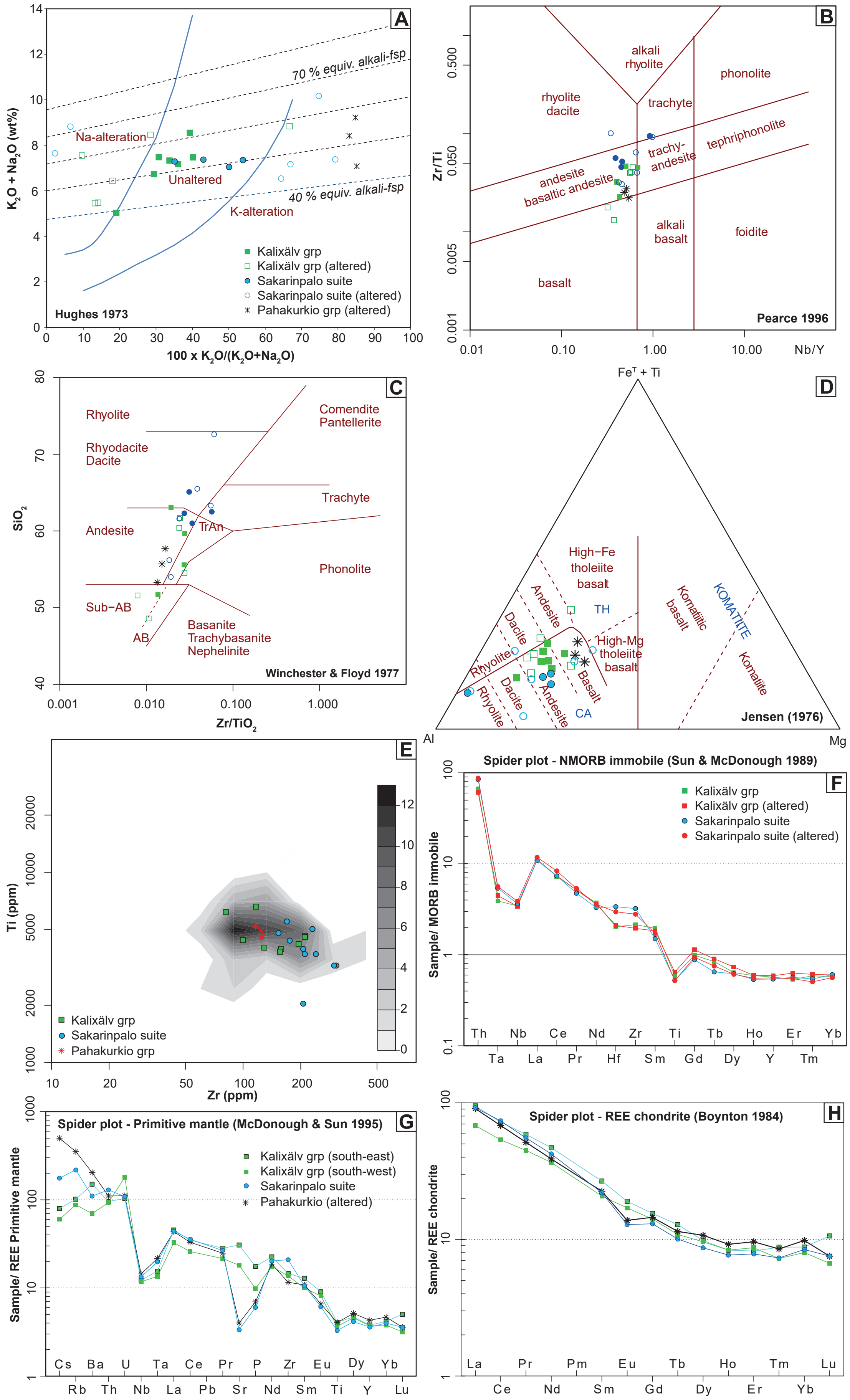
A
Hughes 1973
Na-alteration
Unaltered
K-alteration
70 % equiv. alkali-fsp
40 % equiv. alkali-fsp
Kalixälv grp
Kalixälv grp (altered)
Sakarinpalo suite
Sakarinpalo suite (altered)
Pahakurkio grp (altered)
B
Pearce 1996
alkali rhyolite
rhyolite dacite
trachyte
phonolite
trachy-andesite
tephriphonolite
andesite basaltic andesite
alkali basalt
foidite
basalt
C
Winchester & Floyd 1977
Rhyolite
Rhyodacite Dacite
Comendite Pantellerite
Trachyte
Andesite
TrAn
Phonolite
Sub-AB
AB
Basanite Trachybasanite Nephelinite
D
Jensen (1976)
High-Fe tholeiite basalt
TH
High-Mg tholeiite basalt
CA
Komatiitic basalt
KOMATIITE
Komatiite
E
Kalixälv grp
Sakarinpalo suite
Pahakurkio grp
F
Spider plot - NMORB immobile (Sun & McDonough 1989)
Kalixälv grp
Kalixälv grp (altered)
Sakarinpalo suite
Sakarinpalo suite (altered)
G
Spider plot - Primitive mantle (McDonough & Sun 1995)
Kalixälv grp (south-east)
Kalixälv grp (south-west)
Sakarinpalo suite
Pahakurkio (altered)
H
Spider plot - REE chondrite (Boynton 1984)

◄ Figure 9. Geochemistry of metavolcanic rocks. **A.** Hughes igneous spectrum. **B.** Nb/Y – Zr/Ti classification diagram (Pearce 1996, based on Winchester and Floyd 1977). **C.** Zr/TiO_2 – SiO_2 classification diagram (Winchester & Floyd 1977). **D.** (Fe^T + Ti) – Al – Mg classification diagram (Jensen 1976). **E.** Zr – Ti diagram. Data from metavolcanic rocks classified as "Porphyrite group" in the Norrbotten ore province are shown as grey, contoured background (n = 67, SGU database). **F.** Spider plot with data normalised to normal mid-ocean ridge basalt (N-MORB, Sun & McDonough 1989), comparing averaged data from unaltered versus altered rocks of the Kalixälv group and the Sakarinpalo suite, respectively. **G.** Spider plot with mean data of groups normalised to primitive mantle (McDonough & Sun 1995). **H.** REE spider plot with averaged data of groups normalised to chondrite (Boynton 1984).

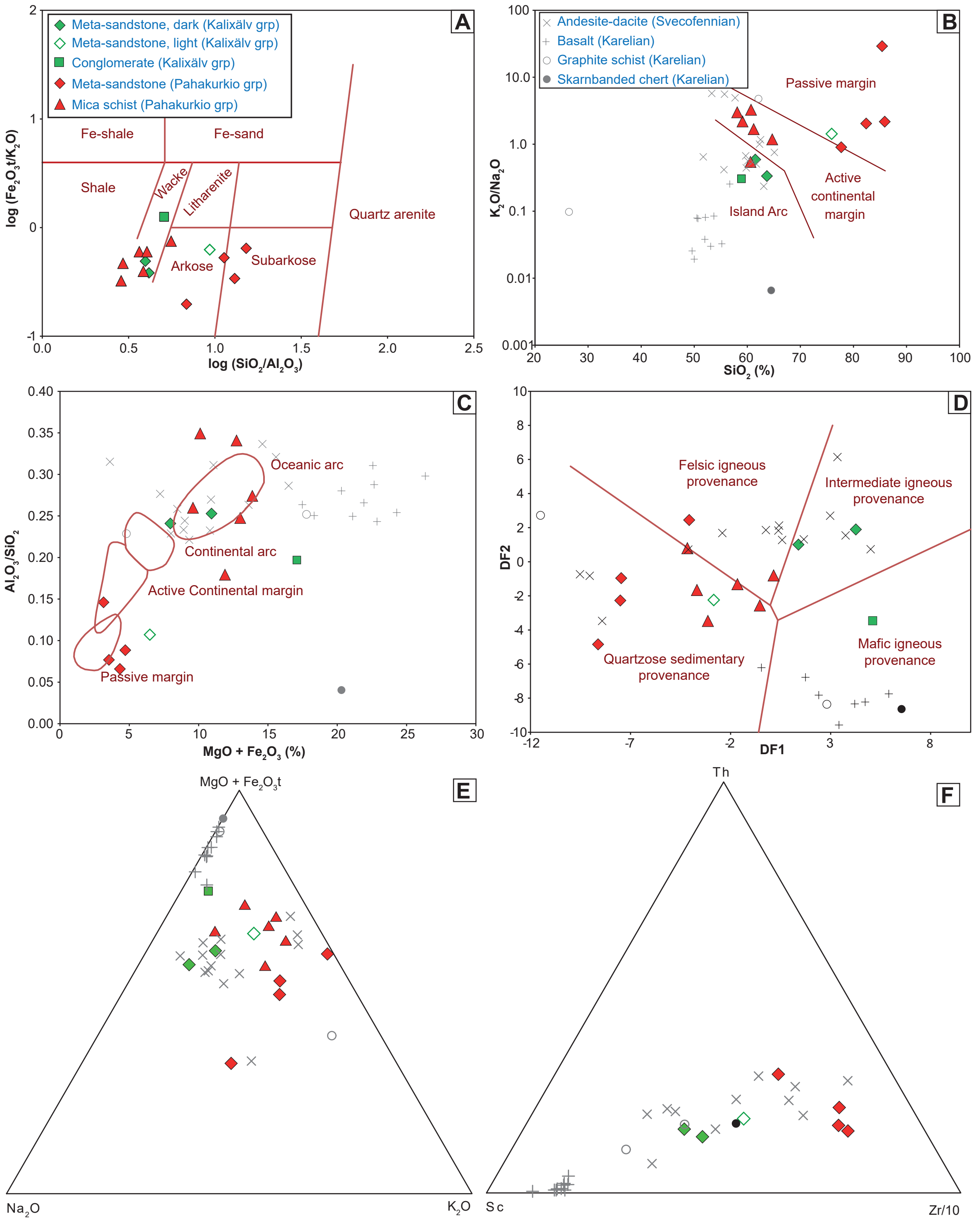

Figure 10. Geochemistry of sedimentary rocks in the Masugnsbyn area. **A.** Log(Fe_2O_3/K_2O) – log(SiO_2/Al_2O_3) classification diagram of terrigenous sandstones and shales (Herron 1988). **B.** Log(K_2O/Na_2O) – SiO_2 discrimination diagram for sandstone-mudstone suites (Roser & Korsch 1986). **C.** Al_2O_3/SiO_2 – MgO + Fe_2O_3t discrimination diagram for sandstones (Bathia 1983). **D.** DF2 – DF1 discrimination function diagram for sandstone-mudstone suites. DF1 = -1.773*TiO2+0.607*Al_2O_3+0.76*Fe_2O_3t- 1.5*MgO+0.616*CaO +0.509* Na_2O-1.224*K_2O-9.09). DF2 = 0.445*TiO_2+0.07*Al_2O_3-0.25*Fe_2O_3- 1.142*MgO+0.438*CaO +1.475*Na_2O+ 1.426*K_2O-6.861 (Roser & Korsch 1988). **E.** Na_2O – MgO+Fe_2O_3t – K_2O. F. Sc – La – Zr/10.

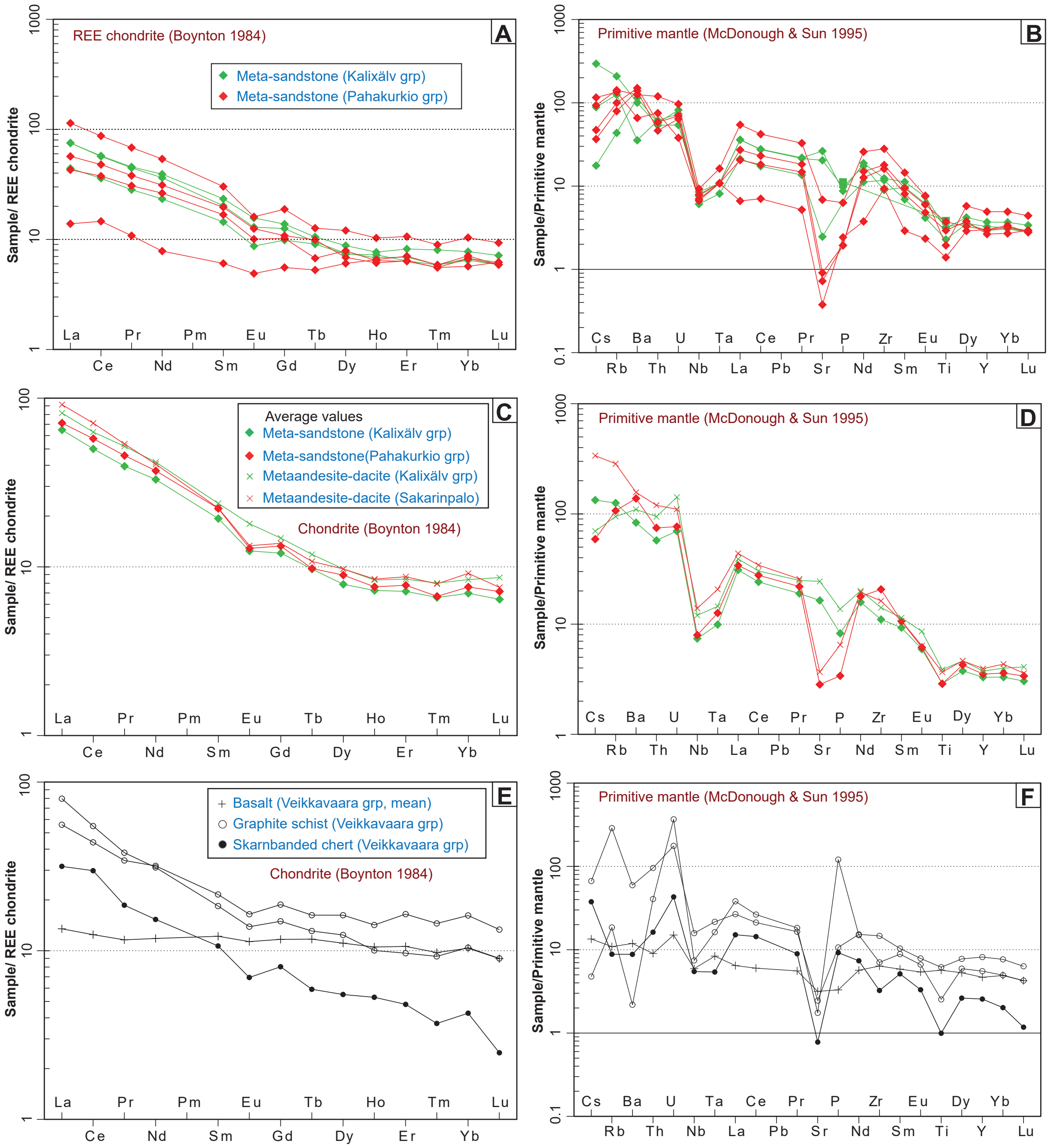

Figure 11. Trace element spider diagrams showing data on sedimentary rocks in the Masugnsbyn area. **A–B.** Spider diagram with data from meta-sandstones in the Pahakurkio and Kalixälv groups normalised to chondrite (A) and primitive mantle (B), respectively. **C–D.** Spider diagrams with averaged data from meta-sandstones in the Pahakurkio and Kalixälv groups normalised to chondrite (C) and primitive mantle (D), respectively. Averaged values of Svecofennian volcanic rocks from Masugnsbyn are shown for comparison. **E–F.** Spider diagrams with data on the Veikkavaara greenstone group rocks normalised to chondrite (E) and primitive mantle (F), respectively, for comparison of trace element patterns with the Svecofennian rocks above.

Geochronology

Methods

SIMS analysis

Zircons were obtained from a density separate of a crushed rock sample using a Wilfley water table. Magnetic minerals were removed with a hand magnet. Handpicked crystals were mounted in transparent epoxy resin together with chips of the reference zircon 91500. The zircon mounts were polished and, after gold coating, examined by Back Scattered Electron (BSE) and Cathodoluminescence (CL) imaging using electron microscopy at EBC, Uppsala University and at the Swedish Museum of Natural History in Stockholm. High-spatial resolution secondary ion mass spectrometer (SIMS) analysis was carried out in November and December 2014 using a Cameca IMS 1280 at the Nordsim facility at the Swedish Museum of Natural History in Stockholm. Detailed descriptions of the analytical procedures are given in Whitehouse et al. (1997, 1999), and Whitehouse & Kamber (2005). An approximately 6 nA O^{2-} primary ion beam was used, yielding spot sizes of approximately 15 μm. Pb/U ratios, elemental concentrations and Th/U ratios were calibrated relative to the Geostandards zircon 91500 reference, which has an age of approximately 1065 Ma (Wiedenbeck et al. 1995, 2004). Common Pb-corrected isotope values were calculated using modern common Pb composition (Stacey & Kramers 1975), and measured ^{204}Pb where the ^{204}Pb count exceeded the detection limit. Decay constants follow the recommendations of Steiger & Jäger (1977). Diagrams and age calculations of isotopic data were made using Isoplot 4.15 software (Ludwig 2012). CL imaging using electron microscopy was also carried out after the SIMS analysis at the Swedish Museum of Natural History in Stockholm to confirm the location of analysed spots.

Laser ablation ICP-MS analysis

Zircon U-Pb geochronology was carried out on mineral separates embedded in epoxy mounts by laser ablation inductively coupled plasma mass spectrometry (LA-ICP-MS) at the Geological Survey of Denmark and Greenland (GEUS). An NWR213 frequency-quintupled solid state Nd:YAG laser system from New Wave Research/ESI mounted with a TV2 ablation cell was coupled to an ELEMENT 2 double-focusing single-collector magnetic sector-field ICPMS from Thermo-Fisher Scientific. The mass spectrometer was equipped with a Fassel-type quartz torch shielded with a grounded Pt electrode and a quartz bonnet. To ensure stable laser output energy, a laser warm-up time of ~15 minutes was used before operation, providing stable laser power and flat ablation craters from a "resonator-flat" laser beam. The mass spectrometer was run for at least one hour before analyses to stabilise the background signal. Before loading, samples and standards were carefully cleaned with ethanol to remove surface contamination. After insertion, the ablation cell was flushed with helium gas to minimise gas blank level. The ablated material was swept by the helium carrier gas and mixed with argon (sample) gas of the spectrometer approximately 0.5 m before entering the plasma in the mass spectrometer. Immediately before the analyses, the ICP-MS was optimised for dry plasma conditions by continuous linear ablation of the GJ-1 zircon standard. The signal-to-noise ratios for the heavy mass range of interest (i.e. from ^{202}Hg to ^{238}U), emphasising ^{238}U and ^{206}Pb, were maximised, while opting for low element-oxide production levels by minimising the $^{254}UO_2/^{238}U$ ratio. To minimise instrumental drift, a standard-sample-standard analysis protocol was followed, bracketing eight sample analyses by six measurements of the Geostandards zircon 91500 reference. The GJ-1 (Jackson et al. 2004) and Plesovice (Slama et al. 2008) reference zircons were used for quality control of the standard analyses, and yield average age accuracies and precisions of < 3%. Data were acquired from single spot analysis of 25 μm, using nominal laser fluence of ~10 J/cm^2 and a pulse rate of 10 Hz. Total acquisition time for a single analysis was maximum 1.5 minutes, including 30-second gas blank measurement followed by laser ablation for 30 seconds and washout for 20 seconds. Factory-supplied software was used to acquire transient data, obtained through automated running mode of pre-set analytical locations. Data reduction and calculation of ratios and ages were performed offline using Iolite software (Hellstrom et al. 2008, Paton et al. 2011), using the Iolite-integral VizualAge DRS data reduction scheme (Petrus & Kamber 2012). This DRS includes a correction routine for down-hole isotopic fractionation (Paton et al. 2010), and provides procedures for data requiring correction for common Pb.

Sample description and analytical results

Geochronology sample data are summarised in Table 3.

Feldspar porphyric, intermediate metavolcanic rock (FHM140069), Sakarinpalo suite

The rock sampled for dating is a sparsely feldspar porphyric, intermediate metavolcanic rock with 1–2 mm feldspar phenocrysts in a fine-grained matrix (Fig. 3, 12A). The thin section shows a recrystallised, granular, polygonal texture, in which phenocrysts are partly recrystallised to aggregates (Fig. 12C). Parallel-oriented, dispersed grains of biotite define a foliation. The groundmass is dominated by K-feldspar, plagioclase, quartz and biotite, with subordinate amounts of opaques and muscovite, the latter also occurring as veins. There are trace amounts of apatite, zircon and tourmaline. The heavy mineral separate is rich in transparent zircon, mostly with subhedral, prismatic crystal shapes. CL imaging shows a well-developed oscillatory zonation, in some grains apparently forming as different generations (Fig. 12E). However, analyses reveal no age difference between different textural domains. A total of 13 zircon analyses were performed. These contain 81–207 ppm uranium and have rather uniform Th/U ratios of 0.42–0.85 (Table 4). All analyses are concordant and record a concordia age of 1 890 ±5 Ma (Fig. 12G, 2σ, n = 13, MSWD of concordance. + equivalence = 1.2, probability of concordance + equivalence = 0.22).

The $^{207}Pb/^{206}Pb$-weighted mean age is 1 887 ±6 Ma (2σ, MSWD = 1.4, probability = 0.18, n = 13), i.e. within error the same age as the concordia age. The Concordia age is chosen as the best age estimate, interpreted to date igneous crystallisation of the metavolcanic rocks of the Sakarinpalo suite at approximately 1.89 Ga.

Feldspar porphyritic meta-andesite (FHM140084B), Kalixälv group

A feldspar porphyritic meta-andesite was sampled approximately 1 km up-section to the basal conglomerate in the Kalixälv group. The meta-andesite has a high magnetic susceptibility and the outcrop spatially coincides with a north–south-trending, positive magnetic anomaly that continues southwards beyond the river. The rock is grey and contains 1–2 mm plagioclase phenocrysts in a fine-grained matrix of plagioclase, microcline and quartz, with subordinate amounts of magnetite, biotite, green pleochroic hornblende and titanite with traces of zircon (Fig. 12B, D). The plagioclase is partly sericite-altered and contains calcite and very fine opaques.

Table 3. Summary of geochronology sample data.

Sample	Lab-id	Rock type	Stratigraphic unit	N	S	Locality	U-Pb dating	Nd
FHM140069A	n5164	Andesite	Sakarinpalo suite	7502412	803618	Pahtajänkkä	Nordsim, NRM	x
FHM140084B	n5174	Andesite	Kalixälv group	7487854	799400	Sarikoski	Nordsim, NRM	x
FHM140078A		Sandstone (sub-arkose)	Pahakurkio group	7493033	804679	Hietajoki	LA ICP-MS; GEUS	x
FHM140088B		Sandstone (intermediate)	Kalixälv group	7487141	800148	Sarikoski	LA ICP-MS; GEUS	x
RR96128	n1383	Sandstone (sub-arkose)	Pahakurkio group	7486200	803000	Pahakurkio	Nordsim, NRM	

Nd = Sm-Nd isotopic analyses performed at GTK lab, Espoo, Finland.

All rocks are metamorphic with prefix meta- to be added to rock name.

► Figure 12. Geochronology of metavolcanic rocks from the Sakarinpalo suite and the Kalixälv groups. **A.** Dated sample of feldspar porphyric meta-andesite from the Sakarinpalo suite northeast of Masugnsbyn (FHM140069A; (7502412 / 803618). **B.** Dated sample of feldspar porphyric meta-andesite from the Kalixälv group (FHM140084B; 7487854 / 799400). **C–D.** Thin section cross-polarised light views of dated volcanic samples. **E–F.** Cathodoluminescence (CL) images of dated zircons from sample FHM140069A and Back-scattered electron (BSE) images of analysed zircon from FHM140084B. Ellipses mark the locations of analyses. Numbers refer to analytical spot number in Table 4. **G–H.** Tera Wasserburg diagram showing U-Pb SIMS data of zircon. Error ellipse of calculated weighted mean age is shown in red. Coordinates are given in SWEREF 99TM.

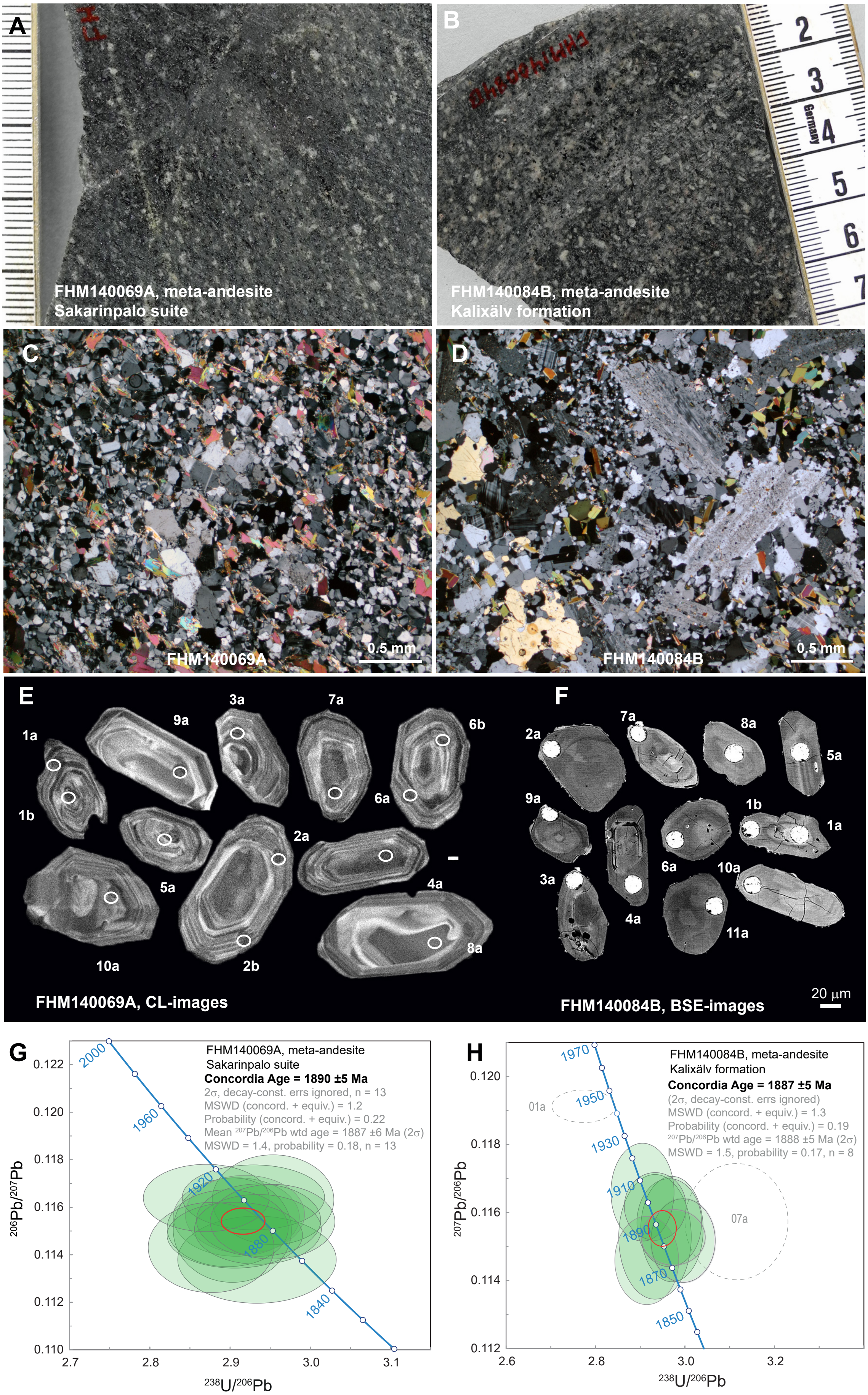
A
FHM140069A, meta-andesite
Sakarinpalo suite
B
FHM140084B, meta-andesite
Kalixälv formation
C
FHM140069A
0.5 mm
D
FHM140084B
0.5 mm
E
FHM140069A, CL-images
F
FHM140084B, BSE-images
20 µm
G
FHM140069A, meta-andesite
Sakarinpalo suite
Concordia Age = 1890 ±5 Ma
2σ, decay-const. errs ignored, n = 13
MSWD (concord. + equiv.) = 1.2
Probability (concord. + equiv.) = 0.22
Mean 207Pb/206Pb wtd age = 1887 ±6 Ma (2σ)
MSWD = 1.4, probability = 0.18, n = 13
206Pb/207Pb
238U/206Pb
H
FHM140084B, meta-andesite
Kalixälv formation
Concordia Age = 1887 ±5 Ma
(2σ, decay-const. errs ignored)
MSWD (concord. + equiv.) = 1.3
Probability (concord. + equiv.) = 0.19
207Pb/206Pb wtd age = 1888 ±5 Ma (2σ)
MSWD = 1.5, probability = 0.17, n = 8
01a
07a
207Pb/206Pb
238U/206Pb

Table 4. SIMS U-Pb-Th zircon data meta-andesite samples (FHM140069A, laboratory id n5164; FHM140084B, laboratory id n5174).

Sample/ spot #	U ppm	Th ppm	Pb ppm	Th/U calc *1	$^{207}Pb/^{235}U$	±σ %	$^{208}Pb/^{232}Th$	±σ %	$^{238}U/^{206}Pb$	±σ %	$^{207}Pb/^{206}Pb$	±σ %	ρ *2	Disc. % conv. *3	Disc. % 2σ lim. *4	$^{207}Pb/^{206}Pb$	±σ Ma	$^{206}Pb/^{238}U$	±σ Ma	$^{206}Pb/^{204}Pb$ measured	f_{206}% *5
FHM140069A, meta-andesite, Sakarinpalo suite																					
n5164_01a	163	73	69	0.45	5.431	1.24	0.0988	2.18	2.954	1.05	0.1163	0.66	0.84	-1.3		1901	12	1880	17	100393	{0.02}
n5164_01b	164	127	75	0.80	5.424	1.20	0.1014	3.34	2.935	1.08	0.1155	0.54	0.89	0.2		1887	10	1890	18	38105	{0.05}
n5164_10a	137	59	59	0.45	5.592	1.22	0.1048	2.22	2.870	1.12	0.1164	0.50	0.91	1.5		1902	9	1927	19	>1e6	{0.00}
n5164_2a	111	50	48	0.47	5.465	1.30	0.1008	2.32	2.903	1.04	0.1151	0.78	0.80	1.7		1881	14	1908	17	313475	{0.01}
n5164_2b	123	53	52	0.44	5.389	1.21	0.1002	2.37	2.953	1.07	0.1154	0.56	0.89	-0.4		1886	10	1880	18	95390	{0.02}
n5164_3a	82	43	36	0.55	5.480	1.30	0.1010	2.32	2.876	1.11	0.1143	0.68	0.85	3.4		1869	12	1923	19	29637	{0.06}
n5164_4a	207	168	96	0.85	5.481	1.33	0.1031	2.39	2.929	1.24	0.1164	0.48	0.93	-0.5		1902	9	1893	20	76620	{0.02}
n5164_5a	108	70	48	0.67	5.467	1.19	0.1018	2.29	2.918	1.04	0.1157	0.58	0.87	0.5		1891	10	1899	17	769102	{0.00}
n5164_6a	131	58	56	0.45	5.407	1.22	0.0999	2.28	2.935	1.10	0.1151	0.52	0.90	0.6		1881	9	1890	18	>1e6	{0.00}
n5164_6b	133	55	57	0.42	5.479	1.21	0.0991	2.37	2.897	1.06	0.1151	0.57	0.88	1.8		1882	10	1912	18	110242	{0.02}
n5164_7a	148	92	66	0.64	5.449	1.28	0.1007	2.47	2.906	1.19	0.1148	0.49	0.92	1.8		1877	9	1907	20	>1e6	{0.00}
n5164_8a	104	46	44	0.44	5.482	1.25	0.0979	2.32	2.908	1.10	0.1156	0.58	0.88	1.0		1889	10	1905	18	41467	{0.05}
n5164_9a	81	55	36	0.72	5.349	1.52	0.1011	3.99	2.933	1.37	0.1138	0.66	0.90	1.9		1861	12	1891	23	215686	{0.01}
FHM140084B, meta-andesite, Kalixälv formation																					
n5174_01b	206	101	88	0.52	5.362	1.10	0.1044	2.24	2.971	0.96	0.1155	0.55	0.87	-1.1		1888	10	1870	16	43645	{0.04}
n5174_02a	99	54	43	0.59	5.420	1.30	0.1056	2.30	2.933	1.13	0.1153	0.65	0.87	0.4		1885	12	1891	19	97302	{0.02}
n5174_03a	151	82	64	0.53	5.301	1.07	0.0947	2.24	2.996	0.98	0.1152	0.44	0.91	-1.6		1883	8	1857	16	12176	0.15
n5174_04a	159	73	67	0.47	5.382	1.10	0.1003	2.16	2.965	1.00	0.1157	0.46	0.91	-1.1		1891	8	1874	16	>1e6	{0.00}
n5174_05a	157	103	71	0.68	5.535	1.11	0.1020	2.07	2.905	0.99	0.1166	0.50	0.89	0.1		1905	9	1907	16	262349	{0.01}
n5174_06a	138	64	60	0.51	5.422	1.10	0.1064	2.13	2.914	1.00	0.1146	0.46	0.91	1.7		1874	8	1902	16	57614	{0.03}
n5174_07a	296	53	108	0.09	5.123	1.63	0.0485	5.55	3.115	1.51	0.1157	0.60	0.93	-5.9	-1.9	1891	11	1795	24	6314	0.30
n5174_08a	211	140	95	0.68	5.461	1.02	0.1015	2.07	2.933	0.96	0.1162	0.35	0.94	-0.4		1898	6	1891	16	>1e6	{0.00}
n5174_09a	287	521	92	0.39	3.894	2.96	0.0201	4.31	3.943	2.87	0.1114	0.73	0.97	-22.3	-16.8	1822	13	1457	38	2655	0.70
n5174_10a	188	145	74	0.51	4.943	1.13	0.0647	2.45	3.231	1.01	0.1158	0.51	0.89	-9.3	-6.4	1893	9	1738	15	4565	0.41
n5174_11a	294	161	126	0.54	5.345	1.02	0.0972	2.12	2.974	0.98	0.1153	0.29	0.96	-0.9		1884	5	1869	16	>1e6	{0.00}

Isotope values are common Pb corrected using modern common Pb composition (Stacey & Kramers 1975) and measured ^{204}Pb.

*1 Th/U ratios calculated from $^{208}Pb/^{206}Pb$ and $^{207}Pb/^{206}Pb$ ratios, assuming a single stage of closed U-Th-Pb evolution

*2 Error correlation in conventional concordia space. Do not use for Tera-Wasserburg plots.

*3 Age discordance in conventional concordia space. Positive numbers are reverse discordant.

*4 Age discordance at closest approach of error ellipse to concordia (2σ level).

*5 Figures in parentheses are given when no correction has been applied, and indicate a value calculated assuming present-day Stacey-Kramers common Pb.

The heavy mineral concentrate is rich in titanite, but there are also small amounts of weakly coloured, greyish and transparent zircon with subhedral to euhedral crystal shapes. Microfractures and inclusions are common. Back-scattered (BSE) imaging shows an internal oscillatory zonation in the zircon, and textural older cores are evident in some grains (Fig. 12F). Altogether, 11 zircon analyses were performed. These contain 99–296 ppm uranium and have rather uniform Th/U ratios of 0.39–0.68, except analysis 7a, which has a ratio of 0.09 (Table 4). Two discordant analyses (9a, 10a) have high values for common lead and are excluded from the age calculations. One analysis (1a) located in an textural older core, records an older age of approximately 1.91 Ga, compared with the other analyses, and is interpreted as inherited. Eight analyses are concordant and record a concordia age of 1887 ±5 Ma (Fig. 12H, 2σ, MSWD of concord. + equiv. = 1.3, probability (concord. + equiv.) = 0.19, n = 8). The $^{207}Pb/^{206}Pb$-weighted mean age is 1888 ±5 Ma (2σ, MSWD = 1.5, probability = 0.17, n = 8) or 1889 ±5 Ma including the discordant analysis 7a (MSWD = 1.3, probability = 0.2, n = 9). The concordia age of 1887 ±5 Ma is chosen as the best age estimate and is interpreted to date igneous crystallisation of the meta-andesite.

Meta-sandstone (FHM140078A), lower sandstone unit Pahakurkio group

A subarkosic meta-sandstone was sampled from the lower sandstone unit in the Pahakurkio group (Fig. 2), approximately 300 m west of the contact with the dolomite of the Veikkavaara greenstone group (Fig. 3). The outcrop at the sampled locality shows a planar bedded meta-arkose, with thin, 1-mm-wide laminas enriched in heavy minerals. The bedding dips steeply eastwards with cross-bedding in the unit showing way-up towards the east. 20 metres above (west of) the sampled rock is a approximately 20 m wide, highly magnetic, skarn-banded rock unit of intermediate composition, possibly of volcanic origin, as suggested by its similar chemical composition to volcanic rocks in Masugnsbyn. The meta-subarkose is dominated by quartz, usually with finer-grained feldspar (microcline and plagioclase). Biotite occurs between the quartz grains in a polygonal to seriate recrystallised texture (Fig. 13A, C). Some feldspar grains are of a similar size to the quartz grains. Parallel-oriented, dispersed grains of biotite define a foliation. There are larger grains of ilmenite enriched in laminas, together with other heavy minerals, rutile (?) and zircon.

The heavy mineral concentrate is rich in zircon, rounded, anhedral to subhedral, colourless transparent to brownish turbid. Ilmenite, rutile, tourmaline, and possibly garnet were also recovered. BSE images show zircons to have variable internal structures, many grains with oscillatory or patchy zonation (Fig. 14A). Some grains contain clearly xenocrystic cores and some have homogenous BSE-bright outer domains. Microcracks in the zircon are common and many grains show irregular BSE-dark, probably metamict domains. Altogether, 149 zircon analyses were carried out. 104 of these were less than 5% discordant and selected for plotting in the age distribution diagram (Table 5, Fig. 14C–D). The zircon age population is dominated by 2.15–1.90 Ga Karelian–Svecofennian ages (66% of the entire zircon population) and 2.95–2.62 Ga Archaean ages (30%), with a few results outside these ranges. Two analyses have ages at 2.44 & 2.50 Ga (2%) and a single analysis is dated at approximately 3.29 Ga (1%). The younger age group peaks at 2.04 Ga, with a smaller peak at 1.92 Ga (Fig. 14C). The nine youngest zircons give a $^{207}Pb/^{206}Pb$-weighted mean age of 1911 ±10 Ma (Fig. 14F, MSWD = 0.14, probability = 0.997), suggesting a maximum depositional age of Pahakurkio group sedimentary rocks of approximately 1.91 Ga.

Meta-sandstone (RR96128), upper sandstone unit, Pahakurkio group

A meta-sandstone was previously sampled by Roy Rutland in the upper sandstone unit of the Pahakurkio group, upstream of the Pahakurkio rapids on the river Kalixälven. The locality contains flat-lying ripple- and rill-marked meta-sandstones of subarkosic composition. Zircons from this sample were previously dated at Nordsim in 2004. 13 analyses from 8 zircon grains were carried out. These contain 101–793 ppm U and Th/U ratios of 0.26–0.99, except two CL-dark rim analyses, which have Th/U

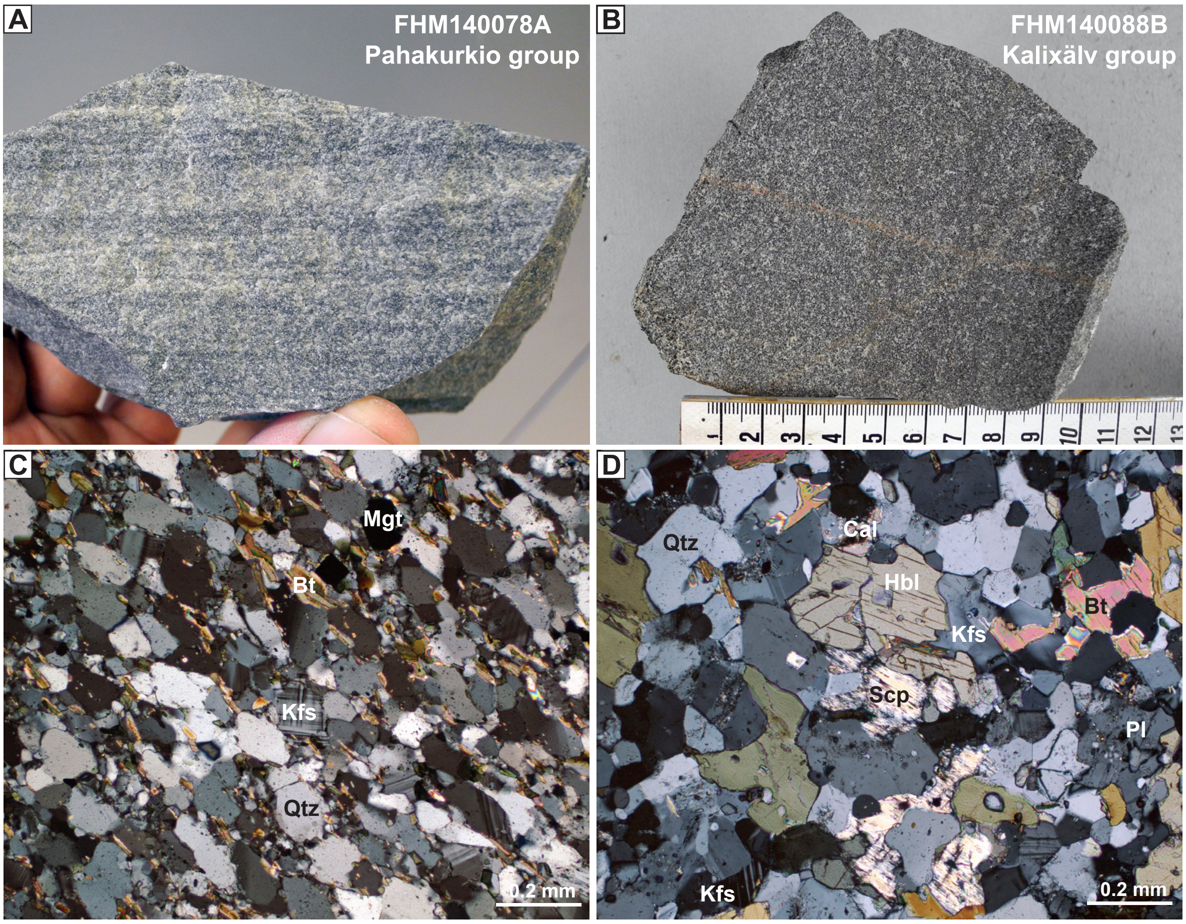

Figure 13. Provenance geochronology of meta-sandstones of the Pahakurkio and the Kalixälv groups. **A–B.** Dated samples of meta-sandstone from the Pahakurkio group (A, sub-arkose) and Kalixälv group (B, intermediate amphibole-bearing). **C–D.** Photomicrographs in cross-polarised light of dated samples of meta-sandstones from the Pahakurkio group (C) and the Kalixälv group (D).

ratios of 0.06 and 0.09 (Table 6). The analyses are concordant or weakly discordant at the two-sigma error level, with low amounts of common lead. Although a very limited number of analyses were made, these give similar age results to the dated sample from the lower sandstone unit. The $^{207}Pb/^{206}Pb$ zircon ages range from 1.89 to 2.09 Ga, with one analysis at 2.65 Ga (Fig. 15). The three youngest zircons give a $^{207}Pb/^{206}Pb$-weighted mean age of 1896 ±10 Ma (Fig. 15), suggesting a maximum depositional age of approximately 1.90 Ga, i.e. similar to the lower Pahakurkio sandstone unit.

► Figure 14. Provenance geochronology of meta-sandstones of the Pahakurkio and Kalixälv groups. **A–B.** Selection of BSE-images of dated zircons from the two provenance samples. **C.** Probability density diagram showing $^{207}Pb/^{206}Pb$ zircon age spectra (<5% discordant) from the Pahakurkio group sample (red) and Kalixälv group sample (green). n = number of zircon analyses measured in each sample used to construct the curves in the diagram. >5% discordant analyses are excluded; see Table 5. **D–E.** Diagrams showing <5% discordant $^{207}Pb/^{206}Pb$ zircon ages from the Pahakurkio group sample(D) and the Kalixälv group sample (E). **F–G.** Estimated maximum depositional ages from the youngest group of zircon analyses from the Pahakurkio meta-sandstone (F) and the Kalixälv meta-sandstone (G). The three youngest ages from the Kalixälv group sample were excluded from the maximum depositional age calculation, assuming secondary partial resetting of the U-Pb isotopic system in these.

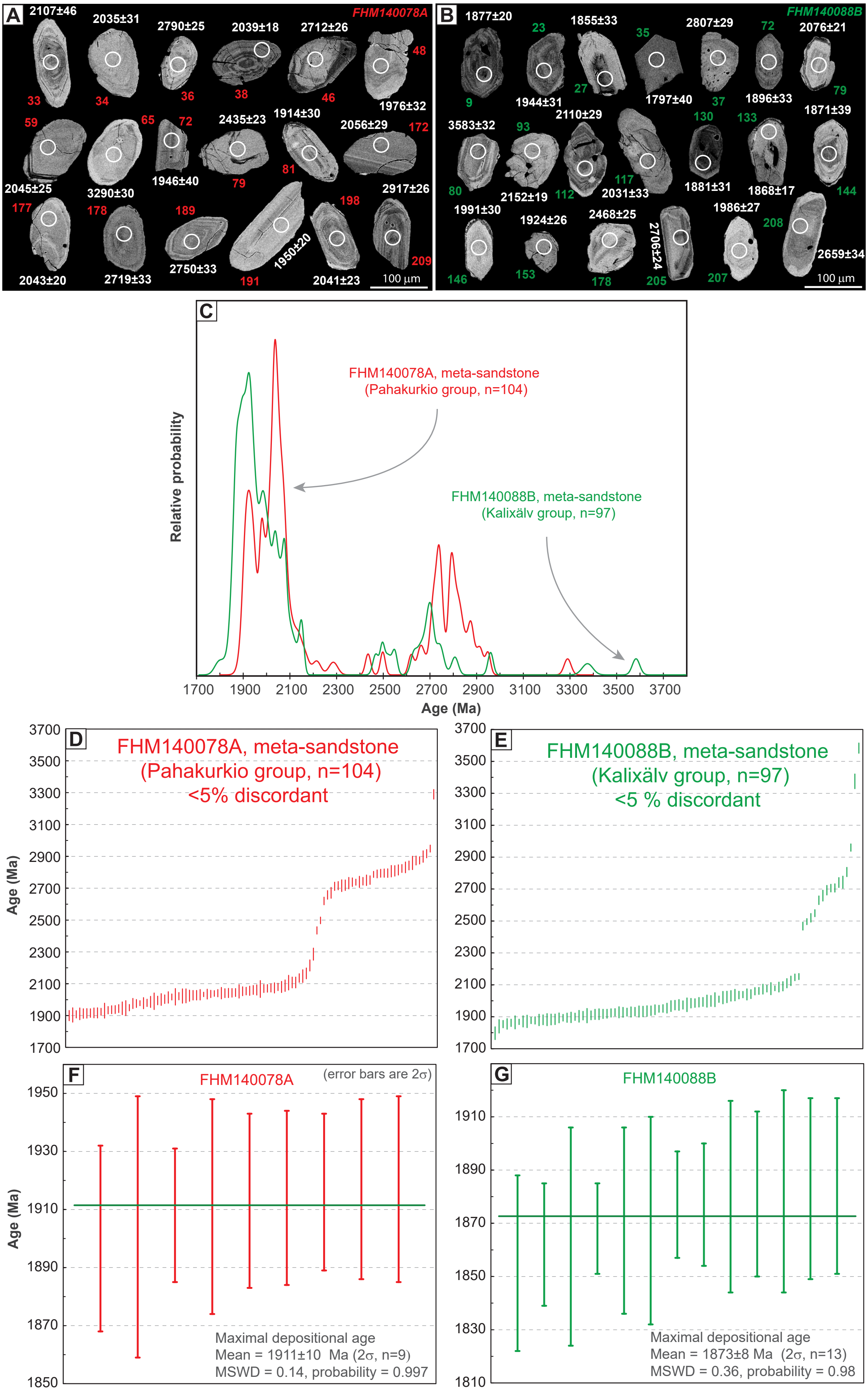
A
FHM140078A
B
FHM140088B
100 µm
C
FHM140078A, meta-sandstone
(Pahakurkio group, n=104)
FHM140088B, meta-sandstone
(Kalixälv group, n=97)
Relative probability
Age (Ma)
D
FHM140078A, meta-sandstone
(Pahakurkio group, n=104)
<5% discordant
E
FHM140088B, meta-sandstone
(Kalixälv group, n=97)
<5 % discordant
Age (Ma)
F
FHM140078A
(error bars are 2σ)
Maximal depositional age
Mean = 1911±10 Ma (2σ, n=9)
MSWD = 0.14, probability = 0.997
G
FHM140088B
Maximal depositional age
Mean = 1873±8 Ma (2σ, n=13)
MSWD = 0.36, probability = 0.98

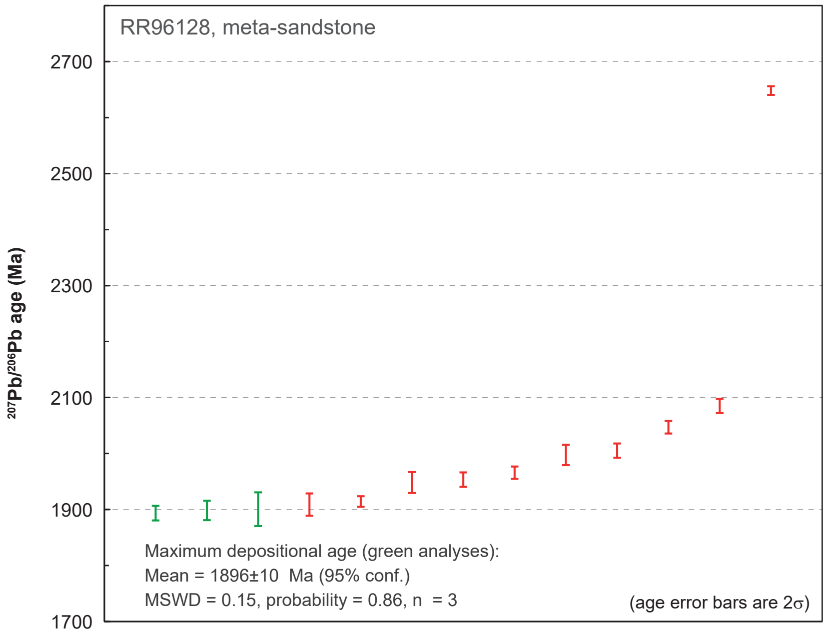

Figure 15. Diagram showing U-Pb SIMS data on a meta-sandstone sample from the upper part of Pahakurkio group. A maximum depositional age is calculated from the three youngest zircons (in green).

Meta-sandstone (FHM140088B), Kalixälv group

A cross-bedded, amphibole-bearing meta-sandstone was sampled immediately above the basal conglomerate, approximately 250 m west of the contact with the Pahakurkio group (Fig. 2–3, 13B). The rock is fine-grained with a recrystallised evenly-grained, polygonal texture, but grains of hornblende tend to be slightly larger (Fig. 13D). The main minerals are quartz, K-feldspar, plagioclase, green hornblende and biotite, with subordinate amounts of cordierite and calcite, the latter interstitial between quartz grains. Accessory phases are epidote, monazite, zircon, magnetite and fluorite. A few metres above the sampled rock is a laminated (1–10 mm) cordierite, quartz, and hornblende meta-sandstone, where magnetite-rich laminas alternate with laminates with subordinate amounts of opaques (Fig. 8C). Other layers consist of larger proportions of quartz, K-feldspar and amphibole, with subordinate amounts of biotite and cordierite.

The heavy mineral concentrate is rich in zircon, with subhedral to rounded, anhedral crystal shapes, generally with better developed crystal shapes than in the Pahakurkio group sample. Some grains of monazite, amphibole and magnetite are also seen. BSE images show variable internal structures, many grains showing oscillatory or patchy zonation (Fig. 14B). Some grains have clearly xenocrystic cores. Microcracks in the zircons are common and many grains show BSE-dark, probably metamict domains. 149 zircon analyses were carried out. 92 analyses of these were less than 5% discordant and selected for plotting in the age distribution diagram (Table 5, Fig. 14C, E). This sample shows a similar age distribution to the Pahakurkio meta-sandstone sample (FHM140078), but generally trends towards somewhat younger ages (Fig. 14C). The zircon age population is dominated by 2.15–1.86 Ga ages (81%) and 2.96–2.55 Ga ages (11%), with a few analyses outside these ranges. Two analyses have ages of approximately 3.38 and 3.58 Ga (2%), three analyses of 2.52–2.47 Ga (3%) and three of approximately 1.85–1.84 and 1.80 Ga (3%). The significance of young ages is uncertain, but they may reflect secondary partial resetting of the U-Pb isotopic system, or lab contamination. The youngest zircon (no 35, Fig. 14B) is homogenous BSE-dark. Excluding this, the second and third-youngest zircons (no 63, 111), the $^{207}Pb/^{206}Pb$-weighted mean age of the 13 youngest analyses is 1 873 ±8 Ma (Fig. 14G). Including analyses 63 and 111 marginally lowers the mean age to 1 870 ±7 Ma. The maximum depositional age is estimated to be approximately 1.87 Ga.

Table 5. Laser ICP-MS U-Pb zircon provenance data of Pahakurkio group, lower sandstone sample (FHM140078A), and Kalixälv group intermediate sandstone sample (FHM140088B).

Analysis	Concentrations (ppm)[a]						Ratios								Ages (Ma)						CONC.
No	U	2σ	Th	2σ	Pb	2σ	U/Th[a]	$^{207}Pb/^{235}U$[b]	2σ[d]	$^{206}Pb/^{238}U$[b]	2σ[d]	rho[c]	$^{207}Pb/^{206}Pb$[e]	2σ[d]	$^{207}Pb/^{235}U$[b]	2σ[d]	$^{206}Pb/^{238}U$[b]	2σ[d]	$^{207}Pb/^{206}Pb$[e]	2σ[d]	%
FHM140078A, meta-sandstone, Pahakurkio group																					
7	150	12	35	3	444	30	4.4	17.110	0.420	0.602	0.015	0.733	0.2086	0.0047	2940	24	3038	61	2892	37	105
8	272	47	58	8	418	53	5.3	5.960	0.110	0.368	0.009	0.847	0.1173	0.0016	1970	15	2018	40	1915	24	105
10	218	6	245	12	2210	140	0.9	6.550	0.210	0.369	0.016	0.858	0.1308	0.0026	2052	28	2024	75	2108	34	96
11	710	160	245	31	1800	330	3.1	6.060	0.160	0.356	0.011	0.915	0.1233	0.0019	1983	23	1964	52	2003	27	98
12	472	70	157	11	1120	140	3.1	6.030	0.150	0.373	0.009	0.882	0.1173	0.0010	1980	21	2041	42	1915	16	107
13	773	52	177	18	1830	190	4.7	11.780	0.300	0.465	0.014	0.815	0.1817	0.0028	2585	24	2458	62	2667	26	92
14	294	16	17	1	162	12	17.1	6.420	0.130	0.358	0.007	0.717	0.1283	0.0019	2034	18	1973	32	2074	26	95
15	919	64	283	31	2220	200	3.4	5.575	0.084	0.344	0.011	0.740	0.1167	0.0029	1912	13	1903	54	1904	45	100
16	590	100	166	34	1790	330	3.6	11.260	0.240	0.494	0.015	0.808	0.1641	0.0020	2544	20	2588	63	2498	21	104
20	700	130	287	70	2730	690	2.5	9.320	0.750	0.418	0.031	0.973	0.1606	0.0041	2354	84	2240	150	2459	43	91
21	259	15	17	2	203	27	15.5	14.980	0.200	0.540	0.013	0.706	0.1989	0.0040	2814	13	2797	50	2815	32	99
24	193	34	162	33	610	63	1.5	13.410	0.410	0.492	0.017	0.800	0.1922	0.0043	2707	29	2576	75	2776	36	93
25	348	24	23	1	280	18	14.6	14.860	0.390	0.536	0.017	0.818	0.2023	0.0034	2805	25	2763	72	2843	28	97
26	442	57	72	7	645	54	6.0	7.260	0.260	0.406	0.015	0.929	0.1286	0.0013	2142	33	2194	70	2079	17	106
27	607	64	59	11	499	99	11.3	6.480	0.110	0.364	0.007	0.719	0.1280	0.0019	2047	14	1998	34	2070	25	97
28	331	38	73	8	571	75	4.3	6.550	0.240	0.365	0.013	0.897	0.1294	0.0027	2051	32	2003	61	2088	36	96
33	193	29	18	3	151	20	11.4	7.150	0.240	0.395	0.016	0.587	0.1309	0.0034	2127	31	2144	75	2107	46	102
34	383	24	58	2	473	15	6.7	6.530	0.150	0.377	0.010	0.721	0.1256	0.0022	2050	20	2060	49	2035	31	101
35	263	35	107	8	797	44	2.5	5.440	0.130	0.329	0.012	0.866	0.1199	0.0025	1890	21	1832	57	1962	35	93
36	384	52	105	10	1080	140	3.7	13.820	0.440	0.514	0.017	0.913	0.1958	0.0030	2735	31	2673	71	2790	25	96
37	312	31	117	13	829	92	2.6	6.670	0.130	0.385	0.009	0.910	0.1253	0.0010	2068	17	2099	39	2033	14	103
38	397	33	59	4	418	36	7.0	6.360	0.180	0.361	0.010	0.960	0.1258	0.0013	2025	24	1985	47	2039	18	97
40	347	39	103	19	1060	200	3.9	13.880	0.390	0.527	0.015	0.805	0.1894	0.0030	2740	27	2727	62	2751	27	99
41	186	16	65	3	491	25	2.9	5.480	0.220	0.340	0.015	0.871	0.1177	0.0033	1895	35	1886	74	1931	47	98
42	393	44	73	9	546	61	5.6	6.900	0.230	0.392	0.015	0.947	0.1283	0.0023	2097	29	2129	69	2074	32	103
46	458	52	108	13	1310	150	3.9	13.100	0.470	0.509	0.018	0.868	0.1867	0.0029	2684	34	2649	79	2712	26	98
48	133	18	25	4	207	31	5.0	5.800	0.190	0.347	0.013	0.875	0.1215	0.0022	1944	30	1919	61	1976	32	97
49	295	33	86	6	974	52	3.2	12.430	0.480	0.497	0.019	0.901	0.1806	0.0030	2634	37	2599	81	2658	27	98
52	1400	140	469	91	6100	1500	3.2	11.270	0.380	0.432	0.016	0.892	0.1874	0.0043	2544	31	2313	71	2717	38	85
53	129	10	45	4	372	47	2.8	7.510	0.530	0.339	0.028	0.935	0.1614	0.0038	2169	64	1880	140	2468	40	76
59	259	17	26	3	211	17	10.8	6.540	0.190	0.372	0.011	0.865	0.1262	0.0018	2050	26	2036	52	2045	25	100
60	436	46	205	28	2260	330	2.3	14.350	0.390	0.537	0.016	0.848	0.1955	0.0032	2771	26	2771	67	2794	25	99
61	209	20	100	8	1086	95	2.2	13.510	0.300	0.521	0.014	0.762	0.1896	0.0031	2715	21	2700	60	2738	27	99
62	141	20	69	9	606	82	2.2	7.320	0.160	0.391	0.009	0.624	0.1353	0.0026	2150	19	2128	40	2165	34	98
63	255	35	35	7	285	46	7.2	6.430	0.290	0.378	0.018	0.902	0.1245	0.0019	2041	43	2083	81	2028	30	103
64	630	160	177	54	1080	340	4.1	5.750	0.310	0.351	0.018	0.994	0.1187	0.0016	1935	49	1939	87	1937	25	100

Table 5 continues

Analysis	Concentrations (ppm)[a]						Ratios								Ages (Ma)						CONC.
No	U	2 σ	Th	2 σ	Pb	2 σ	U/Th[a]	$^{207}Pb/^{235}U$[b]	2 σ[d]	$^{206}Pb/^{238}U$[b]	2 σ[d]	rho[c]	$^{207}Pb/^{206}Pb$[e]	2 σ[d]	$^{207}Pb/^{235}U$[b]	2 σ[d]	$^{206}Pb/^{238}U$[b]	2 σ[d]	$^{207}Pb/^{206}Pb$[e]	2 σ[d]	%
FHM140078A, meta-sandstone, Pahakurkio group																					
65	351	15	41	2	530	40	8.9	25.130	0.550	0.679	0.020	0.828	0.2674	0.0050	3312	21	3338	76	3290	30	101
66	194	20	76	13	599	80	2.9	6.850	0.300	0.387	0.016	0.887	0.1268	0.0020	2088	39	2107	72	2053	28	103
67	260	14	115	7	874	56	2.3	5.860	0.160	0.363	0.012	0.941	0.1157	0.0019	1954	23	1995	57	1896	27	105
68	847	56	300	17	3180	180	2.8	13.830	0.620	0.511	0.022	0.989	0.1954	0.0023	2734	42	2660	94	2787	19	95
72	216	12	75	4	580	33	2.8	5.920	0.170	0.357	0.012	0.809	0.1195	0.0027	1962	25	1967	59	1946	40	101
74	255	7	15	2	208	31	19.3	14.940	0.360	0.521	0.012	0.778	0.2047	0.0028	2810	23	2703	49	2863	23	94
75	474	30	216	17	2350	200	2.2	13.490	0.320	0.523	0.010	0.739	0.1896	0.0022	2720	25	2712	43	2738	19	99
77	624	35	130	12	983	51	4.9	5.480	0.120	0.324	0.009	0.710	0.1242	0.0016	1897	19	1808	44	2017	22	90
79	736	50	103	8	907	57	7.3	10.540	0.180	0.474	0.012	0.830	0.1581	0.0021	2484	15	2502	53	2435	23	103
80	738	66	447	28	3700	300	1.6	6.130	0.100	0.357	0.008	0.478	0.1222	0.0024	1995	14	1968	40	1986	35	99
81	529	14	279	14	2084	91	1.9	5.340	0.150	0.329	0.005	0.911	0.1173	0.0020	1875	23	1834	25	1914	30	96
85	309	17	20	2	259	22	15.1	13.770	0.280	0.504	0.011	0.617	0.1959	0.0031	2733	19	2629	49	2791	26	94
87	334	34	63	8	718	93	5.4	12.020	0.320	0.485	0.015	0.917	0.1765	0.0025	2605	25	2546	63	2620	24	97
88	910	57	231	8	1958	93	4.1	6.400	0.120	0.375	0.010	0.638	0.1232	0.0026	2031	16	2052	46	2001	37	103
89	404	34	106	24	1260	300	4.8	13.200	0.490	0.501	0.018	0.919	0.1903	0.0028	2691	35	2617	76	2744	24	95
90	448	38	25	1	261	11	19.5	14.620	0.210	0.539	0.011	0.653	0.1963	0.0032	2790	14	2778	44	2795	26	99
91	1710	170	259	25	1940	220	7.0	5.020	0.230	0.302	0.011	0.735	0.1211	0.0027	1821	39	1701	54	1970	40	86
92	86	8	11	2	127	20	9.0	15.600	0.350	0.566	0.018	0.891	0.1999	0.0031	2852	21	2888	76	2824	25	102
93	951	90	198	25	1530	210	5.3	5.590	0.130	0.343	0.008	0.791	0.1169	0.0015	1914	20	1903	37	1908	23	100
98	1070	120	260	25	2470	300	4.2	7.510	0.240	0.396	0.010	0.789	0.1392	0.0028	2172	29	2150	45	2215	35	97
99	1266	49	232	24	1957	94	5.7	5.800	0.120	0.331	0.011	0.760	0.1251	0.0021	1946	18	1842	54	2029	29	91
100	962	76	223	10	1950	130	4.3	6.090	0.110	0.369	0.009	0.687	0.1241	0.0025	1988	17	2026	42	2014	36	101
101	356	30	49	6	548	47	7.6	5.690	0.210	0.354	0.012	0.709	0.1172	0.0020	1935	34	1964	53	1913	30	103
103	297	22	49	3	487	22	5.9	7.330	0.240	0.395	0.015	0.717	0.1339	0.0030	2151	30	2144	68	2148	40	100
104	486	31	71	3	561	46	6.7	5.555	0.087	0.343	0.006	0.603	0.1164	0.0021	1909	13	1901	29	1900	32	100
112	557	50	152	13	1310	130	3.8	6.120	0.160	0.355	0.013	0.692	0.1249	0.0031	1991	22	1956	60	2024	44	97
114	432	41	126	11	1370	150	3.6	12.140	0.290	0.481	0.013	0.904	0.1830	0.0017	2614	22	2532	57	2680	15	94
115	234	29	163	31	1830	380	1.6	14.390	0.490	0.524	0.013	0.794	0.1979	0.0043	2773	33	2717	55	2807	36	97
116	1080	140	343	43	2760	370	3.4	6.330	0.120	0.368	0.007	0.478	0.1269	0.0018	2022	16	2019	33	2054	24	98
117	559	31	154	14	1224	47	3.7	7.410	0.170	0.398	0.009	0.717	0.1329	0.0021	2161	21	2159	43	2136	27	101
118	888	91	35	4	330	34	27.7	6.670	0.200	0.378	0.014	0.889	0.1288	0.0017	2073	29	2063	67	2080	23	99
119	234	49	52	12	570	120	4.9	13.280	0.490	0.492	0.017	0.895	0.1963	0.0035	2696	35	2576	72	2794	29	92
120	583	59	30	2	336	18	20.4	12.260	0.290	0.486	0.014	0.731	0.1822	0.0037	2623	22	2553	63	2671	34	96
124	550	110	135	41	1090	310	4.8	5.920	0.200	0.359	0.015	0.834	0.1196	0.0031	1962	31	1976	70	1947	47	101
125	549	41	3	1	70	7	146.0	14.510	0.390	0.525	0.013	0.782	0.1982	0.0040	2782	26	2721	54	2809	33	97
127	579	26	122	6	1036	65	4.6	6.190	0.130	0.361	0.011	0.718	0.1253	0.0023	2002	19	1987	53	2031	33	98
128	90	19	19	5	280	44	4.8	15.770	0.590	0.608	0.024	0.921	0.1917	0.0021	2872	31	3062	95	2756	18	111

Table 5 continues

Analysis	Concentrations (ppm)[a]						Ratios								Ages (Ma)						CONC.
No	U	2 σ	Th	2 σ	Pb	2 σ	U/Th[a]	$^{207}Pb/^{235}U$[b]	2 σ[d]	$^{206}Pb/^{238}U$[b]	2 σ[d]	rho[c]	$^{207}Pb/^{206}Pb$[e]	2 σ[d]	$^{207}Pb/^{235}U$[b]	2 σ[d]	$^{206}Pb/^{238}U$[b]	2 σ[d]	$^{207}Pb/^{206}Pb$[e]	2 σ[d]	%
FHM140078A, meta-sandstone, Pahakurkio group																					
129	140	11	84	7	686	69	1.6	6.320	0.078	0.360	0.007	0.713	0.1273	0.0020	2021	11	1980	34	2061	28	96
131	482	44	92	32	1020	390	6.5	13.210	0.230	0.518	0.013	0.491	0.1872	0.0041	2694	17	2691	57	2716	37	99
132	313	13	119	3	969	50	2.6	6.270	0.170	0.362	0.012	0.765	0.1274	0.0023	2013	24	1989	59	2061	32	97
133	480	110	193	51	1910	540	2.6	10.870	0.530	0.452	0.016	0.649	0.1804	0.0058	2509	46	2404	71	2654	54	91
137	240	13	59	3	497	25	4.1	6.460	0.230	0.384	0.019	0.917	0.1246	0.0016	2039	32	2093	87	2022	23	104
140	334	32	119	26	990	220	3.0	9.540	0.420	0.417	0.023	0.817	0.1675	0.0039	2389	41	2240	110	2531	40	89
141	253	29	115	6	746	97	2.3	6.000	0.160	0.353	0.014	0.654	0.1216	0.0024	1974	24	1948	67	1978	35	98
142	141	10	42	6	454	68	3.5	15.830	0.350	0.557	0.014	0.888	0.2061	0.0029	2865	21	2853	59	2875	23	99
143	134	52	34	6	255	26	3.9	6.770	0.310	0.383	0.022	0.679	0.1260	0.0020	2088	45	2090	110	2041	28	102
144	181	21	56	8	629	72	3.3	16.060	0.370	0.564	0.017	0.610	0.2094	0.0047	2879	22	2880	69	2899	36	99
145	740	100	455	75	2970	500	1.8	5.390	0.370	0.337	0.025	0.988	0.1179	0.0014	1876	65	1870	120	1924	22	97
146	147	12	58	4	470	29	2.6	6.030	0.170	0.353	0.013	0.816	0.1250	0.0021	1978	24	1948	61	2028	30	96
150	116	5	46	2	562	32	2.6	16.930	0.420	0.568	0.016	0.923	0.2158	0.0029	2930	24	2900	65	2949	22	98
151	145	9	43	6	348	42	3.6	6.440	0.130	0.371	0.015	0.794	0.1261	0.0032	2037	19	2034	70	2052	42	99
152	285	16	111	3	935	31	2.6	6.490	0.160	0.379	0.012	0.835	0.1243	0.0026	2044	22	2086	60	2025	35	103
153	48	3	36	3	404	23	1.3	13.790	0.500	0.530	0.021	0.816	0.1891	0.0041	2742	31	2761	96	2732	36	101
154	361	25	55	9	450	52	6.5	6.270	0.190	0.376	0.012	0.845	0.1217	0.0016	2013	25	2055	57	1980	23	104
155	255	19	63	3	472	31	4.1	5.890	0.190	0.369	0.015	0.865	0.1189	0.0017	1958	29	2023	71	1938	25	104
156	70	4	24	2	285	18	2.8	14.780	0.360	0.552	0.017	0.796	0.1964	0.0032	2800	24	2833	71	2795	27	101
157	147	20	69	17	900	230	2.4	19.980	0.800	0.580	0.022	0.932	0.2530	0.0035	3096	36	2946	89	3203	22	92
163	147	8	34	1	275	9	4.4	6.510	0.140	0.377	0.008	0.766	0.1256	0.0016	2046	19	2063	36	2036	23	101
164	398	23	93	6	744	56	4.3	5.570	0.100	0.348	0.009	0.572	0.1170	0.0019	1911	16	1923	44	1916	27	100
165	344	13	58	2	469	13	5.8	5.660	0.150	0.354	0.013	0.886	0.1170	0.0019	1924	23	1953	60	1917	32	102
166	240	17	72	3	810	71	3.4	15.260	0.500	0.549	0.023	0.829	0.2061	0.0035	2829	31	2817	95	2874	28	98
167	207	29	47	8	390	70	4.2	6.500	0.220	0.383	0.015	0.909	0.1242	0.0014	2044	30	2087	71	2017	19	103
168	126	5	43	2	343	15	2.9	5.860	0.140	0.372	0.007	0.665	0.1162	0.0017	1954	21	2039	31	1897	26	107
169	257	14	50	3	409	19	5.0	6.310	0.150	0.368	0.010	0.646	0.1260	0.0025	2020	21	2018	49	2041	36	99
170	193	8	49	4	377	39	3.9	6.440	0.140	0.390	0.012	0.626	0.1217	0.0020	2036	19	2123	56	1980	29	107
171	419	58	179	24	1300	180	2.3	5.540	0.170	0.343	0.010	0.920	0.1186	0.0015	1916	32	1900	48	1934	23	98
172	167	11	45	2	380	22	3.5	6.410	0.290	0.375	0.011	0.920	0.1270	0.0020	2031	43	2051	51	2056	29	100
176	162	12	75	8	805	84	2.2	13.150	0.270	0.515	0.018	0.767	0.1870	0.0029	2690	19	2678	77	2716	26	99
177	176	14	66	3	536	23	2.6	6.340	0.150	0.363	0.009	0.773	0.1261	0.0019	2024	20	1996	45	2043	27	98
178	350	22	77	7	882	70	4.7	14.330	0.620	0.556	0.024	0.901	0.1875	0.0038	2768	42	2848	98	2719	33	105
179	315	80	93	32	570	140	4.0	6.490	0.280	0.376	0.017	0.899	0.1260	0.0021	2041	38	2058	77	2042	29	101
181	293	83	190	59	2010	650	1.8	13.500	0.730	0.506	0.028	0.776	0.1941	0.0056	2721	58	2630	120	2773	47	95
182	706	55	109	5	834	51	6.7	5.974	0.090	0.361	0.007	0.551	0.1227	0.0019	1972	13	1984	32	1995	27	99
183	880	190	28	6	192	57	30.7	5.790	0.520	0.345	0.031	0.988	0.1215	0.0011	1935	80	1900	150	1978	16	96
185	137	28	30	5	231	27	4.9	6.910	0.550	0.368	0.023	0.958	0.1362	0.0032	2091	74	2020	110	2178	41	93

Table 5 continues

Analysis	Concentrations (ppm)[a]						Ratios								Ages (Ma)						CONC.
No	U	2 σ	Th	2 σ	Pb	2 σ	U/Th[a]	$^{207}Pb/^{235}U$[b]	2 σ[d]	$^{206}Pb/^{238}U$[b]	2 σ[d]	rho[c]	$^{207}Pb/^{206}Pb$[e]	2 σ[d]	$^{207}Pb/^{235}U$[b]	2 σ[d]	$^{206}Pb/^{238}U$[b]	2 σ[d]	$^{207}Pb/^{206}Pb$[e]	2 σ[d]	%
FHM140078A, meta-sandstone, Pahakurkio group																					
189	163	6	81	5	923	57	2.0	13.260	0.340	0.504	0.015	0.800	0.1911	0.0038	2697	24	2631	64	2750	33	96
190	359	28	131	7	1450	160	2.8	15.140	0.330	0.550	0.015	0.759	0.2009	0.0042	2823	21	2825	62	2831	34	100
191	454	40	184	19	1340	120	2.6	5.800	0.100	0.357	0.008	0.728	0.1196	0.0013	1946	15	1967	36	1950	20	101
193	252	69	74	16	650	120	3.5	7.200	0.210	0.403	0.014	0.800	0.1289	0.0025	2134	26	2182	66	2080	35	105
194	243	19	61	7	458	63	4.2	5.630	0.160	0.348	0.012	0.910	0.1170	0.0019	1919	26	1925	56	1917	31	100
196	308	27	53	5	405	43	5.9	5.580	0.140	0.346	0.009	0.740	0.1171	0.0024	1912	22	1933	53	1911	37	101
198	186	13	26	2	208	17	6.9	6.250	0.150	0.363	0.010	0.697	0.1259	0.0016	2010	21	1995	46	2041	23	98
202	53	4	30	3	346	31	1.7	14.120	0.490	0.541	0.019	0.846	0.1900	0.0040	2756	33	2785	78	2740	35	102
203	714	62	218	37	1870	350	3.6	8.480	0.290	0.426	0.012	0.759	0.1451	0.0033	2281	31	2287	53	2286	38	100
204	440	41	209	24	1680	270	2.2	6.080	0.130	0.367	0.008	0.798	0.1214	0.0017	1987	19	2014	39	1976	25	102
205	187	7	23	0	182	6	8.0	5.610	0.130	0.341	0.009	0.822	0.1193	0.0017	1917	20	1892	45	1944	25	97
206	375	41	107	13	1157	73	3.6	11.040	0.980	0.453	0.034	0.943	0.1787	0.0037	2513	81	2400	150	2639	35	91
207	195	8	45	1	353	11	4.4	6.125	0.098	0.358	0.011	0.518	0.1248	0.0032	1993	14	1971	55	2023	45	97
208	307	41	111	19	840	190	2.9	6.230	0.220	0.349	0.014	0.864	0.1299	0.0028	2006	31	1927	66	2095	38	92
209	186	14	51	4	637	49	3.8	16.560	0.480	0.570	0.018	0.871	0.2116	0.0034	2908	28	2907	72	2917	26	100
Common-Pb corrected[f]																					
9	800	170	215	52	1410	340	3.9	5.000	0.160	0.314	0.010	0.794	0.1160	0.0022	1818	28	1759	49	1902	30	92
22	1000	67	294	18	1880	250	3.4	5.050	0.160	0.316	0.011	0.895	0.1138	0.0017	1826	26	1770	54	1871	20	95
23	658	64	199	9	1410	110	3.3	4.790	0.260	0.296	0.015	0.915	0.1167	0.0031	1779	45	1672	75	1902	48	88
39	396	41	116	22	900	210	3.7	5.570	0.310	0.315	0.018	0.929	0.1275	0.0026	1917	46	1762	90	2061	36	85
47	787	85	121	17	1200	190	6.7	7.480	0.280	0.368	0.012	0.840	0.1464	0.0029	2168	33	2021	56	2302	34	88
50	1112	47	207	15	1261	86	5.3	4.530	0.190	0.280	0.013	0.927	0.1177	0.0019	1733	35	1589	67	1921	29	83
51	934	53	114	24	1000	210	9.1	5.250	0.200	0.319	0.012	0.880	0.1186	0.0020	1858	32	1785	57	1934	31	92
76	259	24	45	6	430	62	5.5	11.450	0.580	0.465	0.021	0.933	0.1759	0.0028	2566	45	2458	93	2614	27	94
78	321	9	126	5	1135	63	2.6	9.930	0.320	0.398	0.017	0.745	0.1751	0.0045	2428	30	2157	80	2606	43	83
86	900	100	141	38	1240	200	6.1	6.420	0.330	0.359	0.013	0.899	0.1283	0.0037	2032	46	1978	65	2071	24	96
94	2600	130	790	81	5060	370	3.7	4.510	0.250	0.276	0.016	0.933	0.1195	0.0021	1730	47	1570	80	1948	31	81
105	317	24	79	3	709	46	4.1	6.520	0.180	0.368	0.014	0.749	0.1281	0.0038	2047	24	2019	64	2067	53	98
111	2640	330	296	87	1930	520	11.1	3.800	0.340	0.201	0.013	0.954	0.1372	0.0042	1582	72	1181	67	2188	53	54
113	324	15	74	7	631	40	4.8	11.600	0.370	0.460	0.017	0.862	0.1828	0.0032	2571	30	2439	76	2677	29	91
126	1130	230	278	74	1800	340	3.7	4.91	0.21	0.305	0.014	0.94775	0.1156	0.0017	1802	38	1717	70	1888	26	91
130	1850	190	403	33	3200	340	4.5	7.54	0.21	0.339	0.016	0.86893	0.1604	0.0039	2176	25	1882	76	2443	27	77
138	591	56	151	15	827	86	4.0	5.350	0.170	0.325	0.010	0.835	0.1185	0.0025	1876	27	1814	51	1932	37	94
139	371	22	86	8	597	53	4.4	5.130	0.180	0.323	0.015	0.716	0.1169	0.0031	1839	30	1801	71	1906	49	94
180	210	34	83	13	581	95	3.0	5.990	0.330	0.355	0.016	0.874	0.1244	0.0036	1971	49	1958	78	2018	52	97
184	690	140	111	8	810	130	6.4	3.670	0.600	0.233	0.036	0.982	0.1151	0.0023	1580	150	1340	190	1879	36	71
192	330	22	71	11	694	39	4.9	15.4	0.61	0.544	0.03	0.74176	0.2042	0.0053	2838	38	2800	120	2859	42	98
195	432	62	121	19	1000	260	3.7	6.750	0.260	0.379	0.015	0.894	0.1300	0.0028	2077	34	2071	72	2108	34	98
197	240	15	184	19	1560	140	1.3	6.340	0.270	0.378	0.017	0.775	0.1226	0.0036	2021	38	2062	81	1990	52	104

Table 5 continues

Analysis	Concentrations (ppm)[a]						Ratios								Ages (Ma)						CONC.
No	U	2 σ	Th	2 σ	Pb	2 σ	U/Th[a]	$^{207}Pb/^{235}U$[b]	2 σ[d]	$^{206}Pb/^{238}U$[b]	2 σ[d]	rho[c]	$^{207}Pb/^{206}Pb$[e]	2 σ[d]	$^{207}Pb/^{235}U$[b]	2 σ[d]	$^{206}Pb/^{238}U$[b]	2 σ[d]	$^{207}Pb/^{206}Pb$[e]	2 σ[d]	%
FHM140088B, meta-sandstone, Kalixälv group																					
7	339	17	123	7	912	39	2.8	5.446	0.097	0.339	0.008	0.902	0.1159	0.0013	1892	15	1879	39	1894	21	99
8	579	32	237	11	1693	79	2.6	5.480	0.130	0.344	0.009	0.943	0.1148	0.0014	1897	21	1906	44	1877	23	102
9	228	9	78	1	590	12	2.9	5.510	0.140	0.342	0.009	0.898	0.1149	0.0013	1901	23	1896	44	1877	20	101
10	236	39	29	7	158	20	8.8	6.020	0.250	0.378	0.018	0.966	0.1177	0.0016	1976	37	2064	82	1921	24	107
12	143	20	25	2	199	18	6.1	5.860	0.230	0.370	0.016	0.780	0.1174	0.0025	1953	34	2029	75	1915	39	106
13	391	34	100	26	720	180	4.8	6.230	0.250	0.377	0.014	0.887	0.1207	0.0023	2006	36	2073	60	1965	33	105
14	501	25	356	17	2570	150	1.4	5.542	0.091	0.350	0.009	0.739	0.1160	0.0018	1907	14	1932	41	1894	29	102
15	155	9	36	5	232	11	4.7	5.910	0.160	0.367	0.009	0.763	0.1176	0.0018	1962	23	2013	43	1919	28	105
16	228	18	89	9	860	110	2.6	14.190	0.350	0.542	0.013	0.630	0.1904	0.0044	2761	24	2790	56	2743	38	102
21	310	13	189	11	2041	72	1.7	13.270	0.290	0.509	0.013	0.508	0.1862	0.0030	2698	21	2651	57	2707	26	98
23	339	28	98	6	781	63	3.6	5.760	0.110	0.339	0.009	0.645	0.1193	0.0021	1939	17	1906	35	1944	31	98
24	420	32	160	13	1224	90	2.9	5.180	0.140	0.315	0.009	0.933	0.1189	0.0017	1848	23	1767	45	1940	25	91
25	334	27	108	4	911	50	3.2	6.020	0.170	0.343	0.009	0.894	0.1268	0.0019	1978	25	1900	45	2061	24	92
26	204	10	86	4	649	31	2.5	5.150	0.120	0.325	0.009	0.661	0.1154	0.0021	1848	21	1813	41	1884	33	96
27	384	88	210	37	1300	170	1.9	5.330	0.400	0.341	0.026	0.980	0.1135	0.0021	1889	54	1890	130	1855	33	102
28	180	57	40	11	500	110	5.2	17.630	0.880	0.660	0.036	0.917	0.1978	0.0027	2965	49	3260	140	2808	22	116
29	900	130	229	34	2280	430	4.1	11.620	0.240	0.456	0.014	0.706	0.1860	0.0034	2574	19	2422	60	2706	30	90
33	1368	81	56	17	460	140	29.7	5.620	0.130	0.329	0.011	0.747	0.1220	0.0021	1919	20	1831	52	1985	31	92
35	486	16	16	2	121	16	32.2	4.900	0.130	0.323	0.009	0.724	0.1100	0.0024	1802	22	1804	44	1797	40	100
36	754	51	236	14	1710	140	3.1	5.354	0.092	0.333	0.007	0.787	0.1168	0.0017	1882	17	1854	32	1907	27	97
37	334	61	18	8	142	65	25.6	15.900	0.250	0.574	0.014	0.690	0.1968	0.0031	2870	15	2923	57	2807	29	104
38	193	17	32	2	301	25	6.3	9.500	0.300	0.475	0.015	0.770	0.1447	0.0027	2385	30	2502	68	2282	31	110
39	227	12	115	8	1251	67	1.9	14.330	0.230	0.551	0.010	0.691	0.1843	0.0028	2771	15	2829	43	2691	25	105
40	832	36	128	4	1533	72	6.4	16.720	0.290	0.565	0.013	0.780	0.2173	0.0031	2918	17	2884	53	2960	23	97
41	350	25	108	9	802	49	3.4	6.810	0.340	0.406	0.022	0.947	0.1217	0.0019	2083	45	2190	100	1980	28	111
42	412	45	12	5	84	29	66.0	5.610	0.120	0.352	0.008	0.415	0.1139	0.0014	1917	19	1942	39	1862	23	104
46	1276	64	378	49	2830	230	3.6	5.190	0.160	0.319	0.010	0.930	0.1194	0.0015	1849	26	1782	50	1946	22	92
51	987	94	269	51	3300	590	3.9	12.670	0.360	0.485	0.020	0.907	0.1923	0.0053	2655	27	2549	85	2760	45	92
52	657	90	347	25	2530	230	1.8	5.049	0.075	0.316	0.008	0.418	0.1178	0.0025	1827	13	1777	33	1920	38	93
53	360	33	78	3	898	59	4.6	11.830	0.260	0.485	0.014	0.861	0.1777	0.0030	2590	21	2547	62	2630	27	97
59	340	40	209	18	2100	150	1.6	10.540	0.280	0.494	0.018	0.872	0.1514	0.0027	2482	25	2584	78	2360	31	109
60	357	65	54	6	360	17	6.5	13.390	0.460	0.508	0.019	0.895	0.1901	0.0036	2705	33	2646	82	2741	31	97
61	418	72	119	23	700	110	3.8	5.450	0.190	0.340	0.010	0.848	0.1152	0.0023	1891	30	1884	48	1880	36	100
62	551	23	146	13	951	70	4.0	5.180	0.091	0.324	0.009	0.543	0.1140	0.0019	1849	15	1807	42	1882	38	96
64	701	21	180	7	1444	64	4.0	6.660	0.120	0.392	0.011	0.846	0.1216	0.0020	2067	16	2132	51	1979	29	108
65	451	37	156	15	1290	130	2.8	5.730	0.180	0.354	0.012	0.824	0.1170	0.0030	1934	28	1953	59	1907	45	102

Table 5 continues

Analysis	Concentrations (ppm)[a]						Ratios								Ages (Ma)						CONC.
No	U	2 σ	Th	2 σ	Pb	2 σ	U/Th[a]	$^{207}Pb/^{235}U$[b]	2 σ[d]	$^{206}Pb/^{238}U$[b]	2 σ[d]	rho[c]	$^{207}Pb/^{206}Pb$[e]	2 σ[d]	$^{207}Pb/^{235}U$[b]	2 σ[d]	$^{206}Pb/^{238}U$[b]	2 σ[d]	$^{207}Pb/^{206}Pb$[e]	2 σ[d]	%
FHM140088B, meta-sandstone, Kalixälv group																					
66	956	50	395	53	3100	480	2.5	5.810	0.150	0.353	0.009	0.777	0.1189	0.0019	1947	21	1949	43	1938	30	101
67	288	8	144	5	1284	63	2.0	7.020	0.190	0.398	0.009	0.837	0.1286	0.0011	2114	24	2158	41	2078	15	104
72	544	39	130	16	919	60	4.1	5.080	0.140	0.324	0.011	0.764	0.1156	0.0019	1831	22	1808	52	1896	33	95
74	237	49	74	14	710	120	3.8	8.950	0.320	0.450	0.018	0.923	0.1414	0.0024	2331	34	2395	83	2243	29	107
75	555	68	218	34	2190	350	2.6	11.430	0.670	0.456	0.021	0.906	0.1818	0.0044	2552	53	2421	90	2667	40	91
77	377	55	162	34	1170	200	2.3	6.070	0.200	0.354	0.012	0.758	0.1256	0.0025	1984	29	1952	59	2036	36	96
79	545	64	145	26	1230	200	4.0	6.796	0.083	0.380	0.006	0.579	0.1284	0.0015	2085	11	2078	28	2076	21	100
80	209	29	98	18	1370	260	2.3	33.380	0.660	0.753	0.014	0.510	0.3231	0.0067	3591	20	3617	50	3583	32	101
81	301	26	9	2	93	14	36.4	13.630	0.320	0.548	0.014	0.748	0.1820	0.0039	2723	22	2817	60	2668	35	106
85	236	34	73	15	740	200	3.0	6.720	0.170	0.380	0.009	0.361	0.1267	0.0035	2074	22	2085	44	2076	38	100
87	335	23	90	8	746	76	3.5	5.687	0.090	0.338	0.006	0.400	0.1225	0.0025	1932	13	1875	29	1991	36	94
88	233	14	61	3	454	15	3.5	5.960	0.140	0.360	0.007	0.748	0.1174	0.0021	1968	21	1980	34	1915	32	103
89	93	6	43	3	335	20	2.1	6.010	0.140	0.348	0.008	0.494	0.1215	0.0030	1977	21	1925	37	1975	43	97
91	513	69	67	15	397	91	6.5	5.760	0.150	0.347	0.011	0.822	0.1182	0.0017	1938	23	1919	53	1929	25	99
92	362	85	71	14	450	110	4.9	6.140	0.190	0.362	0.015	0.872	0.1246	0.0028	2002	30	1989	70	2020	39	98
93	479	17	64	3	597	29	7.3	7.580	0.150	0.405	0.011	0.758	0.1341	0.0014	2182	18	2193	53	2152	19	102
94	530	36	44	7	420	55	12.2	6.100	0.140	0.357	0.012	0.684	0.1234	0.0030	1989	20	1966	55	2024	36	97
98	765	67	335	60	4060	690	2.5	19.560	0.470	0.576	0.016	0.701	0.2465	0.0036	3069	23	2931	66	3161	23	93
99	425	70	148	24	1210	210	2.8	5.480	0.140	0.343	0.011	0.744	0.1166	0.0024	1897	21	1899	53	1903	37	100
101	660	110	214	46	1880	370	3.3	9.710	0.200	0.425	0.012	0.779	0.1639	0.0027	2407	19	2281	52	2501	30	91
102	1440	190	530	130	3500	1000	2.8	5.030	0.210	0.304	0.014	0.892	0.1161	0.0019	1822	36	1711	69	1895	30	90
103	1164	80	381	28	3430	240	2.8	5.800	0.110	0.338	0.010	0.802	0.1238	0.0020	1951	19	1878	47	2011	28	93
104	501	18	173	11	2060	130	2.6	13.250	0.250	0.495	0.015	0.682	0.1938	0.0032	2697	18	2589	64	2773	28	93
105	143	10	65	10	480	31	2.2	5.530	0.120	0.334	0.008	0.857	0.1182	0.0015	1904	18	1857	36	1928	23	96
111	341	28	75	9	398	31	4.8	4.730	0.140	0.301	0.010	0.771	0.1164	0.0026	1772	24	1694	50	1909	36	89
112	210	11	96	3	738	23	2.3	6.780	0.120	0.395	0.008	0.618	0.1310	0.0022	2083	16	2147	37	2110	29	102
115	277	23	155	13	1032	97	2.0	5.490	0.110	0.351	0.008	0.744	0.1182	0.0021	1898	17	1940	37	1928	31	101
116	913	47	691	62	4620	510	1.5	6.150	0.110	0.369	0.007	0.552	0.1260	0.0020	1997	15	2025	35	2042	28	99
117	470	35	221	13	1499	70	2.2	5.900	0.100	0.349	0.007	0.675	0.1252	0.0023	1965	17	1932	32	2031	33	95
118	1569	51	465	84	3130	550	3.7	5.510	0.130	0.349	0.009	0.826	0.1170	0.0018	1901	20	1929	45	1909	28	101
119	416	29	168	28	933	93	2.8	5.400	0.120	0.344	0.010	0.767	0.1175	0.0019	1883	20	1905	47	1918	29	99
120	524	70	177	13	1398	90	2.9	6.550	0.120	0.377	0.009	0.870	0.1274	0.0016	2053	16	2063	43	2062	22	100
124	804	27	512	44	4610	390	1.5	10.470	0.230	0.461	0.011	0.822	0.1633	0.0022	2476	21	2442	50	2496	19	98
127	992	60	158	12	1270	120	6.2	6.590	0.110	0.381	0.009	0.203	0.1249	0.0031	2057	15	2081	41	2040	35	102
128	358	10	122	4	1010	43	2.9	5.790	0.110	0.343	0.009	0.771	0.1230	0.0026	1945	16	1901	45	1998	38	95
129	708	78	236	81	1650	520	3.3	5.640	0.180	0.343	0.013	0.852	0.1184	0.0018	1920	28	1901	62	1932	27	98
130	154	10	49	3	382	26	3.1	5.170	0.110	0.322	0.008	0.721	0.1152	0.0019	1846	17	1798	38	1881	31	96

Table 5 continues

Analysis	Concentrations (ppm)[a]						Ratios								Ages (Ma)						CONC.
No	U	2 σ	Th	2 σ	Pb	2 σ	U/Th[a]	$^{207}Pb/^{235}U$[b]	2 σ[d]	$^{206}Pb/^{238}U$[b]	2 σ[d]	rho[c]	$^{207}Pb/^{206}Pb$[e]	2 σ[d]	$^{207}Pb/^{235}U$[b]	2 σ[d]	$^{206}Pb/^{238}U$[b]	2 σ[d]	$^{207}Pb/^{206}Pb$[e]	2 σ[d]	%
FHM140088B, meta-sandstone, Kalixälv group																					
131	725	89	137	25	1110	210	5.8	5.800	0.210	0.332	0.010	0.752	0.1269	0.0026	1944	31	1847	48	2053	37	90
132	331	28	262	44	1970	310	1.4	6.070	0.120	0.338	0.012	0.866	0.1308	0.0025	1985	18	1877	58	2107	34	89
133	354	38	255	40	1920	330	1.4	5.370	0.110	0.340	0.006	0.733	0.1142	0.0011	1879	18	1887	30	1868	17	101
138	548	93	199	59	1380	400	3.3	5.075	0.088	0.310	0.008	0.848	0.1164	0.0017	1831	15	1742	41	1900	27	92
139	433	53	32	4	246	35	14.7	5.720	0.160	0.343	0.010	0.912	0.1196	0.0015	1933	24	1902	49	1950	22	98
140	221	25	101	3	749	24	2.3	5.820	0.140	0.352	0.009	0.689	0.1198	0.0016	1949	21	1943	44	1952	24	100
141	948	61	217	10	2510	130	4.5	12.720	0.390	0.473	0.019	0.806	0.1928	0.0045	2658	29	2493	83	2765	38	90
144	325	16	31	3	226	15	11.3	5.640	0.210	0.347	0.013	0.644	0.1145	0.0024	1921	33	1920	61	1871	39	103
145	396	44	165	35	1300	280	2.3	7.120	0.180	0.386	0.010	0.725	0.1337	0.0016	2126	22	2104	46	2147	21	98
146	377	27	70	8	490	39	5.7	6.240	0.200	0.362	0.010	0.876	0.1225	0.0020	2008	29	2003	51	1991	30	101
150	316	52	65	9	477	80	4.7	5.884	0.093	0.351	0.007	0.591	0.1220	0.0021	1958	14	1941	32	1985	30	98
151	640	130	152	26	1180	210	3.9	5.740	0.130	0.350	0.009	0.736	0.1199	0.0021	1936	20	1935	43	1954	31	99
152	260	33	61	5	507	40	4.1	6.190	0.140	0.368	0.011	0.905	0.1237	0.0014	2003	20	2018	50	2010	20	100
153	550	150	148	37	910	250	3.3	5.590	0.170	0.352	0.010	0.927	0.1171	0.0017	1913	26	1944	50	1924	26	101
154	623	80	113	27	930	210	5.7	6.760	0.260	0.366	0.014	0.903	0.1352	0.0023	2078	34	2010	65	2165	30	93
155	185	37	150	19	1010	180	1.2	5.840	0.260	0.355	0.013	0.945	0.1212	0.0017	1951	38	1956	62	1974	26	99
156	151	15	87	18	664	92	1.8	7.140	0.110	0.402	0.011	0.804	0.1296	0.0021	2129	14	2178	49	2091	29	104
157	1780	190	384	35	2880	260	4.5	5.270	0.140	0.311	0.011	0.840	0.1236	0.0016	1864	23	1746	53	2008	23	87
163	630	120	143	22	1230	170	4.5	6.720	0.170	0.381	0.012	0.934	0.1283	0.0023	2073	24	2078	57	2073	31	100
164	548	46	59	6	669	73	9.9	12.930	0.440	0.507	0.019	0.889	0.1846	0.0033	2681	28	2639	83	2693	30	98
165	242	20	125	16	1150	150	2.0	7.400	0.190	0.403	0.014	0.828	0.1321	0.0022	2159	23	2182	63	2125	30	103
166	609	19	105	5	723	41	5.9	5.220	0.140	0.332	0.010	0.877	0.1145	0.0022	1855	22	1845	46	1871	35	99
167	278	42	34	3	258	30	8.3	5.820	0.160	0.357	0.007	0.691	0.1188	0.0022	1947	23	1967	34	1936	33	102
168	728	21	268	21	2460	140	2.8	8.690	0.230	0.407	0.012	0.803	0.1529	0.0021	2305	24	2199	54	2378	23	92
169	876	79	293	24	2400	190	3.0	6.710	0.150	0.382	0.011	0.906	0.1255	0.0017	2073	20	2084	53	2036	24	102
170	678	45	166	49	2370	450	3.8	25.400	2.300	0.652	0.046	0.964	0.2825	0.0082	3317	78	3230	170	3375	46	96
171	807	37	135	6	800	28	6.0	5.322	0.091	0.331	0.005	0.662	0.1160	0.0013	1872	15	1842	26	1900	23	97
172	520	140	143	44	1070	400	3.5	6.250	0.200	0.360	0.015	0.922	0.1273	0.0017	2017	24	1982	70	2060	23	96
176	377	95	320	110	3000	1100	1.6	11.320	0.450	0.495	0.020	0.919	0.1663	0.0027	2556	34	2588	87	2520	27	103
177	1424	75	278	41	1980	280	5.1	5.450	0.120	0.328	0.006	0.654	0.1190	0.0018	1892	18	1826	28	1941	27	94
178	576	94	291	66	2640	600	2.2	10.490	0.270	0.475	0.016	0.910	0.1613	0.0024	2478	23	2504	70	2468	25	101
179	286	28	121	17	740	120	3.0	5.670	0.170	0.346	0.011	0.906	0.1186	0.0021	1925	27	1916	53	1933	33	99
180	365	19	108	5	813	32	3.5	6.120	0.160	0.370	0.010	0.689	0.1230	0.0024	1991	22	2028	48	1999	34	101
181	298	28	149	23	1200	240	2.0	6.970	0.270	0.399	0.016	0.842	0.1292	0.0023	2105	35	2163	74	2086	31	104
182	299	28	104	9	756	61	2.9	5.790	0.190	0.365	0.013	0.847	0.1164	0.0024	1942	29	2003	63	1899	37	105
183	820	180	460	140	2420	510	2.0	6.090	0.430	0.353	0.024	0.960	0.1265	0.0024	1995	59	1950	120	2057	31	95
184	344	20	144	9	1026	81	2.4	6.010	0.160	0.364	0.008	0.841	0.1212	0.0020	1975	23	2001	36	1973	30	101

Table 5 continues

Analysis	Concentrations (ppm)[a]						Ratios								Ages (Ma)						CONC.
No	U	2 σ	Th	2 σ	Pb	2 σ	U/Th[a]	$^{207}Pb/^{235}U$[b]	2 σ[d]	$^{206}Pb/^{238}U$[b]	2 σ[d]	rho[c]	$^{207}Pb/^{206}Pb$[e]	2 σ[d]	$^{207}Pb/^{235}U$[b]	2 σ[d]	$^{206}Pb/^{238}U$[b]	2 σ[d]	$^{207}Pb/^{206}Pb$[e]	2 σ[d]	%
FHM140088B, meta-sandstone, Kalixälv group																					
185	1400	110	316	10	2228	63	4.5	5.560	0.110	0.335	0.008	0.334	0.1207	0.0027	1909	16	1862	39	1963	39	95
190	140	11	47	4	352	30	2.9	5.270	0.130	0.326	0.007	0.683	0.1183	0.0020	1863	21	1816	35	1929	31	94
191	510	110	132	28	780	180	3.8	5.770	0.180	0.334	0.010	0.732	0.1220	0.0028	1940	27	1855	49	1984	40	93
192	330	22	84	4	609	34	3.8	5.660	0.110	0.345	0.009	0.792	0.1186	0.0023	1925	17	1912	43	1933	35	99
193	159	10	97	4	707	22	1.7	6.250	0.140	0.375	0.010	0.595	0.1194	0.0023	2011	19	2064	44	1967	34	105
194	297	27	130	11	971	90	2.2	5.530	0.150	0.339	0.011	0.925	0.1184	0.0021	1904	23	1880	55	1930	32	97
195	238	30	24	1	177	12	9.4	6.170	0.120	0.360	0.008	0.845	0.1226	0.0019	1999	17	1983	37	1993	28	99
196	189	17	49	8	263	18	4.4	6.490	0.150	0.371	0.009	0.942	0.1258	0.0014	2044	20	2031	40	2039	20	100
197	694	44	279	8	1791	55	2.5	5.360	0.120	0.333	0.005	0.591	0.1153	0.0022	1877	19	1851	25	1883	34	98
202	950	120	193	47	1310	330	5.2	5.220	0.130	0.324	0.008	0.798	0.1155	0.0019	1854	21	1810	38	1893	31	96
203	289	24	94	7	677	44	3.1	5.620	0.110	0.335	0.010	0.740	0.1214	0.0023	1919	18	1863	50	1975	33	94
204	209	11	67	2	623	29	3.2	10.770	0.170	0.474	0.008	0.545	0.1692	0.0022	2503	14	2500	35	2549	22	98
205	200	11	23	4	344	58	9.2	13.270	0.290	0.525	0.015	0.260	0.1850	0.0030	2698	21	2721	64	2706	24	101
206	127	6	26	1	186	7	5.0	5.140	0.100	0.324	0.007	0.531	0.1165	0.0024	1845	16	1809	34	1909	39	95
207	235	5	63	3	498	30	3.9	5.960	0.110	0.359	0.008	0.695	0.1221	0.0018	1970	16	1977	37	1986	27	100
208	223	7	129	4	1320	75	1.8	12.470	0.300	0.509	0.012	0.587	0.1793	0.0044	2640	23	2653	51	2659	34	100
209	106	9	43	4	293	22	2.6	5.140	0.110	0.334	0.011	0.603	0.1142	0.0026	1842	19	1859	51	1865	41	100
Common-Pb corrected[f]																					
11	415	71	195	22	1690	110	2.2	8.320	0.440	0.391	0.020	0.914	0.1551	0.0031	2263	49	2124	92	2402	34	88
20	1558	88	799	38	5510	290	2.0	4.890	0.120	0.284	0.011	0.709	0.1258	0.0028	1800	21	1609	53	2039	40	79
22	970	240	322	84	3330	900	3.2	12.040	0.340	0.427	0.031	0.564	0.1990	0.0120	2607	26	2280	140	2804	96	81
34	1200	380	248	61	1090	330	4.5	5.120	0.500	0.317	0.031	0.975	0.1154	0.0018	1831	80	1770	150	1886	28	94
47	318	22	46	3	930	160	7.2	6.310	0.250	0.370	0.015	0.785	0.1237	0.0030	2016	35	2048	64	2007	44	102
48	382	29	115	11	348	58	3.4	4.810	0.130	0.298	0.009	0.781	0.1167	0.0018	1785	23	1682	42	1906	27	88
49	1036	78	308	27	2280	200	3.6	5.163	0.076	0.317	0.009	0.779	0.1182	0.0021	1850	14	1773	45	1934	34	92
50	740	140	363	58	2570	550	1.9	5.760	0.160	0.342	0.012	0.896	0.1229	0.0020	1939	24	1897	59	1997	29	95
63	381	60	470	160	1360	220	1.3	5.420	0.550	0.339	0.028	0.967	0.1126	0.0026	1876	83	1880	130	1840	42	102
68	251	12	117	10	954	63	2.1	6.380	0.120	0.390	0.015	0.776	0.1175	0.0032	2029	16	2121	71	1914	49	111
73	1930	480	580	140	2530	530	3.2	3.130	0.310	0.211	0.018	0.988	0.1081	0.0016	1454	85	1231	99	1767	26	70
76	393	28	66	14	585	87	6.4	5.570	0.130	0.350	0.007	0.754	0.1183	0.0023	1910	21	1935	34	1928	35	100
78	560	95	248	44	1420	300	2.3	12.070	0.430	0.463	0.015	0.777	0.1913	0.0032	2607	33	2450	68	2752	28	89
86	865	83	190	24	1820	300	4.2	9.19	0.24	0.417	0.017	0.92872	0.159	0.0023	2357	24	2246	76	2444	25	92
90	1220	210	497	81	3280	740	2.5	5.06	0.29	0.305	0.018	0.96848	0.1193	0.0013	1826	50	1712	92	1945	20	88
113	700	160	255	74	1220	290	3.4	5.060	0.410	0.335	0.027	0.988	0.1134	0.0014	1818	70	1860	130	1854	23	100
114	552	49	168	11	1240	100	3.5	5.610	0.110	0.358	0.006	0.587	0.1175	0.0022	1917	17	1974	30	1916	34	103
126	668	30	831	33	7150	260	0.8	8.060	0.160	0.392	0.008	0.908	0.1476	0.0022	2237	18	2133	38	2323	28	92
137	468	76	220	41	1230	250	2.2	5.740	0.200	0.344	0.009	0.900	0.1208	0.0025	1935	31	1903	43	1974	34	96

Table 5 continues

Analysis	Concentrations (ppm)[a]						Ratios									Ages (Ma)						CONC.
No	U	2 σ	Th	2 σ	Pb	2 σ	U/Th[a]	^{207}Pb/^{235}U[b]	2 σ[d]	^{206}Pb/^{238}U[b]	2 σ[d]	rho[c]	^{207}Pb/^{206}Pb[e]	2 σ[d]		^{207}Pb/^{235}U[b]	2 σ[d]	^{206}Pb/^{238}U[b]	2 σ[d]	^{207}Pb/^{206}Pb[e]	2 σ[d]	%
FHM140088B, meta-sandstone, Kalixälv group																						
142	414.9	9.1	388	48	3330	200	1.1	10.73	0.27	0.431	0.012	0.67121	0.1765	0.004		2498	24	2309	56	2627	41	88
143	160	7	60	3	439	21	2.8	5.320	0.150	0.323	0.007	0.698	0.1187	0.0026		1871	24	1804	35	1935	39	93
198	2580	100	860	35	30900	1200	3.1	4.940	0.180	0.283	0.011	0.933	0.1264	0.0028		1808	32	1605	54	2046	39	78

CONC. = Concorcance (Tera Wasserburg)

[a]U, Th and Pb concentrations with errors (2SE) and U/Th ratios are calculated relative to the GJ-1 reference zircon

[b]Corrected for background, downhole and within-run Pb/U fractionation. Normalised to the reference zircon GJ-1 (TIMS/measured values)

The ^{207}Pb/^{235}U is calculated through: (^{207}Pb/^{206}Pb)/(^{238}U/^{206}Pb * 1/137.88)

[c]Rho is the error correlation defined as the quotient of the propagated errors of the ^{206}Pb/^{238}U and ^{207}/^{235}U ratios

[d]Quadratic addition of within-run errors (2 SE) and the all-session reproducibility of GJ-1 (2 SE)

[e]Normalised to the GJ-1 reference zircon (~0.6 per atomic mass unit)

[f]Common Pb correction through measured Pb^{204} (corrected for Hg^{204} using natural abundance Hg isotopic ratios) and the model Pb composition of Stacey & Kramers (1975)

Table 6. SIMS U-Pb-Th zircon data on Pahakurkio upper sandstone sample (RR96128, laboratory id n1383).

Sample/ spot #	Comment	U ppm	Th ppm	Pb ppm	Th/U calc [*1]	^{238}U/^{206}Pb	±σ %	^{207}Pb/^{206}Pb	±σ %	Disc. % conv. [*2]	Disc. % 2σ lim. [*3]	^{207}Pb/^{206}Pb	±σ Ma	^{206}Pb/^{238}U	±σ Ma	^{206}Pb/^{204}Pb meas.	f_{206}% [*4]
n1383-01a	CL-grey, margin	349	187	164	0.55	2.732	1.29	0.3661	1.29	0.3		2005	6	2011	22	43304	0.04
n1383-01b	CL-grey, central	185	136	89	0.69	2.768	1.31	0.3613	1.31	-0.5		1997	9	1988	22	49945	{0.04}
n1383-02a	CL-dark grey, margin	793	61	301	0.06	2.986	1.29	0.3349	1.29	-3.1	-0.4	1914	5	1862	21	22821	0.08
n1383-02b	CL-light-grey, osc zon, central	327	339	173	0.99	2.673	1.29	0.3742	1.29	-2.0		2085	6	2049	23	85644	{0.02}
n1383-03a	CL-dark grey, margin	476	46	198	0.09	2.752	1.29	0.3634	1.29	1.9		1966	6	1998	22	29054	0.06
n1383-04a	CL-grey, margin	473	197	218	0.40	2.685	1.29	0.3724	1.29	-0.4		2047	6	2041	23	39121	0.05
n1383-05a	CL-grey, margin	256	126	107	0.43	2.966	1.29	0.3371	1.29	-1.5		1898	9	1873	21	13017	0.14
n1383-05b	CL-dark grey, central	366	140	157	0.40	2.863	1.29	0.3493	1.29	2.3		1894	7	1931	22	21331	0.09
n1383-06a	CL-dark grey, osc. zon., margin	482	147	206	0.26	2.794	1.29	0.3579	1.29	1.1		1953	6	1972	22	35459	0.05
n1383-06b	CL-grey, central	181	118	78	0.49	2.946	1.29	0.3395	1.29	-3.8	-0.4	1948	9	1884	21	19157	0.1
n1383-07a	CL-darkgrey	491	243	329	0.49	1.957	1.29	0.5110	1.29	0.6		2648	4	2661	28	104433	0.02
n1383-08a	CL-grey, margin	173	139	76	0.75	3.043	1.29	0.3286	1.29	-4.6	-1.1	1909	10	1832	21	16729	0.11
n1383-08b	CL-grey, osc. zon, central	101	58	44	0.55	2.926	1.29	0.3417	1.29	-0.3		1901	15	1895	21	17843	{0.10}

CL = Cathodoluminescence, osc. Zon = oscillatory zoned (Roye Rutland, pers. com)

Isotope values are common Pb corrected using modern common Pb composition (Stacey & Kramers 1975) and measured ^{204}Pb.

[*1] Th/U ratios calculated from ^{208}Pb/^{206}Pb and ^{207}Pb/^{206}Pb ratios, assuming a single stage of closed U-Th-Pb evolution

[*2] Age discordance in conventional concordia space. Positive numbers are reverse discordant.

[*3] Age discordance at closest approach of error ellipse to concordia (2σ level).

[*4] Figures in parentheses are given when no correction has been applied, and indicate a value calculated assuming present-day Stacey-Kramers common Pb.

Sm-Nd isotopic analysis

Method

For whole-rock Sm-Nd analysis, 120–200 mg of powdered sample was spiked with a ^{149}Sm-^{150}Nd tracer. The sample-spike mixture was dissolved in HF-HNO_3 in sealed Teflon bombs in an oven at 180°C (felsic rocks) or in Savillex screw-cap beakers on a hot plate (mafic rocks) for 48 hours. Before dissolving the residue in 6.2 N HCl, the fluorides were gently evaporated using HNO_3. Conventional cation exchange chromatography was used to separate the light rare earth elements and Sm and Nd were further separated by a modified Teflon-HDEHP (hydrogen di-ethylhexyl phosphate) method (Richard et al. 1976). Total procedural blank was <0.5 ng for Nd. Isotope ratios were measured on a VG Sector 54 TIMS using Ta-Re triple filaments. Nd isotope ratios were measured in dynamic mode and Sm isotopes in static mode. Nd ratios are normalised to $^{146}Nd/^{144}Nd = 0.7219$. Based on several duplicate analyses, the error of the $^{147}Sm/^{144}Nd$ is estimated to be better than 0.6%. The long-term average $^{143}Nd/^{144}Nd$ for the La Jolla standard is 0.511850 ±0.000010 (standard deviation for 220 measurements during 1996–2010). Recent analysis on BCR-1 yielded Sm = 6.63 ppm, Nd = 28.88 ppm, $^{143}Nd/^{144}Nd = 0.512640 \pm 0.000010$. The ε_{Nd} was calculated using $\lambda 147Sm = 6.54 \times 10^{-12}\ a^{-1}$, $^{147}Sm/^{144}Nd = 0.1966$, and $^{143}Nd/^{144}Nd = 0.512640$ for the present CHUR (Jacobsen & Wasserburg 1980). TDM was calculated after DePaolo (1981). Plotting and calculations of isotope data were performed using Isoplot software (Ludwig 2012).

Results and interpretation of data

Sm-Nd isotopic analysis was performed on the same samples as selected for geochronology (see previous section). Two meta-andesitic samples from the Sakarinpalo suite and the Kalixälv group, record $\varepsilon_{Nd(1.89Ga)}$ -3.9 and -2.2 values, and depleted mantle model ages of approximately 2.4 Ga, respectively (Table 7). Volcanic rocks of the Kiirunavaara group as well as early Svecokarelian intrusive rocks record overall negative initial ε_{Nd} signatures (i.e. lie below the CHUR reference value (Fig. 16). This is suggested to be a result of variable anatexis of the Archaean basement rocks, which by approximately 1.9 Ga had acquired distinctly negative ε_{Nd} values (< -10; Fig. 16). Sm-Nd isotopic analyses of Palaeoproterozoic granitoids and metavolcanic rocks approximately delineate the Archaean palaeoboundary zone between the reworked Archaean craton in the north and more juvenile Palaeoproterozoic domains to the south along the Luleå–Jokkmokk zone in Sweden and along the Raahe–Ladoga zone in Finland (Fig. 1, Huhma 1986, Öhlander et al. 1993, Mellqvist et al. 1999, Vaasjoki & Sakko 1988, Nironen 1997). In contrast, Svecofennian arc volcanism in the Skellefte field south of the Norrbotten ore province records positive initial ε_{Nd} signatures ($\varepsilon_{Nd(1.89Ga)}$ 2.7 and 4.0) close to the depleted mantle model line. It is suggested that this is the result of 'juvenile' melts above a north-dipping subduction zone at the continental margin or possibly in an island arc accreted to the craton (Hietanen 1975, Nironen 1997, Weihed et al. 2005). The Veikkavaara greenstones, which are part of Karelian, approximately 2.1 Ga rift-related magmatism in Norrbotten, have whole-rock initial ε_{Nd} values from 0.4 to +3.7 (Fig. 16), indicating juvenile depleted to partly-enriched tholeiitic mantle melts with minor assimilation of older continental crust of the Archaean Norrbotten craton during magma ascent or storage (Lynch et al. 2018b).

Meta-sandstones from the Pahakurkio and Kalixälv groups record similar $\varepsilon_{Nd(1.89Ga)}$ values at -3.0 and -3.9, respectively, consistent with a mixture of debris from predominantly 2.2–1.9 Ga and 3.0–2.6 Ga-old rocks, as suggested by U-Pb provenance zircon dating of these samples.

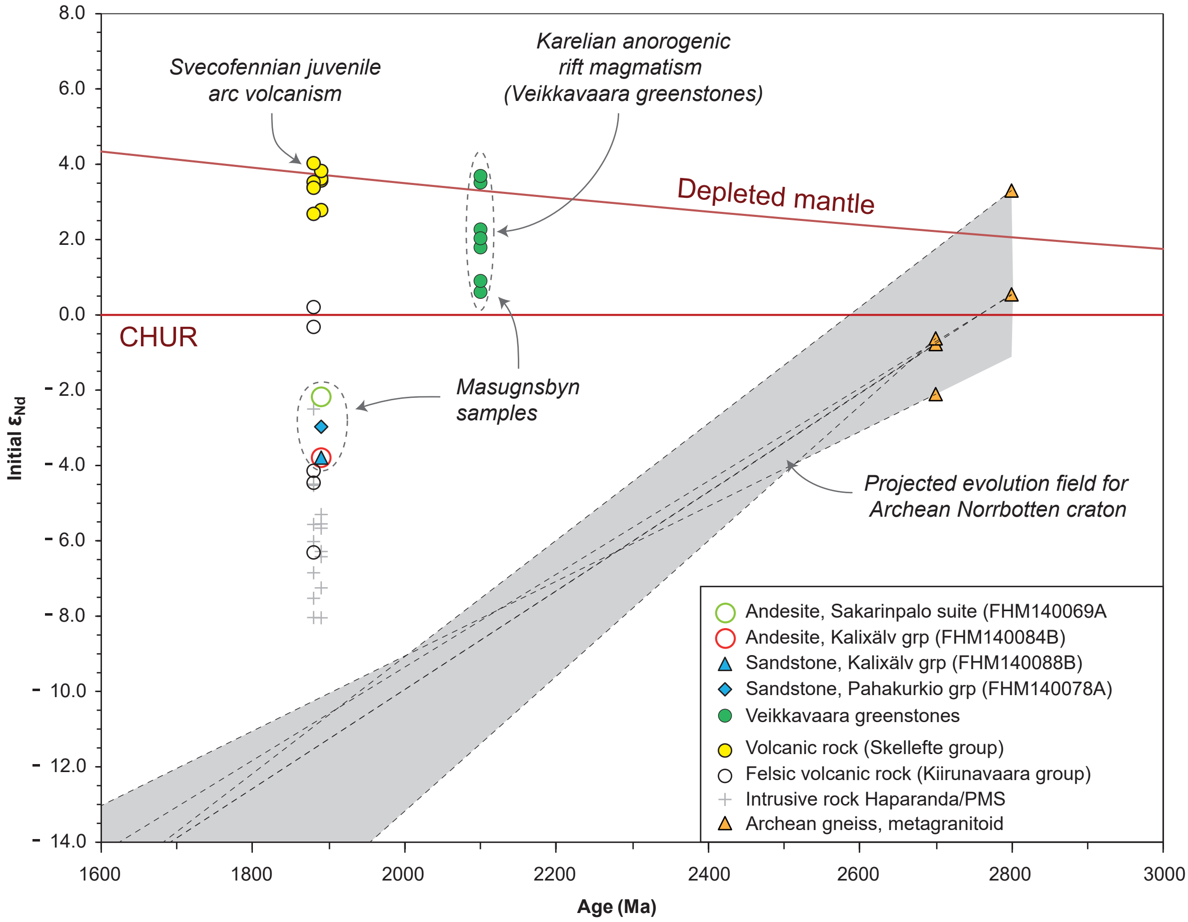

Figure 16. Initial ε_{Nd} versus time plot for rock samples from Masugnsbyn. Data from selected age groups and rock types from northern Norrbotten are shown for comparison, as well as data from the Skellefte group volcanic rocks. DM = depleted mantle model curve, based on DePaolo (1981), CHUR = chondrite uniform reservoir (e.g., DePaolo & Wasserburg 1976). The rocks are metamorphic with the prefix meta- to be added to rock names. References to data: Öhlander et al. (1987a, b, 1993), Skiöld et al. (1988), Kathol & Weihed (2005), Lynch et al. (2018b).

Table 7. Sm-Nd-isotopic data from Svecofennian supracrustal rocks in the Masugnsbyn area. Sm-Nd data from the Veikkavaara greenstones are presented in Lynch et al. (2018b).

Sample	N Sweref	E Sweref	Rock type	Unit	Sm (ppm)	Nd (ppm)	Sm/Nd	$^{147}Sm/^{144}Nd$	Error ±2σ	$^{143}Nd/^{144}Nd$	Error ±2σ	ε_{Nd} 1890 Ma	T-DM (Ma)
FHM140069A	7502412	803618	Andesite	Sakarinpalo suite	4.5	27.5	0.16	0.0991	0.0006	0.511231	0.000010	-3.9	2409
FHM140078A	7493033	804679	Sandstone	Pahakurkio grp	3.9	19.5	0.20	0.1194	0.0007	0.511525	0.000012	-3.0	2455
FHM140084B	7487854	799400	Andesite	Kalixälv grp	8.0	40.0	0.20	0.1204	0.0007	0.511578	0.000010	-2.2	2392
FHM140088B	7487141	800148	Sandstone	Kalixälv grp	4.3	22.4	0.19	0.1150	0.0007	0.511429	0.000010	-3.9	2495

Laboratory assistance by Leena Järvinen and Arto Pulkkinen are acknowledged.
For methods see Huhma et al (2012).
Measurements were made on VG Sector 54 mass-spectrometer.
Error in $^{147}Sm/^{144}Nd$ is 0.6% (spiked Sm and $^{150}/^{144}Nd$ was measured using single collector mode).
$^{143}Nd/^{144}Nd$ ratio is normalized to $^{146}Nd/^{144}Nd$=0.7219.
Long-term average $^{143}Nd/^{144}Nd$ for the La Jolla standard at GTK is 0.511851±0.00008 (standard deviation for 60 measurements during 2012).
Depleted mantle model age (T-DM) was calculated after DePaolo (1981).
Rocks are metamorphic with prefix meta- to be added to rock names.

DISCUSSION AND PRELIMINARY CONCLUSIONS

Interpretation of the depositional environment for supracrustal rocks in the Pahakurkio and Kalixälv groups is given below and mainly follows Padget (1970), Niiniskorpi (1986) and Kumpulainen (2000). Heavy mineral layers and cross-bedding are common in the lower and upper sandstone units of the Pahakurkio group, and ripple and rill marks are found locally, suggesting a coastal marine depositional environment affected by wave and possibly storm activity. The interval of pebbly conglomerates may represent a storm event resulting in erosion on the shelf and transport of pebbly debris from the shoreline setting. The gradual facies change from the deposition characterised by hummocky cross-stratification and low-angle cross-bedding of the lower sandstone unit into the normally graded and ripple-laminated sandy mudstones of the upper shale suggests a gradual increase in relative water depth, where the locally graphite-bearing shales represent deposition in stagnant waters beneath the storm wave base. There appears to be a gradual transition from the upper shale unit to the upper sandstone unit, with localised normally graded bedding in the transition zone. Sandstone deposition gradually takes over and the upper sandstone unit is characterised by horizontal lamination and low-angle cross-bedding, which, together with common wave ripples, indicate a shallow water coastal depositional environment, similar to the lower sandstone unit. Thus, the whole Pahakurkio group represents two consecutive cycles of deepening and shallowing related to corresponding relative sea level changes. The changes in relative water depth could depend on: (a) real sea level changes; (b) changes in input of clastic material; (c) subsidence of the basin floor; or (d) a combination of these factors.

The sandstones of the Pahakurkio group are immature arkoses to subarkoses, and major and trace element chemistry suggests predominantly continental crust source rocks. According to Boggs (2009), feldspar-rich sandstones typically come from rapid erosion of feldspar-rich felsic to intermediate crystalline plutonic or metamorphic rocks, where chemical weathering is subordinate to physical weathering. Transportation of the arkosic material results in better sorting and various degrees of grain rounding, especially when further transported into marine environments, where feldspar-rich sandstone may be inter-bedded with a variety of marine deposits including shales, limestones, and evaporates. A marine depositional environment for the Pahakurkio group sediments is further supported by the presence of tourmaline as a common boron-bearing accessory phase in the sedimentary rocks. Carbonate layers may represent chemically deposited sediments, whereas scapolite-rich rocks may have an evaporitic origin.

The stratigraphically higher Kalixälv group consists of similar types of metasedimentary rocks to the Pahakurkio group, i.e. originally shales and sandstone, but with a generally higher grade of metamorphic alteration and less preserved primary structures. Cross-bedding and wave-ripples can be seen locally in quartzitic rocks, suggesting shallow water deposition. Thus, the depositional environment appears similar to the Pahakurkio group, with vertical facies changes into relatively deeper water where, in part, graphite-bearing shales represent deposition in stagnant waters beneath the storm wave base. A distinct difference is the much greater abundance of volcanic and volcanogenic sedimentary rocks in the Kalixälv group than in the Pahakurkio group. Extensive volcanism is a potentially important heat source driving both hydrothermal alteration and the generation of minor Zn-Pb-Cu and Cu ±Au sulphide mineralisations that occur in the border zone between the Pahakurkio and Kalixälv groups. However, the partly vein-hosted character suggests a later, epigenetic origin. A positive correlation exists between B and Zn + Pb content in lithochemical analyses from the Kurkkionvaara Zn-Pb-Cu mineralisation, suggesting a hydrothermal system with boron-rich fluids containing base metals (Niiniskorpi 1986). Boron-rich fluids probably have a source in the metapelites, originally deposited as marine sediments, and tourmaline-rich rocks could potentially be used as an exploration tool.

A maximum depositional age of the Kalixälv group of approximately 1.87 Ga, as suggested by U-Pb zircon provenance age data, is somewhat lower than the 1 887 ±5 Ma U-Pb zircon age obtained from the plagioclase porphyric meta-andesite within the same group, and the migmatisation age of

1878 ±3 Ma obtained from the high-grade southern part of the Masugnsbyn area (Hellström 2018). The latter age must constrain the deposition of sediments as older than approximately 1.88 Ga. A limited amount of SIMS analyses on zircon core domains from a migmatitic paragneiss record an age distribution similar to the meta-arenite sample in this study, with the majority of ages in the 2.02–1.92 Ga and 2.97–2.75 Ga intervals (Hellström 2018).

The lower sandstone sample (FHM140078A) in the Pahakurkio group shows a zircon age distribution pattern dominated by 2.15–1.90 Ga (66%) and 2.95–2.62 Ga ages (30%), similar to the intermediate sandstone in the Kalixälv group, dominated by 2.15–1.86 Ga ages (81%) and 2.96–2.55 Ga ages (11%). The younger age interval of the Pahakurkio group, however, has slightly older ages, peaking at 2.04 Ga and with a maximum depositional age estimated at approximately 1.91 Ga from the youngest zircons. Zircon age data from the Pahakurkio upper sandstone unit (sample RR96128) show a similar age distribution pattern to the lower sandstone unit, although based on a very limited number of analyses (n = 13) of the former. The maximum depositional age is calculated from the three youngest zircon grains at approximately 1.90 Ga, and is similar or slightly younger than the maximum depositional age from the lower Pahakurkio sandstone unit.

Overall, the zircon age distribution patterns are consistent with the Kalixälv group being younger than the Pahakurkio group, according with field-based way-up determinations. The lower quantity of Archaean zircons in the Kalixälv group sample (13%) compared with the Pahakurkio group sample (31%), suggests that the Archaean basement was covered by Svecofennian rocks as the Svecokarelian orogeny progressed, and thus erosion and deposition of debris from the latter were more predominant. This scenario could explain the peak offset seen in the 2.2–1.9 Ga age interval between the Pahakurkio and Kalixälv groups, with maximum peaks shifting from 2.04 to 1.93 Ga, although the Pahakurkio sample does have a pronounced peak at approximately 1.92 Ga. Archaean rocks are exposed in the Råstojaure complex in northernmost Sweden (Martinsson et al. 1999, Lauri et al. 2016). Sm-Nd isotopic analyses of Proterozoic granitoids and metavolcanic rocks suggest a covered Archaean basement south of the Råstojaure complex (Öhlander et al. 1993, Mellqvist et al. 1999). So far, there are few age determinations from felsic to intermediate igneous rocks in the 2.2–1.92 Ga interval, but some do exist from the Savo schist belt within the Raahe–Ladoga zone in Finland, at Norvijaur in the Jokkmokk area and in the Rombak–Sjangeli basement window of the Caledonides, all along the Archaean–Palaeoproterozoic boundary (Helovuori 1979, Korsman et al. 1984, Vaasjoki & Sakko 1988, Kousa et al. 1994, Lahtinen & Huhma 1997, Vaasjoki et al. 2003, Kousa et al. 2013, Skiöld et al. 1993, Romer et al. 1992; Hellström 2015). In addition, 1.96–1.94 Ga calc-alkaline rocks with island arc affinity occur in the northern part of the Bothnian basin, south of the Skellefte district (Wasström 1993, 1996, Lundqvist et al. 1998, Eliasson et al. 2001, Skiöld & Rutland 2006). It can be concluded from zircon age provenance data that 2.2–1.9 Ga felsic to intermediate rocks can be expected to be present to a far greater extent than is known from present age determination of the rocks within the Svecokarelian orogen, or suggest the presence of a still unlocated major continental block that must have existed somewhere nearby to supply the abundant detritus material. This pattern is observed in several other provenance studies of Svecofennian sedimentary rocks (e.g. Huhma et al. 1991, Claeson et al. 1993, Huhma et al. 2011, Lahtinen et al. 2015). The 2.5–2.2 Ga age interval seems to have been a "quiet" period with no major rock-forming events, except for minor mafic magmatism (see compilation in Huhma et al. 2011). Meta-sandstones from the Pahakurkio and Kalixälv group record similar $\varepsilon_{Nd(1.89Ga)}$ values at -3.0 and -3.9, respectively, which are consistent with mixture of debris from predominantly 2.2–1.9 Ga and 3.0–2.6 Ga old rocks, as suggested by U-Pb provenance zircon dating of these samples (cf. Huhma 1987).

It is suggested that deposition of epiclastic material occurred contemporaneously with volcanism at approximately 1.89–1.88 Ga, with erosion and redeposition of volcanic material to form mixed epiclastic and volcanoclastic sediments of the Kalixälv group. Sub-arkosic sandstone of the Pahakurkio group has a more mature, quartz-rich composition than the amphibole-bearing sandstones of the Kalixälv group. Volcanic rocks seem to be much less abundant in the Pahakurkio group, except for the correlated Sakarinpalo suite

The Sakarinpalo metavolcanic rocks occur spatially with rocks of the Veikkavaara greenstone group, and are tentatively correlated with units within the Viscaria formation in the Kiruna Greenstone group (cf. Martinsson 1997). However, U-Pb SIMS zircon geochronology dates an intermediate metavolcanic rock sample of the Sakarinpalo suite at 1 890 ±5 Ma, a Svecofennian age. Magnetic anomaly patterns reveal a complexly folded internal structure for the Veikkavaara greenstones. Poly-phase deformation and folding, together with the very low rock exposure complicates interpretation of way-up in the stratigraphic succession. The Svecofennian age of the Sakarinpalo suite may even suggest inverted younging, with way-up towards the core of the V-shaped Veikkavaara greenstone structure.

Strongly scapolite-biotite-altered intermediate rocks of the Pahakurkio group show an identical trace element pattern to volcanic rocks in the Sakarinpalo suite, suggesting these units may be correlated. The meta-andesite in the Kalixälv group is dated at 1 887 ±5 Ma and is thus of a similar age to the rocks in the Sakarinpalo suite. In a regional context, the metavolcanic rocks in the Masugnsbyn area are of a similar or possibly slightly older age to the intermediate metavolcanic rocks in the Sammakkovaara group in the Pajala area of northeastern Norrbotten, dated at 1 882 ±3 and 1 880 ±3 Ma (Martinsson et al. 2018b), as well as intermediate volcanic rocks of the "Porphyrite group" in the Kiruna area, dated at 1 878 ±7 Ma (minimum age; Edfelt et al. 2006), intermediate metavolcanic rocks of the Muorjevaara group in the Gällivare area, dated at 1 882 ±6 Ma and 1 878 ±7 Ma (Claeson & Antal Lundin 2012, Lynch et al. 2018a) and felsic metavolcanic rocks in the Boden area, dated at 1 886 ±4 and 1 884 ±5 Ma (Sadeghi & Hellström 2015).

Chemically, the metavolcanic rocks in the Masugnsbyn area are intermediate to weakly felsic, low-Fe-Ti and calc-alkaline, thus of similar composition to "Porphyrite group" rocks in Norrbotten. A detailed, regional comparison of data from volcanic rocks in Norrbotten has not been carried out here, however. Most samples from Masugnsbyn are classified as andesite according to the Nb/Y –Zr/Ti classification diagram (Pearce 1996), but basalts, trachy-andesites, trachytes and dacites-rhyolites also occur. Volcanic rocks record similar chondrite-normalised rare earth element (REE) patterns, enriched in light REE over heavy REE, $(La/Yb)_N = 10.5 \pm 3.3$ (1σ, n = 26), but with a relatively flat pattern in the HREE end ($(Gd/Lu)_N = 1.6 \pm 0.38$ (1σ)). Primitive mantle-normalised spider diagrams show enrichment in the large ion lithophile elements, with a pronounced negative Nb-Ta anomaly, as well as negative anomalies in Ti and P. The normalised element patterns thus show a typical subduction zone signature, but also a typical upper continental crustal signature. Alternatively, this signature could be inherited from partial melting of crustal source rock. Although they have very similar averaged normalised element patterns, the volcanic rocks from the southeastern part of the Masugnsbyn area can be grouped with the Kalixälv group, and the highly altered rocks in the Pahakurkio group with the Sakarinpalo suite, only distinguished by a strong negative anomaly in Sr in the latter groups. In part, strong potassium or sodium alteration of the volcanic rocks in the Sakarinpalo suite suggest that this poorly exposed area could have potential for hydrothermal sulphide mineralisations.

Overall, negative initial ε_{Nd} signatures of metavolcanic rocks from the Sakarinpalo and Kalixälv groups ($\varepsilon_{Nd(1.89Ga)}$ at -3.9 and -2.2), metavolcanic rocks of the Kiirunavaara Group, as well as early Svecokarelian intrusive rocks in the Northern Norrbotten ore province suggest a source of juvenile arc-generated melts mixed with variable amounts of assimilated older continental crust of the Archaean craton, which by approximately 1.9 Ga had acquired distinctly negative ε_{Nd} values (< -10). Svecofennian igneous activity was related to partial melting above a subduction zone dipping under the older continental crust of the Archaean Norrbotten craton.

ACKNOWLEDGEMENTS

Our sincere thanks go to George Morris, Nikolaos Arvanitidis, Stefan Bergman and Veikko Niiniskorpi for their comments on the manuscript. Roy Rutland and Martin Whitehouse are gratefully acknowledged for providing unpublished SIMS zircon data from a meta-sandstone sample (RR96128) of the Pahakurkio group. U-Pb isotopic zircon data were obtained from fruitful cooperation with the Laboratory for Isotope Geology of the Swedish Museum of Natural History (NRM) in Stockholm. The Nordsim facility is operated under an agreement between the research funding agencies of Denmark, Norway and Sweden, the Geological Survey of Finland and the Swedish Museum of Natural History. Martin Whitehouse, Lev Ilyinsky and Kerstin Lindén at the Nordsim analytical facility are gratefully acknowledged for their first-class analytical support with SIMS analyses. Martin Whitehouse reduced the zircon analytical data, Lev Ilyinsky assisted during ion probe analyses and Kerstin Lindén prepared the zircon mounts. Milos Bartol at the Evolutionary Biology Centre and Jaroslaw Majka at the Department of Geology, Uppsala University, along with Kerstin Lindén at NRM are all warmly thanked for their support during BSE/CL imaging of zircons. Laboratory assistance with Sm-Nd isotopic analyses by Leena Järvinen and Arto Pulkkinen at GTK is gratefully acknowledged. Magnetic data from areas adjacent to northern Sweden used in Figure 1 were supplied by the geological surveys of Norway (ngu.no), and Finland (gtk.fi). Veikko Niiniskorpi is thanked for permission to use his photo of cross-bedding at Saarikoski in Figure 8B. Tone Gellerstedt and Maxwell Arding are much thanked for editing and proofreading.

REFERENCES

Bhatia, M.R., 1983: Plate Tectonics and Geochemical Composition of Sandstones. *The Journal of Geology 91*, 611–627.

Bergman, S., Billström, K., Persson, P.-O., Skiöld, T. & Evins, P., 2006: U-Pb age evidence for repeated Palaeoproterozoic metamorphism and deformation near the Pajala shear zone in the northern Fennoscandian shield. *GFF 128*, 7–20.

Bergman, S., Kübler, L. & Martinsson, O., 2001: Description of Regional Geological and Geophysical Maps of Northern Norrbotten County (east of the Caledonian Orogen). *Sveriges geologiska undersökning Ba 56*, 110 pp.

Bergman, T., Hellström, F. & Ripa, M., 2015: Verksamhetsrapport 2014: Norrbottens malm och mineral. *SGU-rapport 2015:08,* Sveriges geologiska undersökning. 20 pp.

Boggs, S., 2009: *Petrology of Sedimentary Rocks.* Cambridge University Press, 600 pp.

Boynton, W., 1984: Cosmochemistry of the rare earth elements: meteorite studies. Rare Earth Element Geochemistry.-Developments in Geochemistry 2 (Henderson, R., ed.), 89-92. Elsevier, Amsterdam.

Carlson, L., 1982a: Guld i Norrbotten del 1. *Sveriges geologiska undersökning BRAP 82039*, 140 pp.

Carlson, L., 1982b: Guld i Norrbotten. Del 2. *Sveriges geologiska undersökning BRAP 82040*, 133 pp.

Claeson, D. & Lundin, I.A., 2012: Beskrivning till berggrundskartorna 27K Nattavaara NV, NO, SV & SO. *Sveriges geologiska undersökning K383–386*, 22 pp.

Claesson, S., Huhma, H., Kinny, P.D. & Williams, I.S., 1993: The Baltic Shield Svecofennian detrital zircon ages—implications for the Precambrian evolution of the Baltic Shield. *Precambrian Research 64,* 109–130.

DePaolo, D.J., 1981: Neodymium isotopes in the Colorado Front Range and crust-mantle evolution in the Proterozoic. *Nature 291*, 684–687.

DePaolo, D.J. & Wasserburg, G.J., 1976: Nd isotopic variations and petrogenetic models. *Geophysical Research Letters 3*, 249–252.

Eliasson, T., Greiling, R., Sträng, T. & Triumf, C., 2001: Bedrock map 23H Stensele NV, scale 1:50 000. *Sveriges geologiska undersökning Ai 126*.

Edfelt, Å., Sandrin, A., Evins, P., Jeffries, T., Storey, C., Elming, S.-Å. & Martinsson, O., 2006: Stratigraphy and tectonic setting of the host rocks to the Tjårrojåkka Fe-oxide Cu-Au deposits, Kiruna area, northern Sweden. *GFF 128*, 221–232.

Eriksson, T., 1954: Pre-Cambrian Geology of the Pajala District, Northern Sweden. *Sveriges geologiska undersökning C 522*, 38 pp.

Frietsch, R., 1997: The iron ore inventory program 1963-1972 in Norrbotten County. *Sveriges geologiska undersökning Rapporter och meddelanden 92*, 77 pp.

Geijer, P., 1918: Nautanenområdet. En malmgeologisk undersökning. *Sveriges geologiska undersökning C 283*, 105 pp.

Geijer, P., 1929: Masugnsbyfältens geologi. *Sveriges geologiska undersökning C 351*, 39 pp.

Geijer, P., 1930: Pre-Cambrian geology of the iron bearing region Kiruna Gällivare Pajala. *Sveriges geologiska undersökning C 366*, 225 pp.

Grigull, S., Berggren, R., Jönberger, J., Jönsson, C., Hellström, F.A. & Luth, S., 2018: Folding observed in Palaeoproterozoic supracrustal rocks in northern Sweden. *In:* Bergman, S. (ed): Geology of the Northern Norrbotten ore province, northern Sweden. *Rapporter och Meddelanden 141,* Sveriges geologiska undersökning. This volume pp 205–257.

Grip, E. & Frietsch, R., 1973: *Malm i Sverige 2. Norra Sverige*. Almqvist & Wiksell, 295 pp.

Hellström, F., 2015: SIMS geochronology of a 1.93 Ga basement metagranitoid at Norvijaur west of Jokkmokk, northern Sweden. *SGU-rapport 2015:01,* Sveriges geologiska undersökning. 18 pp.

Hellström, F.A., 2018: Early Svecokarelian migmatisation west of the Pajala Shear Zone in the northeastern part of the Norrbotten Province, northern Sweden. *In:* Bergman, S. (ed): Geology of the Northern Norrbotten ore province, northern Sweden. *Rapporter och Meddelanden 141,* Sveriges geologiska undersökning. This volume pp 361–379.

Hellström, F.A. & Bergman, S., 2016: Is there a 1.85 Ga magmatic event in northern Norrbotten? – U-Pb SIMS zircon dating of the Pingisvaara metagranodiorite and the Jyryjoki granite, northern Sweden. *GFF 138, 526–532.*

Hellström, F. & Jönsson, C., 2014: Barents project 2014: Summary of geological and geophysical information of the Masugnsbyn key area. *SGU-rapport 2014:21*, Sveriges geologiska undersökning. 84 pp.

Hellström, F., Carlsäter Ekdahl, M. & Kero, L., 2012: Beskrivning till berggrundskartorna 27L Lansjärv NV, NO, SV & SO. *Sveriges geologiska undersökning K 387–390*, 27 pp.

Hellstrom, J., Paton, C, Woodhead, J. & Hergt, J., 2008: Iolite: Software for spatially resolved LA- (quad and MC) ICPMS analysis. *In:* Sylvester P (Ed.): *Laser Ablation ICP–MS in the Earth Sciences: Current Practices and Outstanding Issues*. Mineral. Assoc. of Canada, Quebec, Canada., 343–348.

Helovuori, O., 1979: Geology of the Pyhäsalmi ore deposit, Finland. *Economic Geology 74*, 1 084–1 101.

Hermelin, S.G., 1804: *Försök till mineral historia öfver Lappmarken och Vesterbotten; af friherre S.G. Hermelin. Stockholm, tryckt hos Carl Delén, 1804.* Stockholm.

Herron, M.M., 1988: Geochemical classification of terrigenous sands and shales from core or log data. *Journal of Sedimentary Research 58*, 820-829.

Hietanen, A., 1975: Generation of potassium-poor magmas in the northern Sierra Nevada and the Svecofennian of Finland. *J. Res. US Geol. Surv 3*, 631–645.

Högdahl, K., Andersson, U.B. & Eklund, O., 2004: The Transscandinavian Igneous Belt (TIB) in Sweden: a review of its character and evolution. *Geological Survey of Finland, Special Paper 37*, 123 pp.

Hughes, C.J., 1973: Spilites, keratophyres, and the igneous spectrum. *Geological Magazine 109*, 513–527.

Huhma, H., 1986: Sm-Nd, U-Pb and Pb-Pb isotopic evidence for the origin of the Early Proterozoic Svecokarelian crust in Finland. *Geologian survey of Finland Bulletin 337,* 48 pp.

Huhma, H., 1987: Precambrian Geology and Evolution of the Cental Baltic Shield Provenance of early proterozoic and archaean metasediments in Finland: a Sm-Nd isotopic study. *Precambrian Research 35*, 127–143.

Huhma, H., Claesson, S., Kinny, P. & Williams, I., 1991: The growth of Early Proterozoic crust: new evidence from Svecofennian detrital zircons. *Terra Nova 3*, 175–178.

Huhma, H., O'Brien, H., Lahaye, Y. & Mänttäri, I. 2011. Isotope geology and Fennoscandian lithosphere evolution. *Geological Survey of Finland, Special Paper 49,* 35–48

Huhma, H., Kontinen, A., Mikkola, P., Halkoaho, T., Hokkanen, T., Hölttä, P., Juopperi, H., Konnunaho, J., Luukkonen, E., Mutanen, T., Peltonen, P., Pietikäinen,K. & Pulkkinen, A. 2012: Nd isotopic evidence for Archaean crustal growth in Finland. *In*: P. Hölttä (ed.) *The Archaean of the Karelia Province in Finland. Geological Survey of Finland (GTK) Special Paper 54*, 176–213.

Jacobsen S.B. & Wasserburg G.J., 1980. Sm-Nd isotopic evolution of chondrites. *Earth and Planetary Science Letters, 50,* 139–155.

Jackson S.E., Pearson, N.J., Griffin W.L., Belousova E.A., 2004: The application of laser ablation-inductively coupled plasma-mass spectrometry to in situ U–Pb zircon geochronology. *Chemical Geology 211*, 47–69.

Janoušek, V., Farrow, C.M. & Erban, V., 2006: Interpretation of whole-rock geochemical data in igneous geochemistry: introducing Geochemical Data Toolkit (GCDkit). *Journal of Petrology 47,* 1255–1259.

Jensen, L.S., 1976: A new cation plot for classifying subakalic volcanic rocks. *Ontario Division of Mines Miscellaneous Paper 66,* 22 pp.

Jönberger, J., Jönsson, C., & Luth, S., 2018: Geophysical 2D and 3D modeling in the areas around Nunasvaara and Masugnsbyn, northern Sweden. *In:* Bergman, S. (ed): Geology of the Northern Norrbotten ore province, northern Sweden. *Rapporter och Meddelanden 141,* Sveriges geologiska undersökning. This volume pp 311–339.

Kathol, B. & Persson, P.-O., 2007: U-Pb zircon age of an ignimbritic rhyolite from Benbryteforsen in the area between Moskosel and Vidsel, southern Norrbotten County, Sweden. *In:* F. Hellström & J. Andersson (eds.): Results from radiometric datings and other isotope analyses 1. *SGU-rapport 2007:28*, Sveriges geologiska undersökning, 17–19.

Kathol, B. & Triumf, C.-A., 2004: Bedrock map 24J Arvidsjaur SO, scale 1:50 000. *Sveriges geologiska undersökning Ai 151.*

Kathol, B. & Weihed, P., (eds.) 2005: Description of regional geological and geophysical maps of the Skellefte District and surrounding areas. *Sveriges geologiska undersökning Ba 57*, 197 pp.

Korsman, K., Hölttä, P., Hautala, T. & Wasenius, P., 1984: Metamorphism as indicator of evolution and structure of the crust in eastern Finland. *Geological Survey of Finland Bulletin 328*, 40 pp.

Kousa, J., Luukas, J., Huhma, H. & Mänttäri, I., 2013: Palaeoproterozoic 1.93–1.92 Ga Svecofennian rock units in the northwestern part of the Raahe–Ladoga zone, central Finland. *In:* P. Hölttä (ed.): Current research: GTK Mineral potential workshop, Kuopio, May 2012. *Geological Survey of Finland Report of Investigation 198*, 91–96.

Kousa, J., Marttila, E. & Vaasjoki, M., 1994: Petrology, geochemistry and dating of Palaeoproterozoic metavolcanic rocks in the Pyhäjärvi area, central Finland. *In:* M. Nironen & Y. Kähkönen (eds.): Geochemistry of Proterozoic supracrustal rocks in Finland. *Geological Survey of Finland, Special Paper 19*, 7–27.

Kumpulainen, R.A., 2000: The Palaeoproterozoic sedimentary record of northernmost Norrbotten, Sweden. Unpublished report. *Sveriges geologiska undersökning BRAP 200030*, 45 pp.

Lahtinen, R. & Huhma, H., 1997: Isotopic and geochemical constraints on the evolution of the 1.93–1.79 Ga Svecofennian crust and mantle. *Precambrian Research 82*, 13–34.

Lahtinen, R., Huhma, H., Lahaye, Y., Jonsson, E., Manninen, T., Lauri, L.S., Bergman, S., Hellström, F., Niiranen, T. & Nironen, M., 2015: New geochronological and Sm–Nd constraints across the Pajala shear zone of northern Fennoscandia: Reactivation of a Paleoproterozoic suture. *Precambrian Research 256*, 102–119.

Lauri, L.S., Hellström, F., Bergman, S., Huhma, H. & Lepistö, S., 2016: New insights into the geological evolution of the Archaean Norrbotten province, Fennoscandian shield. *32nd Nordic Geological Winter Meeting, Helsingfors.*

LKAB Prospektering K-8656, 74 pp.

Ludwig, K.R., 2012: User's manual for Isoplot 3.75. A Geochronological Toolkit for Microsoft Excel. *Berkeley Geochronology Center Special Publication No. 5*, 75 pp.

Lundqvist, T., Vaasjoki, M. & Persson, P.-O., 1998: U-Pb ages of plutonic and volcanic rocks in the Svecofennian Bothnian Basin, central Sweden, and their implications for the Palaeoproterozoic evolution of the basin. *GFF 120*, 357–363.

Luth, S., Jönsson, C., Hellström, F., Jönberger, J., Djuly, T., Van Assema, B., Smoor, W., 2016: Structural and geochronological studies of the crustal-scale Pajala Deformation Zone, northern Sweden. *32nd Nordic Geological Winter Meeting, Helsingfors.*

Luth, S., Jönsson, C., Jönberger, J., Grigull, S., Berggren, R., van Assema, B., Smoor, W. & Djuly, T., 2018: The Pajala deformation belt in northeast Sweden: Structural geological mapping and 3D modelling around Pajala. *In:* Bergman, S. (ed): Geology of the Northern Norrbotten ore province, northern Sweden. *Rapporter och Meddelanden 141,* Sveriges geologiska undersökning. This volume pp 259–285.

Lynch, E.P., Bauer, T.E., Jönberger, J., Sarlus, Z., Morris, G.A. & Persson, P.-O., 2018a: Lithological and deformation characteristics of c. 1.88 Ga meta-volcanosedimentary rocks hosting iron oxide-copper-gold (IOCG) and related mineralisation in the Nautanen-Gällivare area, northern Sweden. *In:* Bergman, S. (ed): Geology of the Northern Norrbotten ore province, northern Sweden. *Rapporter och Meddelanden 141,* Sveriges geologiska undersökning. This volume pp 107–149.

Lynch, E.P., Hellström, F.A., Huhma, H., Jönberger, J., Persson, P.-O.& Morris, G.A., 2018b: Geology, lithostratigraphy and petrogenesis of c. 2.14 Ga greenstones in the Nunasvaara and Masugnsbyn areas, northernmost Sweden. *In:* Bergman, S. (ed): Geology of the Northern Norrbotten ore province, northern Sweden. *Rapporter och Meddelanden 141,* Sveriges geologiska undersökning. This volume pp 19–77.

Martinsson, O., 2004: Geology and Metallogeny of the Northern Norrbotten Fe-Cu-Au Province. *In:* R.L Allen, O. Martinsson & P. Weihed (eds.): Svecofennian ore-forming environments: volcanic-associated Zn-Cu-Au- Ag, intrusion associated Cu-Au, sedimenthostedPb-Zn, and magnetite-apatite deposits in northern Sweden. *Economic Geology Guidebook series 33*, 131–148.

Martinsson, O., 1997: Tectonic setting and metallogeny of the Kiruna greenstones. *Doctoral thesis, Luleå University of Technology*, 19 pp.

Martinsson, O. & Wanhainen, C., 2013: Fe oxide and Cu-Au deposits in the northern Norrbotten ore district: excursion held 16–20 August 2013. 12th Biennial SGA Meeting. Excursion guidebook SWE5, 70 pp.

Martinsson, O. & Perdahl, J.-A., 1995: Paleoproterozoic extensional and compressional magmatism in northern Sweden. *In:* J.-A. Perdahl: *Svecofennian volcanism in northern Sweden, Doctoral thesis 1995:169D, Paper II,* 1–13. Luleå University of Technology.

Martinsson, O., Vaasjoki, M. & Persson, P.-O., 1999: U-Pb ages of Archaean to Palaeoproterozoic granitoids in the Torneträsk-Råstojaure area, northern Sweden. *In:* S. Bergman (ed.): Radiometric dating results 4. *Sveriges geologiska undersökning C 831*, 70–90.

Martinsson, O., Van der Stilj, I., Debras, C. & Thompson, M., 2013: Day 3. The Masugnsbyn, Gruvberget and Mertainen iron deposits. *In:* O. Martinsson & C. Wanhainen (eds.): *12th Biennial SGA Meeting, Uppsala, Sweden. Excursion guidebook SWE5*, 37–44.

Martinsson, O., Billström, K., Broman, C., Weihed, P. & Wanhainen, C., 2016: Metallogeny of the Northern Norrbotten Ore Province, northern Fennoscandian Shield with emphasis on IOCG and apatite-iron ore deposits. *Ore Geology Reviews 78*, 447–492.

Martinsson, O., Bergman, S., Persson, P.-O. & Hellström, F.A., 2018a: Age and character of late-Svecokarelian monzonitic intrusions in north-eastern Norrbotten, northern Sweden. *In:* Bergman, S. (ed): Geology of the Northern Norrbotten ore province, northern Sweden. *Rapporter och Meddelanden 141,* Sveriges geologiska undersökning. This volume pp 381–399.

Martinsson, O., Bergman, S., Persson, P.-O., Schöberg, H., Billström, K. & Shumlyanskyy, L., 2018b: Stratigraphy and ages of Palaeoproterozoic metavolcanic and metasedimentary rocks at Käymäjärvi, northern Sweden. *In:* Bergman, S. (ed): Geology of the Northern Norrbotten ore province, northern Sweden. *Rapporter och Meddelanden 141,* Sveriges geologiska undersökning. This volume pp 79–105.

McDonough, W.F. & Sun, S.s., 1995: The composition of the Earth. *Chemical Geology 120*, 223–253.

Mellqvist, C., Öhlander, B. & Skiöld, T., 1999: Traces of Archaean crust in the Jokkmokk area, northern Sweden: a way of defining the Archaean-Proterozoic boundary. *In:* C. Mellqvist: *Proterozoic crustal growth along the Archaean continental margin in the Luleå and Jokkmokk areas, northern Sweden.* Doctoral thesis, Luleå University, 24 pp.

Niiniskorpi, V., 1982: Kurkkionvaara. Årsrapport 1981. *LKAB Ki 8207*, 5 pp.

Niiniskorpi, V., 1986: *En Zn-Pb-Cu-mineralisering i norra Sverige, en case-studie.* Licenciate thesis., geological department of Åba Akademi, 74 pp.

Nironen, M., 1997: The Svecofennian orogen: a tectonic model. *Precambrian Research 86*, 21–44.

Ödman, O.H., 1939: Urbergsgeologiska undersökningar inom Norrbottens län. *Sveriges geologiska undersökning C 426*, 100 pp.

Ödman, O.H., 1957: Beskrivning till berggrundskarta över urberget i Norrbottens län. *Sveriges geologiska undersökning Ca 41*, 151 pp.

Offerberg, J., 1967: Beskrivning till berggrundskartbladen Kiruna NV, NO, SV, SO. *Sveriges geologiska undersökning Af 1–4,* 147 pp.

Öhlander, B., Hamilton, P.J., Fallick, A.E. & Wilson, M.R., 1987a: Crustal reactivation in northern Sweden: the Vettasjärvi granite. *Precambrian Research 35*, 277–293.

Öhlander, B., Skiöld, T., Elming, S.Å., Claesson, S. & Nisca, D.H., 1993: Delineation and character of the Archaean-Proterozoic boundary in northern Sweden. *Precambrian Research 64*, 67–84.

Öhlander, B., Skiöld, T., Hamilton, P.J. & Claesson, L.-Å., 1987b: The western border of the Archaean province of the Baltic shield: evidence from northern Sweden. *Contributions to Mineralogy and Petrology 95*, 437–450.

Padget, P., 1970: Beskrivning till berggrundskartbladen Tärendö NV, NO, SV, SO. *Sveriges geologiska undersökning Af 5–8*, 95 pp.

Paton, C., Hellstrom, J.C., Paul P., Woodhead J.D. & Hergt J.M., 2011: Iolite: Freeware for the visualisation and processing of mass spectrometric data. *Journal of Analytical Atomic Spectrometry 26*, 2508–2518.

Paton C., Woodhead J.D., Hellstrom J.C., Hergt J.M., Greig A. & Maas R., 2010: Improved laser ablation U-Pb zircon geochronology through robust downhole fractionation correction. *Geochemistry Geophysics Geosystems 11*, 1–36.

Pearce, J.A., 1996: A user's guide to basalt discrimination diagrams. *Trace element geochemistry of volcanic rocks: applications for massive sulphide exploration. Geological Association of Canada, Short Course Notes 12*, 113.

Perdahl, J.-A. & Frietsch, R., 1993: Petrochemical and petrological characteristics of 1.9 Ga old volcanics in northern Sweden. *Precambrian Research 64*, 239–252.

Petersson, G., 1986: Projektet Nordöstra Norrbotten. Delprojektet Tärendö Ö:a. Årsrapport 1985. Studsvik Analytica AB. *Sveriges geologiska undersökning MINK 97043,* 40 pp.

Petrus, J.A. & Kamber, B.S., 2012: VizualAge: A Novel Approach to Laser Ablation ICP-MS U-Pb Geochronology Data Reduction. *Geostandards and Geoanalytical Research 36*, 247–270.

Quezada, R., 1976: Oriasvaara Kopparmalmsfyndighet: Rapport rörande resultat av SGUs undersökningar under åren 1974-1976. *Sveriges geologiska undersökning Mink 97010*, 15 pp.

Richard, P., Shimizu, N. & Allégre, C.J., 1976: ^{134}Nd/^{146}Nd, a natural tracer: an application to oceanic basalts. *Earth Planetary Science Letter 31*, 269–278.

Romer, R.L., Kjösnes, B., Korneliussen, A., Lindahl, I., Skyseth, T., Stendahl, M. & Sundvoll, B., 1992: The Archaean–Proterozoic boundary beneath the Caledonides of northern Norway and Sweden: U-Pb, Rb-Sr, and εNd isotope data from the Rombak-Tysfjord area. *NGU rapport 91.225*, 67 pp.

Roser, B. & Korsch, R., 1988: Provenance signatures of sandstone-mudstone suites determined using discriminant function analysis of major-element data. *Chemical Geology 67*, 119–139.

Sadeghi, M. & Hellström, F., 2015: U-Pb zircon ages of ignimbritic and porphyritic metarhyolites in the Boden area, northern Sweden. *SGU-rapport 2015:15,* Sveriges geologiska undersökning. 15 pp.

Skiöld, T., 1988: Implications of new U-Pb zircon chronology to early proterozoic crustal accretion in northern Sweden. *Precambrian Research 38*, 147–164.

Skiöld, T. & Rutland, R.W.R., 2006: Successive ~1.94 Ga plutonism and ~1.92 Ga deformation and metamorphism south of the Skellefte district, northern Sweden: Substantiation of the marginal basin accretion hypothesis of Svecofennian evolution. *Precambrian Research 148*, 181–204.

Skiöld, T., Öhlander, B., Markkula, H., Widenfalk, L. & Claesson, L.-Å., 1993: Chronology of Proterozoic orogenic processes at the Archaean continental margin in northern Sweden. *Precambrian Research 64*, 225–238.

Sláma, J., Košler, J., Condon, D.J., Crowley, J.L., Gerdes, A., Hanchar, J.M., Horstwood, M.S.A., Morris, G.A., Nasdala, L., Norberg, N., Schaltegger, U., Schoene, B., Tubrett, M.N. & Whitehouse, M.J., 2008: Plešovice zircon – A new natural reference material for U–Pb and Hf isotopic microanalysis. *Chemical Geology 249*, 1–35.

Stacey, J.S. & Kramers, J.D., 1975: Approximation of terrestrial lead isotope evolution by a two-stage model. *Earth and Planetary Science Letters 26*, 207–221.

Steiger, R.H. & Jäger, E., 1977: Convention on the use of decay constants in geo- and cosmochronology. *Earth and Planetary Science Letters 36*, 359–362.

Sun, S.S. & McDonough, W.F., 1989: Chemical and isotopic systematics of oceanic basalts: implications for mantle composition and processes. *In:* A.D. Saunders, M. Norry (eds.). Magmatism in Ocean Basins. *Geological Society of London Special Publications 42,* 313–345.

Tegengren, F.R., 1924: Sveriges ädlare malmer och bergverk. *Sveriges geologiska undersökning Ca 17*, 406 pp.

Vaasjoki, M. & Sakko, M., 1988: The evolution of the Raahe-Ladoga zone in Finland: isotopic constraints. *In:* K. Korsman (ed.): Tectono-metamorphic evolution of the Raahe Ladoga zone. *Geological Survey of Finland Bulletin 343*, 7–32.

Vaasjoki, M., Huhma, H., Lahtinen, R. & Vestin, J., 2003: Sources of Svecofennian granitoids in the light of ion probe U-Pb measurements on their zircons. *Precambrian Research 121*, 251–262.

Wanhainen, C., Broman, C., Martinsson, O. & Magnor, B., 2012: Modification of a Palaeoproterozoic porphyry-like system: Integration of structural, geochemical, petrographic, and fluid inclusion data from the Aitik Cu–Au–Ag deposit, northern Sweden. *Ore Geology Reviews 48*, 306–331.

Wasström, A., 1993: U-Pb zircon dating of a quartz-feldspar porphyritic dyke in the Knaften area; Västerbotten County; northern Sweden. *In:* T. Lundqvist (ed.): Radiometric dating results 2. *Sveriges geologiska undersökning C 82*8, 34–40.

Wasström, A., 1996: The Knaften granitoids of Västerbotten County, northern Sweden. *In:* T. Lundqvist (Ed.): Radiometric dating results. *Sveriges geologiska undersökning C 823*, 60–64.

Weihed, P., Arndt, N., Billström, K., Duchesne, J.-C., Eilu, P., Martinsson, O., Papunen, H. & Lahtinen, R., 2005: 8: Precambrian geodynamics and ore formation: The Fennoscandian Shield. *Ore Geology Reviews 27*, 273–322.

Wiedenbeck, M., Allé, P., Corfu, F., Griffin, W.L., Meier, M., Oberli, F., Quadt, A.V., Roddick, J.C. & Spiegel, W., 1995: Three natural zircon standards for U-Th-Pb, Lu-Hf, trace element and REE analyses. *Geostandards Newsletter 19*, 1–23.

Wiedenbeck, M., Hanchar, J.M., Peck, W.H., Sylvester, P., Valley, J., Whitehouse, M., Kronz, A., Morishita, Y., Nasdala, L., Fiebig, J., Franchi, I., Girard, J.P., Greenwood, R.C., Hinton, R., Kita, N., Mason, P.R.D., Norman, M., Ogasawara, M., Piccoli, P.M., Rhede, D., Satoh, H., Schulz-Dobrick, B., Skår, O., Spicuzza, M.J., Terada, K., Tindle, A., Togashi, S., Vennemann, T., Xie, Q. & Zheng, Y.F., 2004: Further characterisation of the 91500 zircon crystal. *Geostandards and Geoanalytical Research 28*, 9–39.

Whitehouse, M.J., Claesson, S., Sunde, T. & Vestin, J., 1997: Ion-microprobe U–Pb zircon geochronology and correlation of Archaean gneisses from the Lewisian Complex of Gruinard Bay, northwestern Scotland. *Geochimica et Cosmochimica Acta 61*, 4 429–4 438.

Whitehouse, M.J., Kamber, B.S. & Moorbath, S., 1999: Age significance of U–Th–Pb zircon data from Early Archaean rocks of west Greenland: a reassessment based on combined ion-microprobe and imaging studies. *Chemical Geology (Isotope Geoscience Section) 160*, 201–224.

Whitehouse, M., J. & Kamber, B.S., 2005: Assigning Dates to Thin Gneissic Veins in High-Grade Metamorphic Terranes: A Cautionary Tale from Akilia, Southwest Greenland. *Journal of Petrology 46*, 291–318.

Winchester, J. & Floyd, P., 1977: Geochemical discrimination of different magma series and their differentiation products using immobile elements. *Chemical Geology 20*, 325–343.

Witschard, F., 1970: Description of the geological maps Lainio NV, NO, SV, SO. *Sveriges geologiska undersökning Af 9–12*, 102 pp.

Witschard, F., 1984: The geological and tectonic evolution of the precambrian of northern Sweden – A case for basement reactivation? *Precambrian Research 23*, 273–315.

Witschard, F., Nylund, B. & Mannström, B., 1972: Masugnsbyn iron ore. Report concerning the results of Sveriges geologiska undersökning:s investigations in the years 1965–1970. *Sveriges geologiska undersökning BRAP 734,* 95 pp.

Geological Survey of Sweden
Box 670
SE-751 28 Uppsala
Phone: +46 18 17 90 00
Fax: +46 18 17 92 10
www.sgu.se

Uppsala 2018
ISSN 0349-2176
ISBN 978-91-7403-393-9
Tryck: Elanders Sverige AB